POLITECNICO DI MILANO

Scuola di Ingegneria Industriale e dell'Informazione
Corso di Laurea Magistrale in Ingegneria Elettrica

Research on Overvoltage Analysis and Insulation Coordination for Converter Station of MMC-MTDC

Relatore: Prof. Flavia GRASSI

Correlatore: Associate Prof. Lianhui NING

Tesi di Laurea Magistrale di:
Renqing Chen
Matricola: 876459

Anno Accademico 2018-2019

PREFAZIONE

Le nuove risorse rinnovabili hanno gli svantaggi della capacità ridotta, della potenza di trasmissione instabile ed è ampia e dispersa nella distribuzione. È difficile integrare in modo stabile e affidabile le nuove risorse rinnovabili nella rete già esistente mediante la trasmissione in corrente alternata o attraverso il sistema tradizionale in corrente continua. La tecnologia di trasmissione half-bridge submodule modular multilevel (MMC-HVDC) ha un ampio campo di applicazione. Ha la capacità di trasmissione a lunga distanza e a grandi capacità. Quindi, può fornire un sistema di trasmissione di potenza per le nuove energie pulite, ma in questa tecnologia manca la capacità di eliminare i guasti DC. Il sistema multi-terminal DC (MTDC) con interruttore DC ibrido ad alta tensione, può interrompere rapidamente la linea difettosa interrompendo selettivamente l'interruttore nel circuito DC per garantire un'alimentazione continua ad altre parti del sistema. Al momento, non esiste un'applicazione di ingegneria pratica in cui gli interruttori di circuito DC siano usati nelle linee aeree. Esistono pochi studi sull'influenza del funzionamento dell'interruttore del circuito in dc sulla sovratensione del sistema MTDC e mancano gli standard di coordinamento dell'isolamento per il sistema MMC-HVDC. Il sistema di trasmissione MMC-MTDC da ± 500 kV viene preso come oggetto di ricerca in questa tesi e vengono studiate le caratteristiche di sovratensione della stazione di conversione insieme al coordinamento dell'isolamento delle apparecchiature nella stazione elettrica.

In primo luogo, questa tesi ricava il modello matematico della stazione di conversione del sistema MMC-HVDC e progetta la struttura del controllore di quest’ultima. Inoltre, viene presentato il modello con i punti chiave del sistema per la simulazione di sovratensione da commutazione degli interruttori e dai fulmini. Sulla base del modello matematico derivato, della struttura del controllore e del modello delle apparecchiature, è possibile costruire il modello transitorio elettromagnetico della rete MMC-MTDC. Successivamente, la validità del controllore e del sistema viene verificata mediante la prova della risposta dinamica del modello.

In secondo luogo, questa tesi analizza il processo del transitorio e del livello di sovratensione durante i tipici guasti della stazione di conversione MMC-MTDC e studia i fattori di influenza della sovratensione da commutazione da quattro aspetti: azione dell'interruttore DC, modalità di funzionamento della rete, modalità di messa a terra della stazione di conversione e la logica del sistema di protezione. Inoltre, i fattori che influenzano la sovratensione dai fulmini della stazione di conversione sono studiati attraverso i parametri della torre, dalla topografia e dalla posizione del fulmine. Analizzando i fattori di influenza della sovratensione da commutazione e da fulmine, si ottengono le condizioni di simulazione degli apparecchi chiave della stazione di conversione. Su questa base, vengono riepilogati il livello massimo di sovratensione su ciascun nodo chiave della stazione e le caratteristiche intrinseche della stazione di conversione MMC-MTDC.

Infine, sulla base dell'esperienza ingegneristica nei sistemi MMC-MTDC, questo documento propone cinque tipi di schemi di configurazione per il dispersore di terra della stazione di conversione. Inoltre, in base al livello di tensione e al livello di sovratensione del sistema, vengono selezionati i parametri appropriati del dispersore e il livello di isolamento di ciascuna apparecchiatura della stazione di conversione viene determinato considerando il margine di isolamento. Allo stesso tempo, utilizzando il processo di gerarchia analitica migliorato per considerare in modo completo il livello di isolamento, il margine di isolamento, i costi di ingegneria, le difficoltà di installazione e manutenzione e altri fattori, si ottiene lo schema di configurazione del dispersore con economicità e tecnicità ottimali. Lo schema ottimale è quello di usare solo il dispersore di terra e rimuovere invece il dispersore in parallelo alle apparecchiature, che fornisce le basi teoriche per la progettazione e l'applicazione di successivi progetti pratici.

PAROLE CHIAVI: MMC; Rete multi-livello in DC; Sovratensione; configurazione del dispersore; coordinazione dell’isolamento

ABSTRACT

The new clean energy has the disadvantages of small capacity, unstable transmission power, wide and scattered on distributing. It is difficult to integrate new clean energy into the grid stably by means of AC transmission or traditional DC transmission technology. The half-bridge submodule modular multilevel transmission technology (MMC-HVDC) has a wide application field. It has long-distance and large-capacity transmission capability, which can provide a power transmission platform for a variety of new energy interconnections and transmissions, but lacks the ability to clear DC faults. The multi-terminal DC (MTDC) system with high voltage hybrid DC circuit breaker can quickly cut off the faulty line by selectively breaking the DC circuit breaker to ensure continuous power supply to other parts of the system. At present, there is no practical engineering application in which DC circuit breakers are matched with overhead lines. There are few studies on the influence of DC circuit breaker operation on the overvoltage of MTDC system, and there is a lack of insulation coordination standards for MMC-HVDC system. The ±500kV MMC-MTDC transmission system is taken as the research object in this paper, and the overvoltage characteristics of the converter station and the insulation coordination of the equipment in the station are studied.

Firstly, this thesis deduces the mathematical model of the converter station of the MMC-HVDC system, and designs the controller structure of the converter station. In addition, the key equipment model of system for switching and lightning overvoltage simulation is presented. Based on the derived mathematical model, controller structure and equipment model, the electromagnetic transient model of MMC-MTDC grid can be build. After that, the validity of the controller and model is verified by the dynamic response verification of the model.

Secondly, this thesis analyzes the transient process and overvoltage level under the typical fault of MMC-MTDC converter station, and studies the influencing factors of switching overvoltage from four aspects: DC circuit breaker action, grid operation mode, grounding mode of the converter station and control protection system. Moreover, the factors affecting lightning overvoltage of the converter station are studied from the aspects of tower parameters, topography and lightning strike position. By analyzing the influencing factors of switching and lightning overvoltage, the simulation conditions of the representative overvoltage of the key equipment of the converter station are obtained. On this basis, the maximum overvoltage level at each key node of the converter station and intrinsic characteristics of the overvoltage of MMC-MTDC converter station are summarized.
Finally, based on the engineering experience of MMC-MTDC system, this paper proposes five kinds of arrester configuration schemes of the converter station for different protection modes of converter valve, bridge arm reactor and smoothing reactor. In addition, according

to voltage grade and overvoltage level of the system, the appropriate arrester parameters are selected, and the insulation level of each equipment of the converter station is determined by considering the insulation margin. At the same time, using the improved analytic hierarchy process to comprehensively consider the insulation level, insulation margin, engineering cost, installation and maintenance difficulty and other factors, the arrester configuration scheme with the optimal technicality and economy is obtained. The optimal scheme is to reserve the ground arrester and remove the equipment parallel arrester, which provides the theoretical basis for the design and application of subsequent practical projects.

KEY WORDS: MMC; Multi-terminal DC grid; Overvoltage; Arrester configuration; Insulation coordination

CONTENTS

1 Preface

1.1 Significance and Application Background of Selected Topic

With the increasing shortage of fossil resources and the increasing environmental problems such as pm2.5, the market needs new clean energy to solve the contradiction between environment and energy demand urgently. In recent years, China has continuously increased its investment in clean renewable energy fields such as wind power generation and solar power generation. However, due to small scale, unstable, relatively dispersed of these energy sources and not easy to assemble, which bring many challenges that have never been encountered before. Different from the traditional AC transmission or conventional DC transmission technology, there are still many problems to be solved in the technology of large-scale new energy access. Correspondingly, this also brings great challenges and profound changes to China's traditional power transmission technology. New technologies and equipment must be adopted, and the power grid structure should be appropriately adjusted to meet the needs of the future energy pattern. Flexible DC transmission technology can provide a power transmission platform for the interconnection and transmission of various new energy sources, thus effectively solving this technical problem [1, 2].

In line with the construction of the 2020 Winter Olympics and the Xiong'an New District, the State Grid Corporation plans to construct a Zhangbei flexible DC power grid demonstration project in the Zhangjiakou National New Energy Comprehensive Demonstration Zone and the Winter Olympics Zone. Through the construction of a large-scale clean renewable energy integrated grid such as wind power, photovoltaic, and pumping energy, the coordinated coordination of wind, light and storage can be realized. The project plans to build DC converter stations in Zhangbei, Kangbao, Fengning and Beijing. The four-terminal converter station forms a ±500kV flexible DC grid in the form of a ring-shaped overhead line, which enhances the development level of Zhangjiakou wind power and photovoltaic power generation, strengthens Beijing's power grid construction, and guarantees the capital's energy supply. It will provide safe and reliable power supply to the 2022 Winter Olympic Games venues, respond to the call of “Low Carbon Olympics, Green Olympics”, and take advantage of this opportunity to promote flexible DC key technology upgrades and equipment innovation [3].

Flexible DC transmission technology is a kind of high-voltage DC transmission technology. It originated in the late 1990s, and its commutation part use voltage source converter with fully controlled components (VSC). Flexible DC transmission technology has broad application prospects in many fields. It is mainly used in the field of new energy fields for offshore wind plant, and it can also be applied to long-distance transmission and asynchronous networking. Compared with traditional DC transmission technology, flexible

DC transmission technology has its incomparable advantages [4-7].

1）Small occupied area, low harmonic level, few filtering devices.

2）No reactive compensation problem, and can provide reactive power to the system.

3）Active and reactive power can be independently controlled in the aspect of power flow control, and instantaneous decoupling control of that can be realized by a vector controller.

4）No commutation failure.

5）Access to weak AC systems or passive systems.

6）Suitable for multi-terminal DC system with multi-power supply and multi-point charge.

At present, most of the flexible DC transmission engineering applications that have been put into operation are modular multi-level flexible direct current transmission technologies with half bridge modules (MMC-HVDC). However, the converter stations of these projects lack fault removal capabilities. When a temporary failure occurs in the transmission line, a large fault current will be generated on the converter valve and the transmission line, thereby affecting the safe and stable operation of the DC system. At present, there are two ways to solve this problem [8]. First, the improved MMC adopts full bridge submodule or clamped double submodule, and the controller maintains the module capacitance to be charged by its own control, and provides a back EMF for the fault loop to achieve the purpose of clearing the DC side fault. However, the disadvantage of this approach is that the converter valve is costly and has low operating efficiency. Second, relying on the AC side circuit breaker to achieve DC fault clearance, but this method will cause the converter station to be out of service and cannot meet the requirements of continuous operation. Therefore the third method is adopted, that is, the DC circuit breaker is configured in the multi-terminal system. The DC side fault is cut out rapidly by selective breaking of DC circuit breaker, ensuring continuous power supply to other parts of the system. However, this method puts high requirements on the breaking capacity of the DC circuit breaker and the detection time of the protection system [9, 10].

Similar to the conventional DC transmission system, the overvoltage protection and insulation coordination of the converter station is also one of the core technologies for the implementation of the DC transmission project. It has important significance for the selection, design, manufacture and testing of converter station equipment. Flexible DC transmission systems generate overvoltage due to various operations, faults, lightning strikes, etc., which can seriously threaten the insulation safety life of the converter station equipment and the safe and stable operation of the system. The converter valve use full-control devices, so there is a big difference between the circuit topology, the converter operating principle, the system control strategy and the operation mode of MMC-HVDC system and the conventional DC transmission system. Correspondingly, it also puts forward new demands in

the overvoltage protection and insulation coordination. Therefore, in order to ensure the stability and safety of the system, it is of great significance to study and analyze the overvoltage characteristics of the MMC-HVDC transmission system and the insulation coordination scheme of the converter station. For conventional DC transmission systems, the insulation level and insulation scheme can be determined by referring to the insulation coordination principles and procedures in the national standard GB/T311.3-2017. However, there is no specific national technical standard for MMC-HVDC transmission system to guide the insulation coordination [11, 12].

Compared with the flexible DC transmission system at both ends, the multi-terminal flexible DC transmission system has higher flexibility, reliability and economy. However, the control system will be more complicated, and the coordination control strategy is needed between the converter stations to balance the power of each part of the grid. The operation requirement of the MMC-MTDC grid is that when any converter station is out of operation due to failure or maintenance, the remaining system should operate stably under the condition of power balance and its overvoltage level does not exceed the insulation level of each electrical equipment. In addition, there are more types of faults to be considered in MMC-MTDC system. The MMC-MTDC system with DC breakers should also consider the effect of DC breaker action on the overvoltage level of the converter station. This puts higher requirements on the overvoltage protection of the system, and requires more detailed study on the overvoltage protection and insulation coordination scheme of the MMC-MTDC system.

Zhangbei flexible DC demonstration project uses the technology of DC circuit breaker and overhead line. Due to the short history of this technology, there is a lack of accurate models to reflect the operating characteristics of DC circuit breakers. In addition, few studies have been done on the influence of DC circuit breaker operation on system overvoltage, so it is difficult to find the standard and guideline for flexible DC transmission systems. In summary, it is necessary to analyze the lightning and switching overvoltage of the MMC-MTDC system using DC circuit breaker and overhead line technology. And it is necessary to do research on insulation coordination to provide technical support for practical engineering applications.

1.2 Domestic and Oversea Research Status Review

1.2.1 Research Status of MMC-MTDC Technology

So far, MMC-HVDC technology has been widely applied and developed. The voltage levels and capacities of the two-terminal MMC system are rapidly increasing, and the technology for multi-terminal system and DC grid are becoming more mature [13,14].

In the 1990s, Switzerland successfully applied VSC-HVDC to the field of practical

engineering, which is the first application of fully-controlled power electronic devices in DC. At the beginning of the 21st century, the United States also put into operation the world's first MMC-HVDC project, which is TRANS BAY project. At present, MMC-HVDC is very promising in the international construction and development. The ±525kV North Sea Network project for grid interconnection in the UK and Norway is scheduled to be put into operation in 2021, which will become a submarine interconnection MMC-HVDC project with the longest transmission distance and highest voltage grade. In addition, nearly 100 MMC-HVDC projects are being planned or under construction in the UK and the US to promote and encourage the development of clean energy.

In March 2011, China's first flexible DC transmission demonstration project, Shanghai Nanhui Project, was completed and put into operation, which is also the first flexible DC transmission project in Asia. The Nan'ao ±160kV MMC-MTDC demonstration project started on December 25, 2013 was the world's first MMMC-MTDC project. It fully demonstrates the advantages of flexible DC transmission technology, and realizes the integration of offshore island systems, multiple DC energy grids, and new energy grids. It mainly provides a good solution for wind power access systems with extremely unstable power transmission and poor power quality, and promotes the new development of international DC transmission technology [15].

On July 4, 2014, State Grid of China commissioned a ±200kV Zhoushan five-terminal flexible DC transmission project in Zhoushan, Zhejiang. The power systems of the five islands of Zhoushan are interconnected by submarine DC cables, enabling simultaneous access and power transmission of multiple offshore wind farms. The successful commissioning of the project marked the discovery of effective solutions for the collection and delivery of large-scale clean energy due to weak grids. The MMC-MTDC system can carry clean energy such as wind energy, geothermal energy and solar energy from multi-terminal and transmit through large-capacity long-distance power transmission channels.

The Zhangbei four-terminal MMC-HVDC project, which is based on this research, is scheduled to be put into operation in 2020. The rated voltage level is ±500kV and the rated operating capacity is 3000MW. It will become the flexible DC project with the highest rated capacity in the world. In recent years, the development and utilization of renewable energy in China has developed rapidly but distributed. MMC-MTDC technology has become an inevitable choice to meet the growing demand for urban electricity and to develop smart grids in the future. At present, China has accumulated a lot of experience in the field of MMC-HVDC technology and engineering construction. It will play an important role in China's energy development strategy and will be further developed.

1.2.2 Research Status of Overvoltage and Insulation Coordination of MMC-MTDC

The flexible HVDC transmission projects put into operation in the world are mostly two-terminal systems. For the practical project of multi-terminal flexible HVDC transmission, only the Guangdong Nanao ±160kV three-terminal demonstration project in 2013, the Zhoushan ±200kV five-terminal demonstration project in 2014, the North American Tres Amigas three-terminal project And the three-terminal project of South-West Scheme in Sweden [16]. Most of today's research on multi-terminal MMC-HVDC is related to coordinated control strategies. Moreover, since DC transmission line of these projects are mostly laid by DC cables, there is no problem of overvoltage generated by lightning intruding waves of DC lines, and there is less research on overvoltage of DC overhead lines. Secondly, the multi-terminal system studied in this thesis adopts a true bipolar structure which is equipped with DC circuit breaker. The complex and diverse operation modes put forward higher requirements for overvoltage and insulation coordination.

A complete set of standardized procedures has been developed for the overvoltage and insulation coordination of traditional HVDC transmission system converter stations. Up to now, the traditional HVDC transmission projects in China have been based on the established insulation coordination principle to determine the arrester configuration and insulation level. Reference [17] studies the insulation coordination of the converter stationis which is based on the ±500kV Yunnan-Guangxi DC project. According to the principle of insulation coordination of HVDC converter station, the overvoltage of the station is analyzed and the lightning arrester scheme and equipment insulation level are proposed. In addition, the air clearance of the valve hall is calculated based on the engineering practice. A new type of arrester configuration scheme is proposed in reference [18] based on the traditional ±800kV Changji-Guquan UHV project. This scheme enables the DC system to be boosted to ±1100kV system and verified the effectiveness of the scheme through DC system overvoltage simulation. The insulation coordination of ±1100kV UHVDC transmission project in Zhundong-Chengdu was studied in reference [19]. According to the configuration principle of arrester of UHVDC converter station and the practical engineering experience, the arrester configuration scheme and overvoltage protection strategy are proposed. Finally, the recommended insulation level of the electrical node is obtained.

The research on the insulation coordination of the converter station of the MMC-HVDC system has not formed a unified design principle yet. The arrester configuration of the existing MMC-HVDC project is designed with reference to the experience of the traditional DC converter station. The main wiring scheme, equipment technical parameter and insulation coordination scheme of the converter station are proposed for the Dalian MMC-HVDC project in reference [20]. In reference [21], the transient overvoltage of the bipolar high-voltage and large-capacity flexible DC project with the background of ±320kV

Xiamen project is calculated and analyzed, which provides a reference for the research of converter station equipment. Based on the Transbay project, reference [22] checks the overvoltage level by 14 typical faults of converter stations, and proposes an overvoltage level that limits the critical nodes of the overvoltage protection scheme for MMC-HVDC systems. Then the withstand voltage level of the converter station equipment is obtained by a deterministic insulation coordination. Reference [23] conducted a study on the Luxi back-to-back flexible DC project. By analyzing the overvoltage simulation results of different operating modes of the system, the arrester configuration scheme of the converter station is proposed, and the insulation level of the converter station equipment is determined. In reference [24], based on the Nan'ao three-terminal flexible DC transmission system, lightning intrusion wave overvoltage of DC side is studied, and the voltage stress of the main equipment in the converter station after the DC line is subjected to back flashover and shielding failure is obtained. On this basis, the lightning protection level was checked and the insulation margin of the equipment in the converter station was determined.文 The reference [25,26] analyzes the overvoltage level of electrical equipment and the mechanism of overvoltage generated by faults and lightning strikes for Zhoushan five-terminal MMC-HVDC project. The optimal scheme is selected by comparing the number of arresters and the level of switching overvoltage of the insulation coordination schemes of three different arresters, and finally determining the insulation level of the electrical equipment. It provides an important basis for the study of insulation coordination of the project. Since the project uses a submarine DC cable laying method, the influence of lightning intruding wave overvoltage is not considered.

There are few studies on overvoltage and insulation coordination of converter stations in multi-terminal flexible HVDC transmission systems. Related research is based on the traditional HVDC system or two-terminal MMC-HVDC system to calculate the overvoltage level and equipment insulation level [27-29]. The differences in the insulation configuration of the converter stations of the multi-terminal system are not considered, and a complete design of MMC-HVDC insulation coordination is not formed. Therefore, it is necessary to carry out relevant research on MMC-MTDC system, which can provide theoretical basis for the construction of Zhangbei project and similar projects in the future.

1.3 Main Works of the Thesis

This thesis takes MMC-MTDC system as the research object. Firstly, the coordinated control strategy of multi-terminal system and the electromagnetic transient model of the main equipment of flexible DC converter station are analyzed. Based on this, a four-terminal flexible DC power grid was established based on Zhangbei demonstration project, and the simulation verification of the model was carried out. Secondly, the influencing factors of operating overvoltage and lightning overvoltage of multi-terminal flexible HVDC transmission system are studied and analyzed. Combining the characteristics of the multi-terminal DC system, the optimal arrester configuration scheme of the converter station

is proposed. The specific research work will be carried out in the following sections:

(1) Research on Electromagnetic Transient Model of MMC-MTDC Transmission System
The construction of electromagnetic transient model of MMC-MTDC transmission system should start from the mathematical model derivation. After obtaining the mathematical model of the converter station, the controller structure of station-level is designed based on this, and the coordinated control strategy between multiple converter stations is designed in the upper control part. The main equipment of the MMC-HVDC system includes converter valves, converter transformers, reactors and DC transmission lines. The broadband model of the main equipment is given here to support the subsequent research on lightning overvoltage characteristics. The corresponding electromagnetic transient model is built in the PSCAD simulation software, and the dynamic response simulation verification of the converter station controller parameters and the four-terminal system is carried out.

(2) Research on Switching and Lightning Overvoltage Characteristics of Converter Station in MMC-MTDC
There are many types of faults that can occur in MMC-MTDC system. Starting from the typical faults of the converter station, this paper analyzes the protection action sequence after different faults and the generation mechanism of the overvoltage of the key nodes of the converter station, and deeply studies the characteristics and laws of the overvoltage of the converter station. The lightning intruding wave simulation is carried out in the lightning simulation model, and the characteristics of the lightning intruding wave overvoltage and the overvoltage level on the key equipment of the converter station are deeply studied. The most serious situation of switching and lightning overvoltage are analyzed and the intrinsic characteristics of overvoltage of MMC-MTDC converter station are analyzed, which lays a foundation for the study of insulation coordination of converter station.

(3) Research on Insulation Coordination and Insulation Level of Converter Station in MMC-MTDC
Based on the engineering experience of flexible DC converter station insulation coordination, the arrester configuration scheme of several converter stations is preliminarily estimated, and the appropriate arrester parameters are selected according to the system voltage level and simulation results. The insulation level of equipment in converter station is determined by the idiom, and first we determine the insulation margin of each equipment of converter station. Then determine the insulation level of the equipment according to the maximum overvoltage level of the electrical equipment, and provide a theoretical basis for the actual engineering equipment selection. Finally, according to the characteristics of MMC-MTDC transmission system, five arrester configuration schemes are proposed. The analytic hierarchy process is used to comprehensively consider the technical and economic factors, and determine the optimal configuration of the lightning arrester.

2 Electromagnetic Transient Simulation Modeling of MMC-MTDC System

For MMC-MTDC transmission systems, the controller design and parameter setting are more complicated due to the use of multiple MMC converter stations. The new MMC vector control method adopted in this thesis replaces the more mature internal and external loop current feedback control methods, which makes the tuning of the controller parameters of the converter station simpler and the system response is not affected. Based on the PSCAD simulation software, a four-terminal true bipolar flexible DC transmission ring network model was established, and the effectiveness of the constructed electromagnetic transient simulation model was verified by dynamic response analysis. This laid the foundation for the subsequent calculation of overvoltage and lightning intruding wave overvoltage.

2.1 Topology of MMC-MTDC System

A multi-terminal DC transmission system refers to a DC transmission system containing three or more converter stations under the same DC grid. Its main feature is that the operation mode is flexible and can realize the interconnection of multiple energy systems, and can be applied to various new energy sources and DC distribution networks.

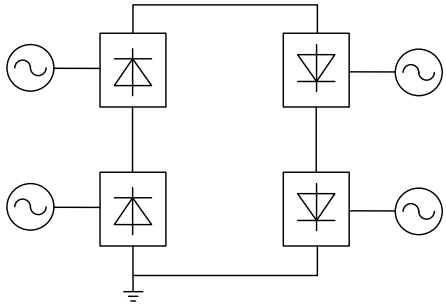

(a) Series

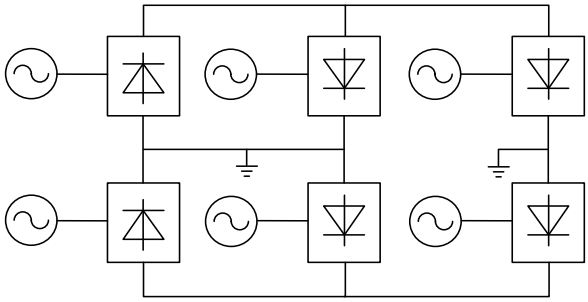

(b) Series-parallel

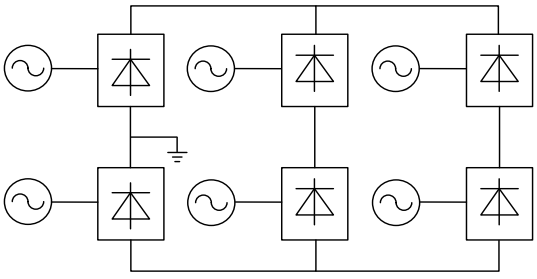

(c) Radial parallel connection

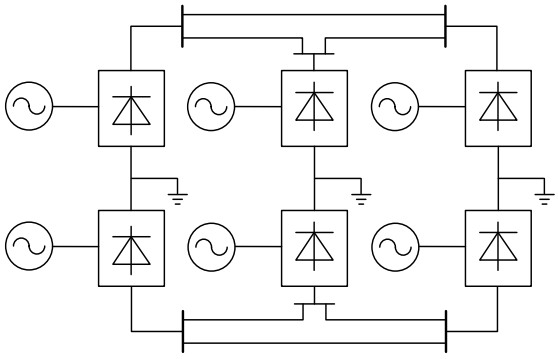

(d) Ring-connected parallel connection

Figure 2-1 Structure of Multi-terminal DC Power Grid

There are four typical wiring methods for multi-terminal DC grids, including series, radial

and ring-connected parallel structures, and series-parallel structures, as shown in figure 2-1. Among them, serial multi-terminal system operates with the same level of DC current, parallel multi-terminal system operates with the same level of DC voltage, and the hybrid multi-terminal system includes series and parallel, which increases the flexibility and complexity of the multi-terminal converter station control. The ultimate goal of these wiring mode controls is to control the power of multiple converter stations to achieve the desired goals and achieve the balance of power delivery. For MMC system using voltage source converter, parallel structure having a stable DC side voltage is often used. In the design of the subsequent controller, one converter station can control the DC voltage to be stable, and the remaining converter stations use fixed active power and fixed reactive power control to realize complete power distribution of all converter stations.

2.2 Control Strategy of MMC-MTDC System

The construction of the control system of MMC-MTDC transmission system will affect the overvoltage level of the system and the determination of the insulation level of the equipment. Therefore, before studying the overvoltage characteristics and insulation coordination of multi-terminal systems, the circuit structure of the converter station should be analyzed. The mathematical model of the converter is obtained by mathematical formula derivation and other methods. On this basis, the controller of station-level is designed [30].

2.2.1 Mathematic Model of the Converter Station

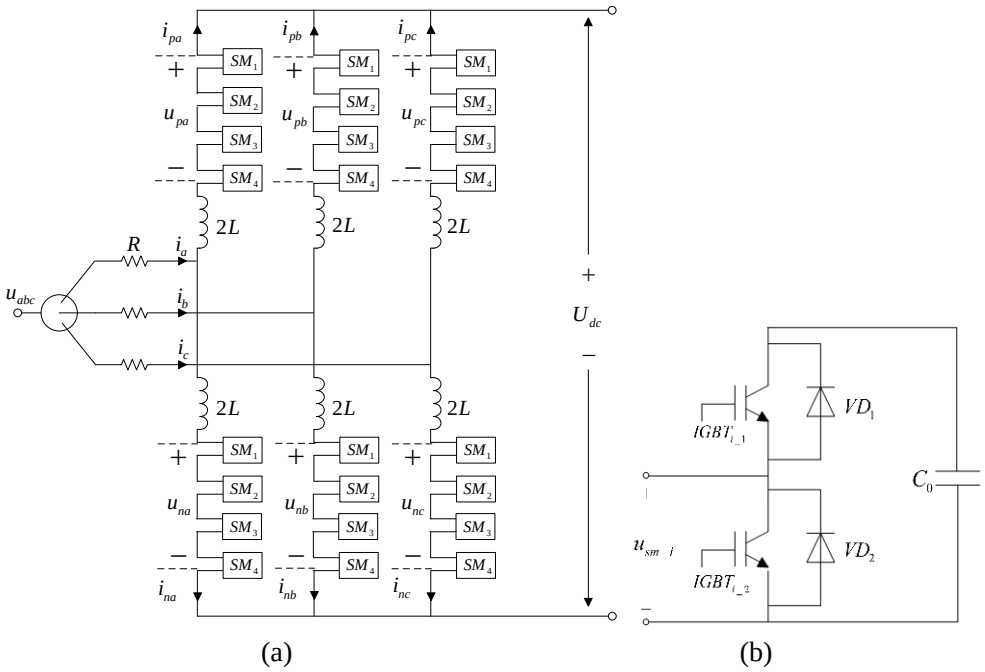

(a) (b)

Figure 2-2 MMC Main Circuit Structure Diagram and Submodule Circuit Structure Diagram

This thesis mainly studies the modular multilevel converter with half bridge module structure. The main circuit structure is shown in figure 2-2 (a). The converter is composed of three-phase commutating bridge arms. Each phase bridge arm is divided into upper and

lower bridge arms, and each bridge arm is composed of N sub-modules. Each submodule consists of two IGBTs, fly-wheel diodes and capacitors, as shown in figure 2-2 (b). By controlling the turn-on and turn-off of the upper and lower IGBTs of each sub-module, the half-bridge sub-module has three working states, namely, latched state, input state, and ablated state.

This thesis studies the true bipolar MMC-MTDC system. The converter stations have the same structure and the positive and negative valve groups in the station are symmetrical. Therefore, the positive valve group of converter station can be selected as the research object. Applying the Kirchhoff's current law to the valve-side AC node of the converter transformer, the phase current can be expressed as the sum of the upper and lower arm currents, as shown in equation (2-1). In the following, k=a,b,c represents three phases.

$$i_k = i_{pk} - i_{nk} \tag{2-1}$$

The Kirchhoff's voltage law is applied to the upper and lower two bridge arms of the three phase units of the MMC converter, and the differential equations can be obtained as

$$2L\frac{di_{pk}}{dt} + 2Ri_{pk} = u_k - (\frac{1}{2}U_{dc} - u_{pk}) \tag{2-2}$$

$$2L\frac{di_{nk}}{dt} + 2Ri_{nk} = u_k - (u_{pk} - \frac{1}{2}U_{dc}) \tag{2-3}$$

Adding equations (2-2) and (2-3) and dividing by 2, and bringing equation (2-1) into the mathematical model of the converter in the three-phase coordinate system

$$L\frac{di_k}{dt} + Ri_k = u_k - v_k \tag{2-4}$$

where, $v_k = (u_{nk} - u_{pk})/2, (k = a,b,c)$.

2.2.2 Control System of Multi-terminal System

According to the current research on MMC-HVDC, the control system can be divided into system level, station level and valve level control. Among them, system level control receives the active and reactive power class command values given by the upper layer, and adjusts the power flow distribution between the converter stations. Station level control realizes fast and stable tracking of DC voltage, active power and reactive power of the converter station through feedback control. Valve level control is the lowest control stage and outputs the trigger pulse signal of the MMC sub-module.

Among them, station level control is the key link of the control system. According to different system control objectives, the appropriate station level control mode is selected to realize the rapid conversion of AC and DC power. According to the traditional MMC vector control principle, the controller can be designed for inner loop and outer loop control. After

the Parker transformation of the equivalent mathematical model of MMC, the P and Q decoupling control is realized by feedforward compensation. There are 8 parameters in the 4 PI regulators of the inner and outer rings that need to be set. It is very difficult to verify the design and dynamic performance of the controller when used in a multi-end system.

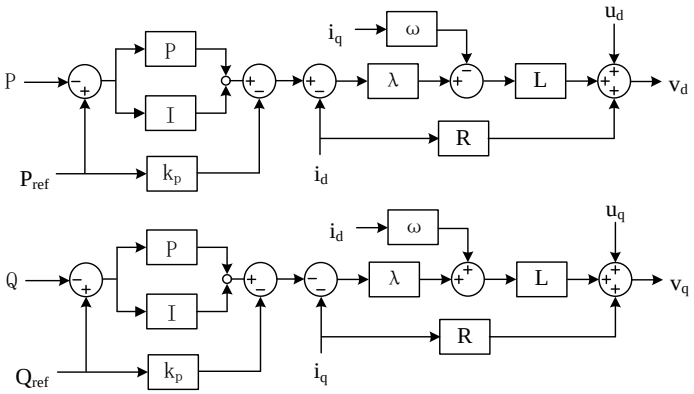

Figure 2-3 Four-terminal MMC System Topology Diagram

According to the new MMC vector control method proposed in reference [31], the control parameter design of multiple converter stations is simplified. The new MMC vector control structure is shown in figure 2-3. The reference power layer controls the active and reactive classes, respectively. In MMC-MTDC system, there is only one converter station control DC side voltage, and the remaining converter stations use active control to regulate the power. Therefore, it is only necessary to select a suitable controllable dynamic parameter λ and a pair of PI regulator parameters to make the MMC fast and no tracking power reference value P_{ref} , Q_{ref} .

When an asymmetrical fault occurs in the multi-terminal system, the MMC controller should suppress the negative-sequence current of the valve side of the converter transformer to avoid the power device current exceeding the limit, so that the MMC can safely pass the AC grid fault period and realize the non-off-line operation. According to the symmetrical component method, the valve side voltage and current can be decomposed into positive sequence component, negative sequence component, and zero sequence component, as shown by equations (2-5) and (2-6),

$$u_k = u_k^+ + u_k^- + u_k^0 \tag{2-5}$$

$$i_k = i_k^+ + i_k^- + i_k^0 \tag{2-6}$$

Taking into account the mathematical equations (2-4) of the converter and the AC side, a simplified mathematical model of the converter station can be obtained,

$$\begin{cases} L\dfrac{di_k^+}{dt} + Ri_k^+ = u_k^+ - v_k^+ \\ L\dfrac{di_k^-}{dt} + Ri_k^- = u_k^- - v_k^- \end{cases} \tag{2-7}$$

The vector control method is applied to transform the mathematical model into the rotating frame, that is, the positive sequence fundamental component is mapped to the coordinate system by the forward rotation frame transformation dq, and the negative sequence fundamental component is mapped to the coordinate system by the inverse rotation frame transformation $d^{-1}q^{-1}$. Let the fundamental frequency of the grid be the initial phase ω, and the above formula can be written as,

$$\begin{aligned}\frac{d}{dt}\begin{bmatrix} i_d^+ \\ i_q^+ \end{bmatrix} &= \begin{bmatrix} -\frac{R}{L} & \omega \\ -\omega & \frac{R}{L} \end{bmatrix}\begin{bmatrix} i_d^+ \\ i_q^+ \end{bmatrix} + \frac{1}{L}\begin{bmatrix} v_d^+ - u_d^+ \\ v_q^+ - u_q^+ \end{bmatrix} \\ \frac{d}{dt}\begin{bmatrix} i_d^- \\ i_q^- \end{bmatrix} &= \begin{bmatrix} -\frac{R}{L} & -\omega \\ \omega & \frac{R}{L} \end{bmatrix}\begin{bmatrix} i_d^- \\ i_q^- \end{bmatrix} + \frac{1}{L}\begin{bmatrix} v_d^- - u_d^- \\ v_q^- - u_q^- \end{bmatrix}\end{aligned} \tag{2-8}$$

Next, using dynamic variable linear transformation, input non-singular transformation and state feedback transformation to achieve system decoupling. First construct a new input χ, and introduce state feedback transformation matrix and input non-singular matrix, which will give the following formula,

$$\begin{aligned}\frac{d}{dt}\begin{bmatrix} i_d^+ \\ i_q^+ \end{bmatrix} &= \begin{bmatrix} -\lambda & 0 \\ 0 & -\lambda \end{bmatrix}\begin{bmatrix} i_d^+ \\ i_q^+ \end{bmatrix} + \frac{2\lambda}{3(u_d^2+u_q^2)}\begin{bmatrix} u_d^+ & u_q^+ \\ u_q^+ & -u_d^+ \end{bmatrix}\begin{bmatrix} \chi_d^+ \\ \chi_q^+ \end{bmatrix} \\ \frac{d}{dt}\begin{bmatrix} i_d^- \\ i_q^- \end{bmatrix} &= \begin{bmatrix} -\lambda & 0 \\ 0 & -\lambda \end{bmatrix}\begin{bmatrix} i_d^- \\ i_q^- \end{bmatrix} + \frac{2\lambda}{3(u_d^2+u_q^2)}\begin{bmatrix} u_d^- & u_q^- \\ u_q^- & -u_d^- \end{bmatrix}\begin{bmatrix} \chi_d^- \\ \chi_q^- \end{bmatrix}\end{aligned} \tag{2-9}$$

The purpose of the controller in the asymmetric fault of the AC grid is to suppress the negative-sequence current of the valve side and avoid the current limit of the power device. Therefore, in the input command of the inner loop control, the negative sequence command χ_d^- and χ_q^- are directly taken to zero to eliminate the valve side negative sequence current component, and the positive sequence component of the active power and the reactive power can be expressed as follows,

$$\begin{bmatrix} P \\ Q \end{bmatrix} = \frac{3}{2}\begin{bmatrix} u_d^+ & u_q^+ \\ u_q^+ & -u_d^+ \end{bmatrix}\begin{bmatrix} i_d^+ \\ i_q^+ \end{bmatrix} \tag{2-10}$$

The converter transformer adopts the Y/△ or △/Y connection method to isolate the zero-sequence component of the grid side voltage, and only the positive sequence and the negative sequence component are transmitted to the converter valve side. Therefore, zero sequence component can be disregarded in this case. By performing the Laplace transform on the equation (2-9), the frequency domain form of the positive and negative sequence fundamental components under dq frame can be obtained, and finally the actual control

variable command value is obtained. At this point, a block diagram of the controller model including the negative sequence control of the converter station can be obtained, as shown in figure 2-4.

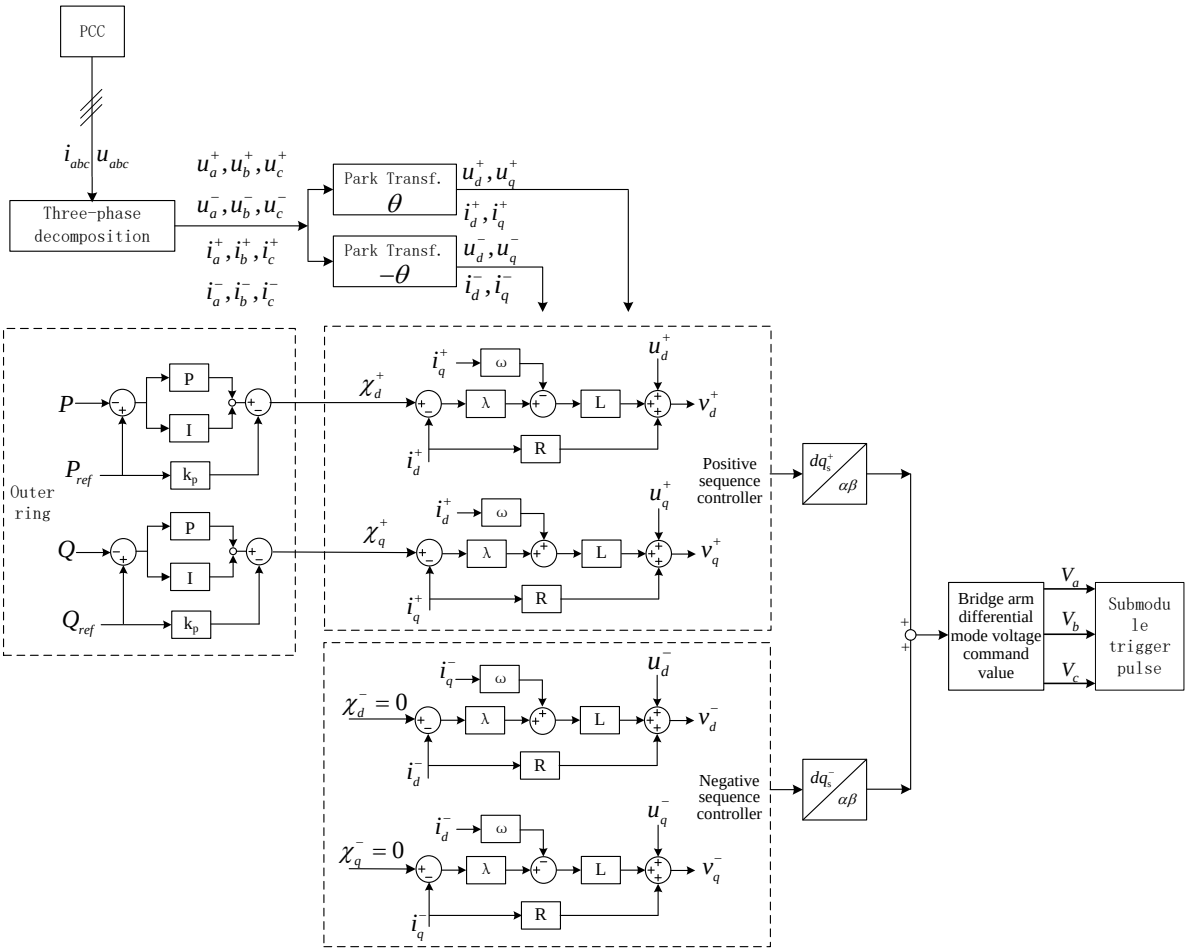

Figure 2-4 MMC Overall Control Block Diagram for AC Grid Asymmetry Fault

In this thesis the decomposition method based on phase-locked loop synchronization technology is used to transform three sequence components in equations (2-5) and (2-6) from *abc* reference frame to *dq* rotating frame. The positive and negative sequence components are obtained by the new vector decoupling controller, and the differential mode voltages of the bridges of the positive and negative sequence components in the *dq* axis are obtained, and then the positive and negative sequence components obtained by the Antipark transformation are superposed to obtain the differential mode voltage command value V_a, V_b, V_c. Finally, according to the voltage command value of each bridge arm, the trigger pulses of each sub-module of MMC are adjusted to realize the control of the converter.

2.3 Equipment Model of MMC-MTDC System

2.3.1 Electromagnetic Transient Model of Flexible DC Converter Valve

When the number of sub-modules of MMC is greater than 30, the detailed sub-module modeling can be very complicated, and a large number of capacitors and switching components can greatly reduce the simulation speed of the running model. The number of sub-modules of practical MMC project is increasing due to the demand for the transmission capacity. Therefore, the research on the simulation modeling of the large-capacity MMC-HVDC is not suitable for the detailed model. Many scholars have proposed a variety of MMC speed-up models for the slow PSCAD simulation, including the average model, the Thevenin equivalent model, etc. [32] Although the simulation speed of the average model is faster than the Thevenin equivalent model, the charging and discharging process cannot be accurately reflected in overvoltage simulation. The simulation speed of the Thevenin equivalent model is between the average model and the detailed model, and its simulation accuracy is also higher than the average model. It has a very wide range of applications [33].

The equivalent circuit of the sub-module of MMC is shown in figure 2-5 (a). The equivalent circuit of N sub-modules of each bridge arm can be connected in series to obtain the Thevenin equivalent model of the bridge arm, as shown in figure 2-5 (b). T_{sm} and V_{sm} are the trigger signals input to the N submodules of the bridge arm and the capacitor voltages output by the N submodules, respectively. By this simplification, the working state of converter can be simulated.

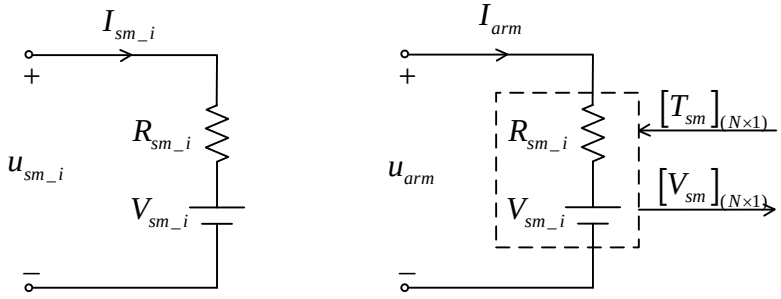

(a) Sub-module (b) Bridge Arm

Figure 2-5 Sub-module and Bridge Arm Thevenin Equivalent Circuit

2.3.2 Model of High Voltage Hybrid DC Circuit Breaker

When the sub-module is blocked after a ground fault, there is still a faulty flow path, so the half-bridge sub-module has no fault isolation and clearance capability. In order to solve the problem that the MMC cannot clear the DC fault, the solution chosen is to configure the DC breaker on the valve side of the smoothing reactor. Therefore, each converter station is equipped with four DC circuit breakers on the positive and negative DC lines, and the breaker is selectively disconnected to achieve rapid removal of the fault line and to ensure continuous power supply to other parts of the multi-terminal system. The full-bridge hybrid

structure of the high-voltage DC circuit breaker is shown in figure 2-6.

The DC circuit breaker has three branches: the main branch routes a small number of full-bridge auxiliary switch IGBT modules and a set of fast mechanical switches; the transfer branch routes a large number of power electronic modules with the same parameters of IGBTs in series; energy consumption branch is composed of metal oxide arresters with the same parameters, and each arrester is connected in parallel with each power electronic module of the transfer branch.

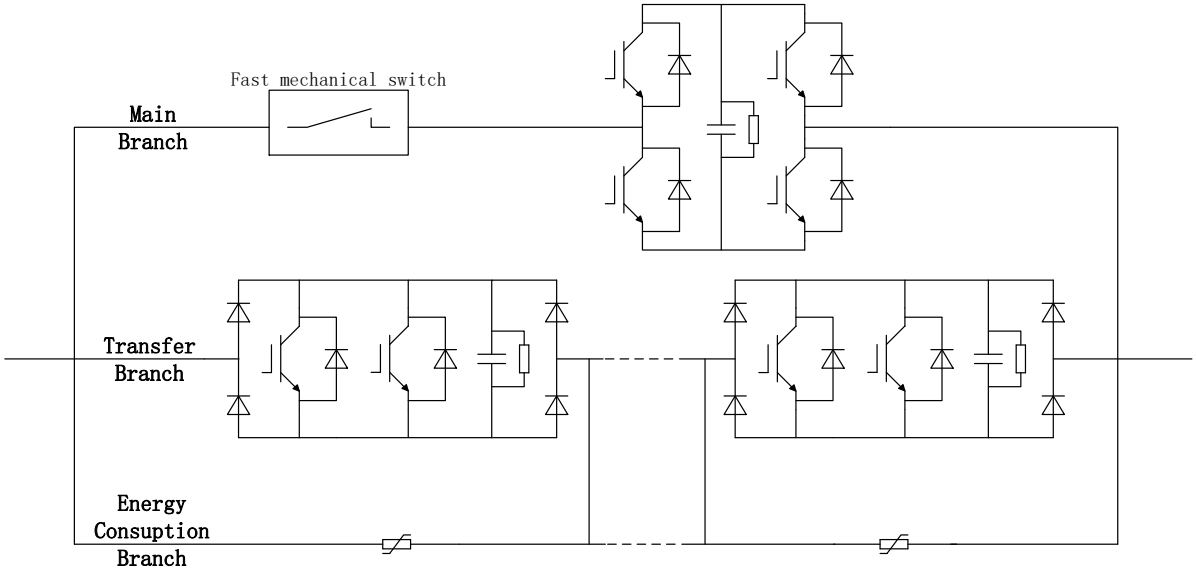

Figure 2-6 Structure of Full-bridge High Voltage Hybrid DC Circuit Breaker

The hybrid DC circuit breaker has four working modes. The equivalent circuit structure and current mode of each mode are shown in figure 2-7. In order to simplify the circuit structure of the DC circuit breaker, we only show one module of the main branch, the transfer branch and the energy-consuming branch.

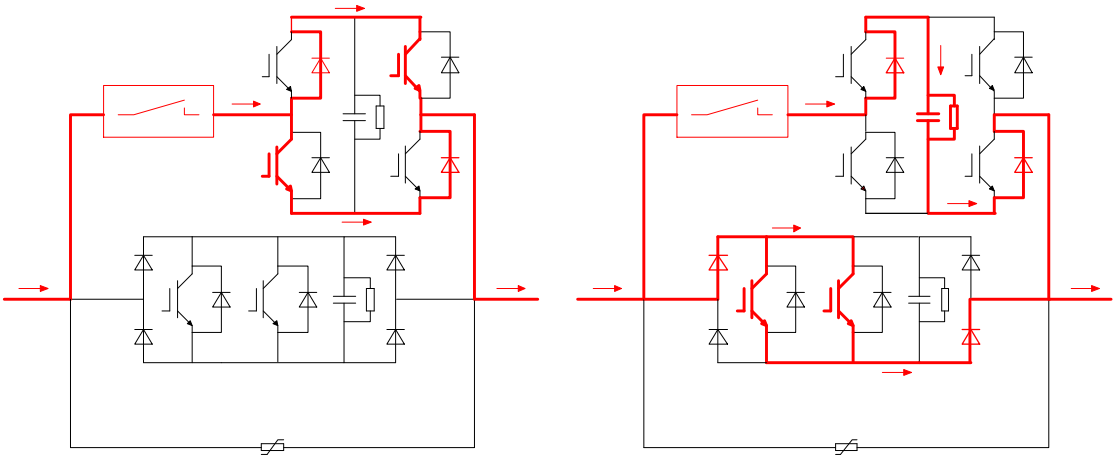

(a) Normal Work Mode

(b) Fault Current Limiting Mode

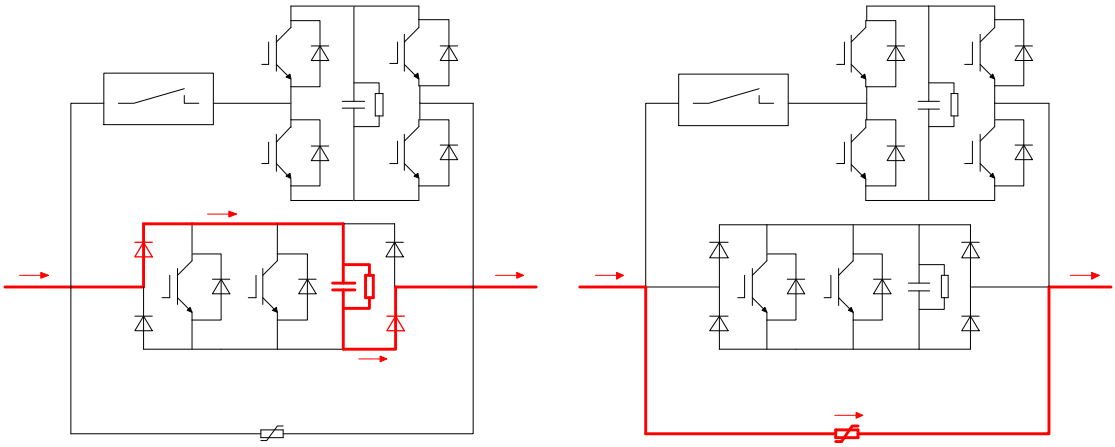

(c) Fault Break Mode (d) Arrester Absorbs Energy Mode

Figure 2-7 Full-bridge Hybrid DC Circuit Breaker Working Mode

Normal working mode: The fast mechanic switch is closed, the IGBT in the main branch power electronic module is turned on at the same time, and the IGBT in the branch power electronic module is turned off at the same time. In this mode of operation, the main branch impedance is less than the transfer branch impedance and current flows through the main branch.

Fault current limiting mode: When a fault is detected, the transfer branch IGBT is turned on at the same time, and the branch circuit resistance is reduced. When the main branch IGBT is turned off at the same time, the resistance of the main branch is large so that the current starts to transfer from the main branch to the transfer branch.

Fault open mode: When the main branch current drops to 0, the current flows only through the IGBT and diode of the transfer branch, at which point the fast mechanic switch of the main branch is opened. At the same time, all the IGBT modules of the transfer branch are blocked, and the fault current starts to charge the capacitance of the transfer branch.

Arrester absorbs energy mode: When the branch capacitor voltage reaches the operating voltage of arrester, the current mainly flows through the energy consuming branch.

2.3.3 Broadband Model of Equipment

In the simulation of lightning overvoltage, the lightning wave front time and half-wave time are in the microsecond level, and the overvoltage results obtained by the conventional converter station equipment model are not accurate enough. Therefore, the broadband characteristics should be considered when modeling the converter station equipment [34,35].

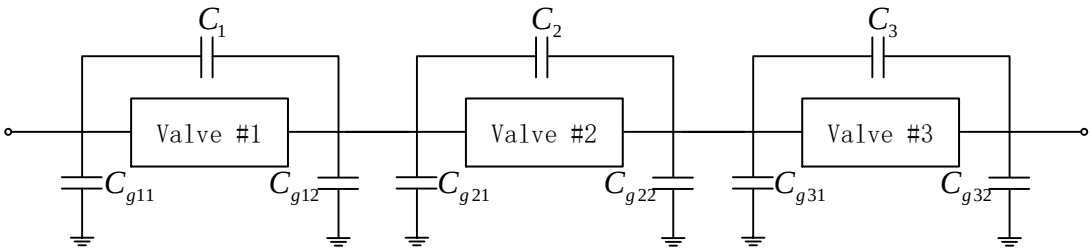

(a) Valve Tower and Port Capacitance Equivalent Model

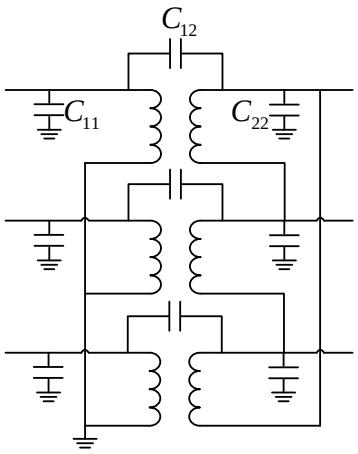

(b) Converter Transformer

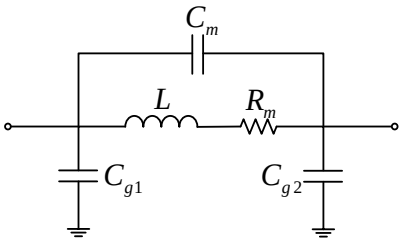

(c) Reactor

Figure 2-8 Broadband Model of Equipment

The broadband model of the converter valve mainly considers the parasitic capacitance of the shield. In reference [36], the two-port stray capacitance extraction method is used to simplify the complex parasitic capacitance into the equivalent model of the valve tower and port capacitance, as shown in figure 2-8(a). The broadband model of the converter transformer, smoothing reactor and neutral line reactance is shown in figure 2-8 (b)(c). The broadband model of the converter transformer considers the ground stray capacitance of the primary and secondary windings and the parasitic capacitance between two sides. The stray parameters should be derived from the 500kV converter transformer used in the actual project. The broadband model of the reactor considers the capacitance of the two sides to ground and the capacitance and loss resistance between the windings. The selection of these parameters should be based on the measured data of the equipment used in the practical project.

It is necessary to consider the lightning strike simulation of the six towers in the inlet section of the converter station, so we adopt the appropriate transmission line model and tower model. The overhead transmission line model considers the distribution parameters using the frequency correlation model of PSCAD. The tower model uses a more realistic multi-wave impedance model, [37] as shown in figure 2-9.

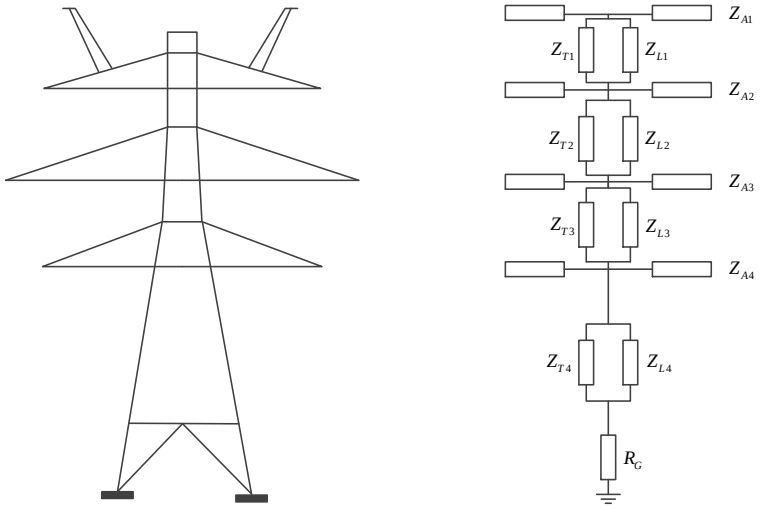

(a) Tower Geometry (b) Multi-wave Impedance Equivalent Model of Tower

Figure 2-9 Tower Model

2.4 Modeling and Simulation Verification of MMC-MTDC System

Taking the ±500kV Zhangbei project as an example, the overvoltage characteristics of MMC-MTDC and the design principle of insulation level are analyzed by PSCAD simulation modeling. This section mainly analyzes the modeling part of the Zhangbei demonstration project and the dynamic response of the simulation model.

2.4.1 Modeling of MMC-MTDC System

The access points for the Zhangbei four-end demonstration project are Zhangbei, Kangbao, Beijing and Fengning. The four converter stations are connected by a ring network, and the middle is connected by overhead lines. In the field of high-voltage and large-capacity, the DC project generally adopts a symmetrical bipolar structure to improve reliability. A simulation model of a four-terminal MMC-HVDC transmission system is built in PSCAD/EMTDC, as shown in figure 2-10.

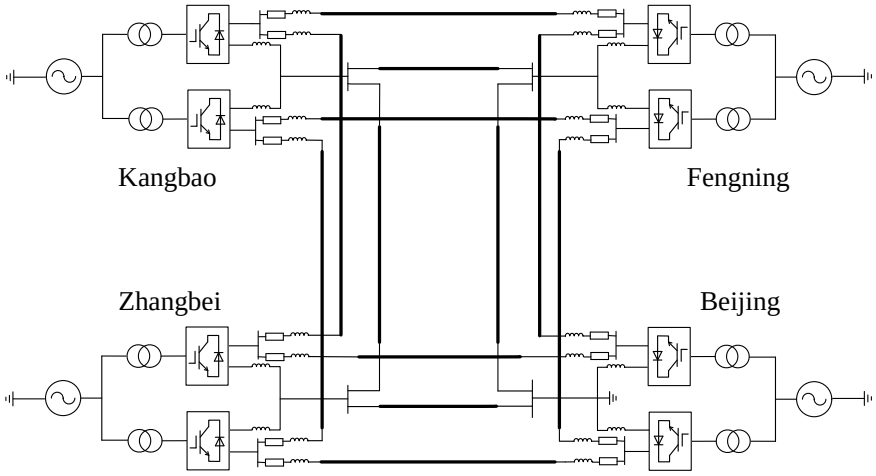

Figure 2-10 Schematic Diagram of Four-terminal MMC-HVDC System

The MMC converter station adopts a modular multilevel converter composed of half bridge modules. The main equipment parameters of the converter station are shown in table 2-1. Among them, the entrance section of Beijing Station is a double-return transmission line, the entrance section of other converter stations is a single transmission line, the AC side of Fengning and Beijing stations are connected to the local 500kV grid, and the AC side of Kangbao and Zhangbei Station is connected to the local 220kV. The grid has a DC side voltage of ±500kV.

Table 2-1Main Equipment Parameters

Equipment	Beijing	Fengning	Kangbao	Zhangbei
Submodule Capacitor/mF	15	8	8	15
Number of Submodules	244	244	244	244
IGBT Parameters	4.5kV/3kA	4.5kV/2kA	4.5kV/2kA	4.5kV/3kA
Capacity /MW	3000	1500	1500	3000
Arm Reactor/mH	75	100	100	75
Line Reactor/mH	150	150	150	150
Neutral Line Reactor/mH	300	300	300	300

2.4.2 Analysis of Model Dynamic Response

In order to verify the validity of the electromagnetic transient model, the dynamic response verification analysis of the four-terminal model is carried out. This section mainly consists of three dynamic response check models: the power step, the negative of the converter station, and the DC voltage step. The active power and DC voltage step response of the four-terminal system is shown in figure 2-11.

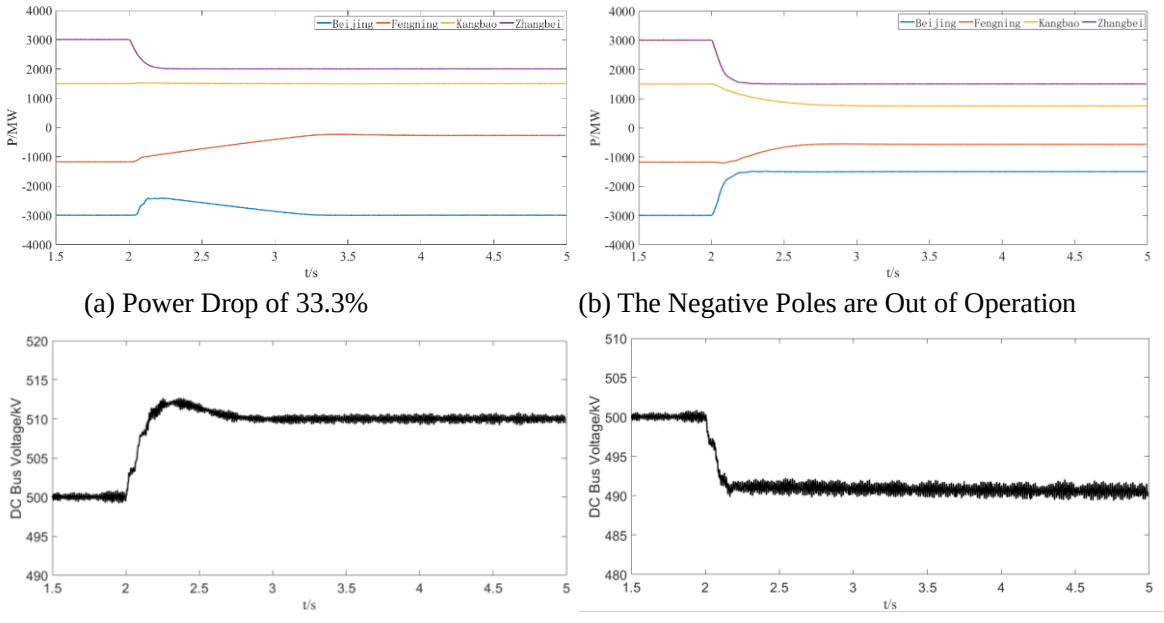

(a) Power Drop of 33.3%

(b) The Negative Poles are Out of Operation

(c) DC Voltage Command Rises 2%

(d) DC Voltage Command Drops 2%

Figure 2-11 Active Power and DC Voltage Step Response Diagram

It can be seen from the DC voltage step diagram that the DC voltage controller has fast response speed and small overshoot. From the active power dynamic response step diagram, the power of the PCC point can quickly track the reference value, and the power of other converter stations will be adjusted together with the power step station to achieve stable operation of the entire system. Table 2-2 summarizes several measured values of four dynamic step response times. The response time of active power step change does not exceed 376ms, the system stabilization time is less than 2235ms, and the overshoot is less than 6.0%. When DC voltage command value rises or falls 2%, the response time does not exceed 169ms, the overshoot is less than 2.5%, and the four-terminal system resumes stable operation within 1326ms, thus verifying the validity of the PSCAD model.

Table 2-2 Multi-terminal System Dynamic Response Time Measurement

Step Test	Response Time /ms	Overshoot /%	Settling Time /ms
Power Drop of 33.3%	320	2.7	2109
Negative Poles Out of Operation	376	6.0	2235
DC Voltage Rises 2%	169	2.5	1205
DC Voltage Drops 2%	165	2.0	1326

2.5 Brief Summary

This chapter introduces in detail the topology of MMC-MTDC system, the mathematical model of the converter station, the key equipment model of the converter station and the modeling and model verification of MMC-MTDC system. Firstly, the mathematical model of the flexible converter is obtained by mathematical formula derivation, and then the controller of the converter station stage is designed by considering the positive and negative sequence control. Then the key equipment model of the converter station is introduced in combination with the working principle and circuit topology. DC converter valve with Thevenin equivalent model, hybrid high-voltage DC circuit breaker, converter transformer, reactor, and tower model for lightning intruding wave simulation. Finally, relying on Zhangbei project, the MMC-MTDC grid was modeled by PSCAD electromagnetic transient simulation software and the dynamic response of the model was verified, which laid a foundation for subsequent overvoltage analysis.

3 Overvoltage Characteristic Analysis of Converter Station in MMC-MTDC

3.1 Switching Overvoltage Analysis in MMC-MTDC

The switching overvoltage experienced by the flexible DC converter station studied in this thesis is mainly caused by system failure and the operation of the control and protection system. This section takes the typical fault of MMC-MTDC system as an example to simulate and calculate the DC circuit breaker action, the grid operation mode, the AC side fault and the influence of the control protection system on the overvoltage in the multi-terminal converter station.

3.1.1 Fault Type of the Converter Station and Protection Action Sequence

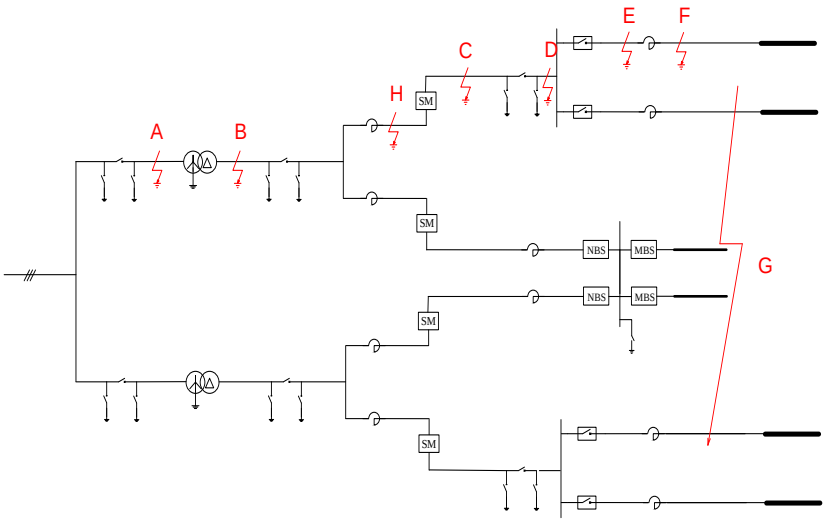

Figure 3-1 Fault Set Point of Converter Station

This section revolves around the effect of DC breaker action on the switching overvoltage in the station after a converter station failure. According to the division of the converter station area, eight position faults are shown in figure 3-1. And for details, see table 3-1.

DC system protection can quickly remove short-circuit faults or improperly operating equipment in the system to prevent damage or interfere with normal operation of other parts of the system. The control and protection strategies of different faults are different. The action and timing of the control and protection system after different positions of the converter station are given below.

When the AC side fails, the converter station protection system starts to operate, that is, the

faulty valve group is locked, AC circuit breaker trips to cut off the fault, and the faulty pole DC circuit breaker and the metal return line switch are tripped to achieve pole isolation.

Table 3-1 Typical Failure of Zhangbei Flexible DC Converter Station

Region	Fault Location	Fault Type
AC Side	A	Four metal ground faults on the AC grid side
	B	Four metal ground faults on the valve side
Converter Station	H	Ground fault on the arm reactance valve side
	C	Ground fault on the valve top
	D	DC bus ground fault
	E	Ground fault between DC circuit breaker and smoothing reactor
DC overhead line	F	Single ground fault on DC line
	G	Bipolar short circuit fault

When the fault occurs in the converter station, the faulty valve group is blocked, AC circuit breaker is tripped to cut off the fault, and at the same time, the metal return switch of the fault pole and the two DC breakers are tripped to achieve pole isolation. Since the fault arc of the fault point in the converter station cannot be extinguished due to the existence of the freewheeling action of the bridge arm reactor, the DC circuit breaker cannot be restarted, and the fault pole is permanently turned into a chain operation mode after the fault.

When the DC line is faulty, the DC circuit breakers at both ends of the faulty line are tripped to clear the fault, and all the converter stations are not locked and do not exit. The DC circuit breaker performs the reclosing operation after the de-free time. If the fault has not disappeared, it is opened again to clear the fault. It should be noted that the DC breaker has no secondary reclosing operation.

The focus of fault analysis is on the switching overvoltage amplitude at the insulation location, which also lays the foundation for the subsequent insulation coordination of the converter station and the study of the insulation level of important equipment. The insulation position of MMC mainly involves two aspects. First, the bracket structure of the valve tower is insulated from the ground (bracket insulation), followed by insulation between the outlet terminals of the valve tower (inter-terminal insulation). For important equipment in the converter station, the ground voltage and the terminal voltage at both ends of the equipment need to be considered separately. The switching overvoltage of the equipment takes the extreme values of the three voltages.

3.1.2 Effect of DC Circuit Breaker Action on Switching Overvoltage

This section focuses on the typical faults of the system, considering that the DC grid is in normal bipolar operation and four converter stations form a four-wire ring network.

According to the control and protection strategy of the grid, the switching overvoltage of the converter station caused by the action of the DC breaker is studied.

1）DC line failure

（1）Single pole ground fault

The single pole ground fault is simulated by taking a permanent ground fault on the side of the Kangbao-Fengning line as an example. After the fault occurred for 6ms, the two circuit breakers on the positive line connected to the Kangning station and Fengning Station cut off the line. After 300ms, the reclosing switch was started. After 6ms, the fault was detected again and the line isolation fault was removed again. The simulation results of overvoltage caused by DC line single pole ground fault under DC circuit breaker are shown in figure 3-2.

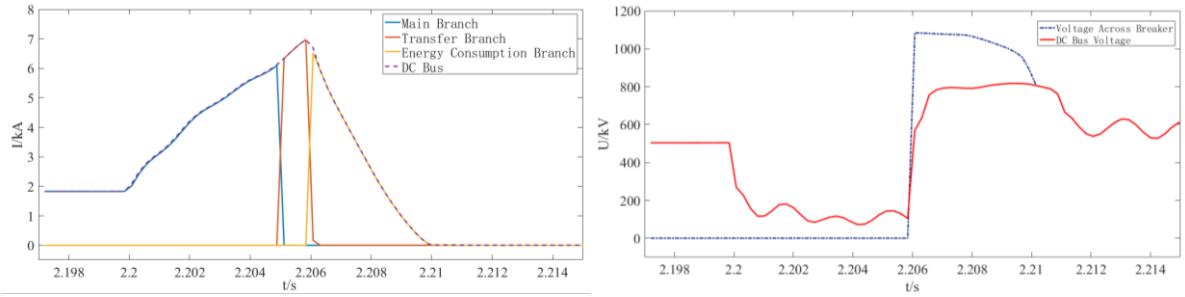

(a) Effect of Circuit Breaker on Fault Current (b) Effect of the Circuit Breaker on the Voltage

Figure 3-2 Effect of Single pole Fault DC Circuit Breaker Action on Current and Voltage

Figure 3-2 (a) shows the effect of the DC circuit breaker on the fault current, and figure 3-2 (b) shows the DC circuit breaker switching overvoltage simulation waveform. It can be seen that during the first commutation of the DC breaker, the voltage across the DC breaker is basically zero, and the system fault current cannot be limited. During the second commutation of the DC breaker, the voltage across the DC breaker rapidly rises until the short-circuit current and energy are consumed after reaching the operating voltage of the energy consuming branch arrester. It can be seen that the peak DC circuit breaker switching overvoltage occurs at the beginning of the energy consumption mode, so this has a significant relationship with the arrester characteristics of the energy consuming branch.

The peak value of the fault current during the opening of the DC circuit breaker reaches 6.97kA, and the peak voltage at both ends of the circuit breaker reaches 1084kV. When the circuit breaker completely consumes the fault current, the voltage at both ends gradually decreases and is clamped at 500kV by the system voltage. When the DC circuit breaker is opened, the overvoltage of the fault pole is 816kV. Because of the inter-electrode coupling between the normal pole and the fault pole, an overvoltage of 781kV will be induced at the normal pole. Calculate the switching overvoltage level generated by the DC circuit breaker opening and reclosing operation of the Zhangbei demonstration project at the DC pole line, and obtain the overvoltage level of each converter station opening and reclosing as shown in

table 3-2.

Table 3-2 DC Bus Switching Overvoltage after Single Pole Ground Fault

Converter Station	DC Circuit Breaker Opening		DC Circuit Breaker Reclosing	
	U/kV	*U*/p.u.	*U*/kV	*U*/p.u.
Beijing	793	1.48	740	1.38
Fengning	796	1.49	773	1.45
Kangbao	816	1.53	767	1.43
Zhangbei	822	1.54	760	1.42

After the DC single pole ground fault, the DC circuit breaker opening switching overvoltage is greater than the reclosing switching overvoltage. The largest opening overvoltage occurred in the Zhangbei-Beijing line, which was 1.54p.u, while the largest reclosing overvoltage was generated in the Fengning-Beijing line, which was 1.45p.u.

（2）Bipolar short circuit fault

The bipolar short-circuit fault is simulated by the Kangbao station-Fengning line. 6ms after the fault, the four circuit breakers on the positive and negative lines connected to the Kangning station and Fengning Station cut off the line. After 300ms, the recloser is started to recover the line. After 6ms, the fault is detected again and the line isolation fault is removed again. The current and voltage simulation waveforms caused by DC circuit breaker operation are shown in figure 3-3.

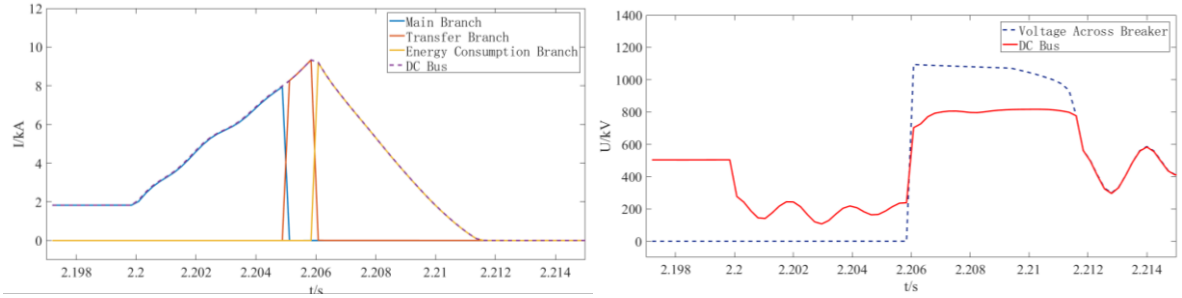

(a) Effect of Circuit Breaker on Fault Current (b) Effect of the Circuit Breaker on the Voltage

Figure 3-3 Effect of Bipolar Short Circuit Fault DC Circuit Breaker Action on Current and Voltage

According to the symmetry of the positive and negative poles of the DC grid, the positive and negative bipolar short circuit faults can be regarded as two single pole ground faults with smaller grounding resistance at the fault point. Therefore, overvoltage and current of bipolar short circuit fault is greater than that of single pole. It can be seen from the simulation waveform that the DC circuit breaker cuts the fault line similarly to the single pole ground fault, but the time that the bipolar short circuit fault consumes the fault current is 0.018 s longer than the time required for the unipolar. The peak value of the fault current during the tripping of the DC circuit breaker reaches 9.33kA, and the peak voltage across the circuit breaker reaches 1094kV. When the circuit breaker completely consumes the fault current, the

voltage at both ends of the circuit breaker gradually drops and is clamped at 500kV by the system voltage. The overvoltage of the DC bus reaches 820kV when the breaker is opened.

2）Ground fault between DC circuit breaker and smoothing reactor

The circuit breaker and the anti-indirect fault are simulated by the Kangbao station-Fengning line as an example. The protection system protects against such faults in a similar manner to a DC line single pole ground fault. When the system detects such faults, it issues a trip command to the two circuit breakers on the fault line. Figure 3-4 shows the voltage waveform of this fault and single pole ground fault.

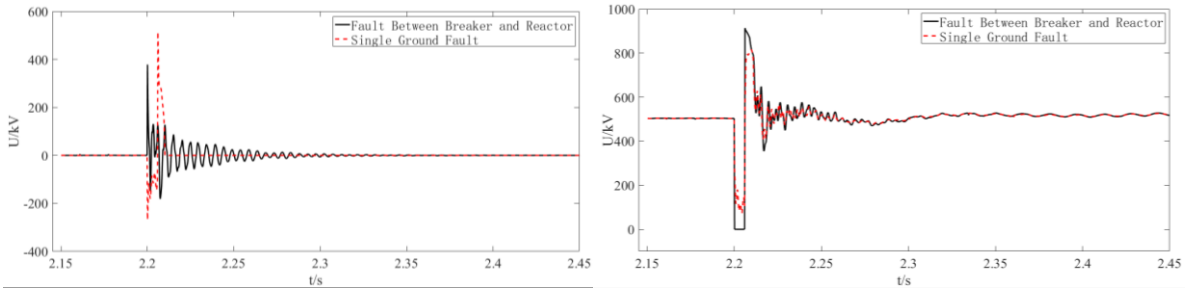

(a) Comparison of Voltage across Reactor (b) Comparison of DC Bus Voltage

Figure 3-4 Overvoltage Comparison of Critical Fault Locations in Two Fault Systems

It can be seen from the above figure that when a ground fault occurs between the circuit breaker and the smoothing reactor, the DC bus voltage drops to zero instantaneously, and the presence of the fault current causes a voltage of 378 kV to be induced across the smoothing reactor. The action of the positive DC circuit breaker raises the DC bus voltage to 913kV, and the voltage across the smoothing reactor fluctuates. Comparing the two faults, the voltage induced by the single pole ground fault at the DC bus is 816kV, which is much lower than the ground fault on the smoothing reactor side. This is because when the fault point is on the smoothing reactor line side, the smoothing reactor can protect the device on the valve side by limiting the rate of current change caused by the rapid voltage change.

3）DC Bus ground fault

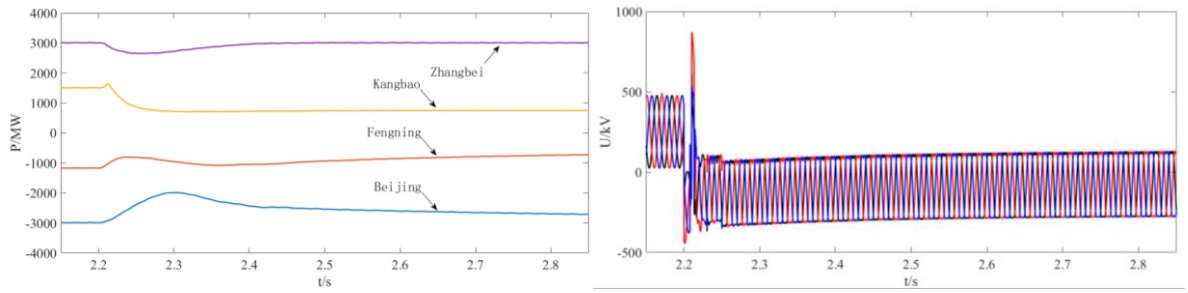

(a) Power of Four-terminal Converter Station (b) Switching Overvoltage of Valve Side

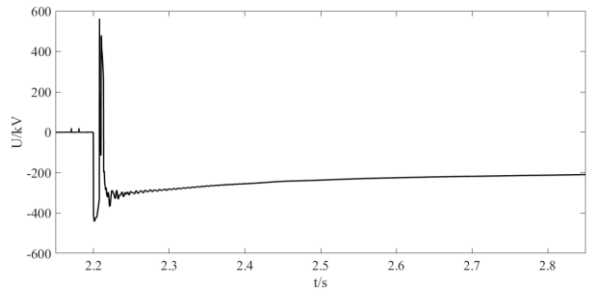

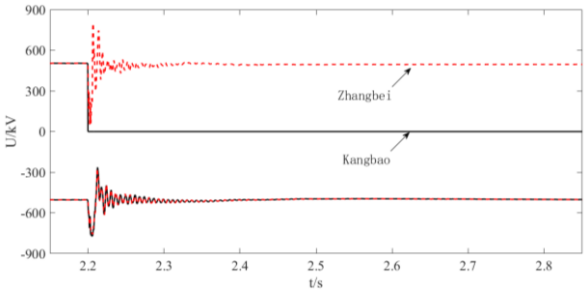

(c) Neutral Bus Switching Voltage of Fault Station (d) DC Bus Overvoltage Comparison

Figure 3-5 Transient Process of DC Bus Ground Fault

The DC bus of the converter station is connected to the lines of two adjacent converter stations. When the DC bus has a ground fault, two fault lines need to be tripped. Moreover, the fault of the converter station needs to be quickly blocked to prevent the impact current from damaging the converter valve. The freewheeling action of the bridge arm reactor makes the fault current drop very slowly, and the fault arc cannot be extinguished in a short time, so the reclosing operation is not performed after the DC breaker is operated.

Take Kangbao Station as an example for simulation analysis. After the DC bus has a ground fault, the two DC breakers on the positive side of the Kangbao station and the two circuit breakers on the opposite side of the line cut off the two lines. The positive valve of the converter valve is blocked and extremely isolated, the positive DC bus is fast switching, and the AC breaker on the converter side is disconnected. The transient process of this type of fault is shown in figure 3-5.

The faulty pole valve locking and pole isolation operation produces significant overvoltage at the system electrical nodes such as the neutral busbar, the converter valve and the converter transformer valve side of the converter station. After the DC circuit breaker is cut off, the output power of the Kangbao station is halved. Other converter stations adjust the positive and negative pole power through the slope control curve to maintain the grid power balance. Comparing the faulty station and unfaulty station DC bus voltage, the switching overvoltage level of the unfaulty station is slightly higher than that of the faulty station, so the switching overvoltage generated on the unfaulty station cannot be ignored.

4）Valve top ground fault

A DC bus fast switch is arranged between the valve top and the DC bus, so the protection methods after the ground faults are similar in these two places. The difference is that the DC bus grounding fault relies on the DC bus fast switch to isolate the valve and the fault point, and the DC bus fast switch does not need to be operated after the valve top ground fault. Figure 3-6 shows the transient process of the valve top overvoltage under these two faults. It can be seen that the rapid switching action of the DC bus will generate a large overvoltage at the top of the converter valve, and voltage fluctuations will also occur at the unfaulty pole.

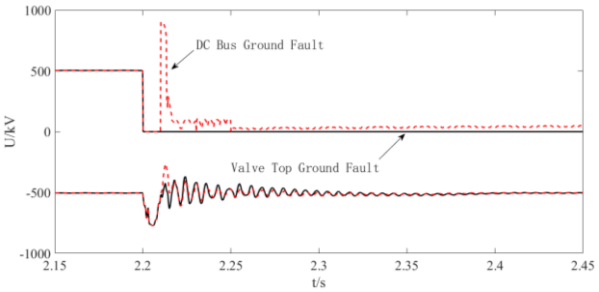

Figure 3-6 Valve Top Overvoltage Transient Process under Two Faults

5）Valve ground fault

The grounding fault of the valve bottom is set on the side of the A-phase bridge arm of the valve group on the positive pole of the converter station, and the Kangbao station is taken as an example for simulation analysis. After the fault, the two DC circuit breakers of the positive pole act, the positive valve block of the converter valve is blocked and pole-isolated, and the AC circuit breaker on the valve side is tripped.

The overvoltage of the key node of the converter station when the valve bottom is grounded is shown in figure 3-7. After the fault occurs, the voltage at the bottom of the fault phase falls to zero. The voltage of the unfaulty phase rises due to the modulation of the control system, causing an overvoltage at the DC side voltage fluctuation. The faults occurring in the converter station are generally permanent faults, regardless of the case of the circuit breaker reclosing. The switching overvoltage at both ends of the faulty phase bridge arm occurs at the moment when the converter valve is blocked and the converter valve side breaker is actuated. The two switching overvoltage of the faulty DC bus are derived from the action of the DC breaker and the AC breaker.

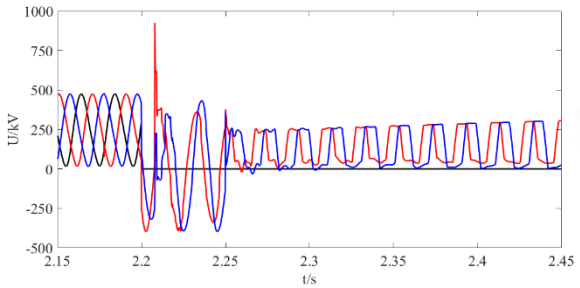

(a) Valve Side Voltage of Three-phase Bridge Arm Reactor

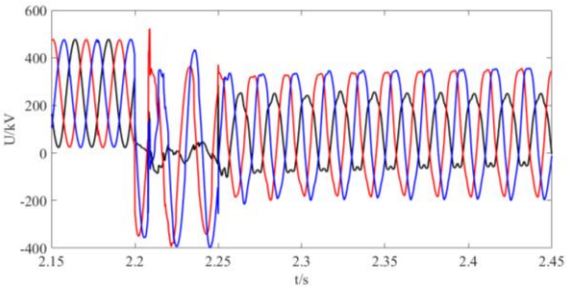

(b) Valve Side Voltage of Transformer

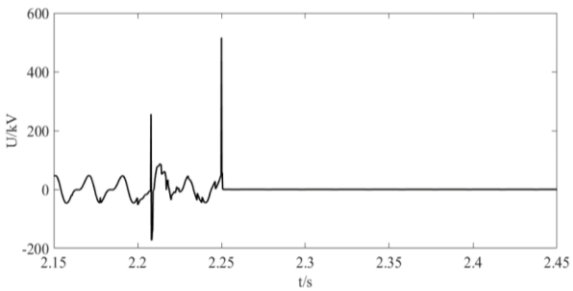

(c) Overvoltage across Faulty Phase Arm Reactor

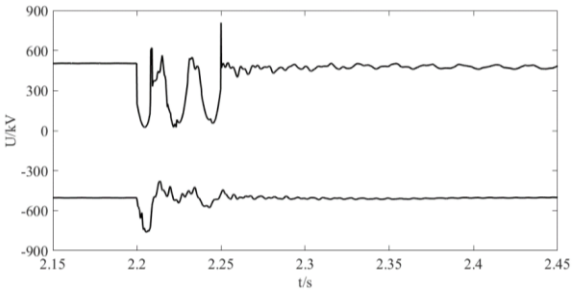

(d) DC Bus Voltage of Transmission Line

Figure 3-7 Switching Overvoltage of Valve Ground Fault

6）Converter valve side failure

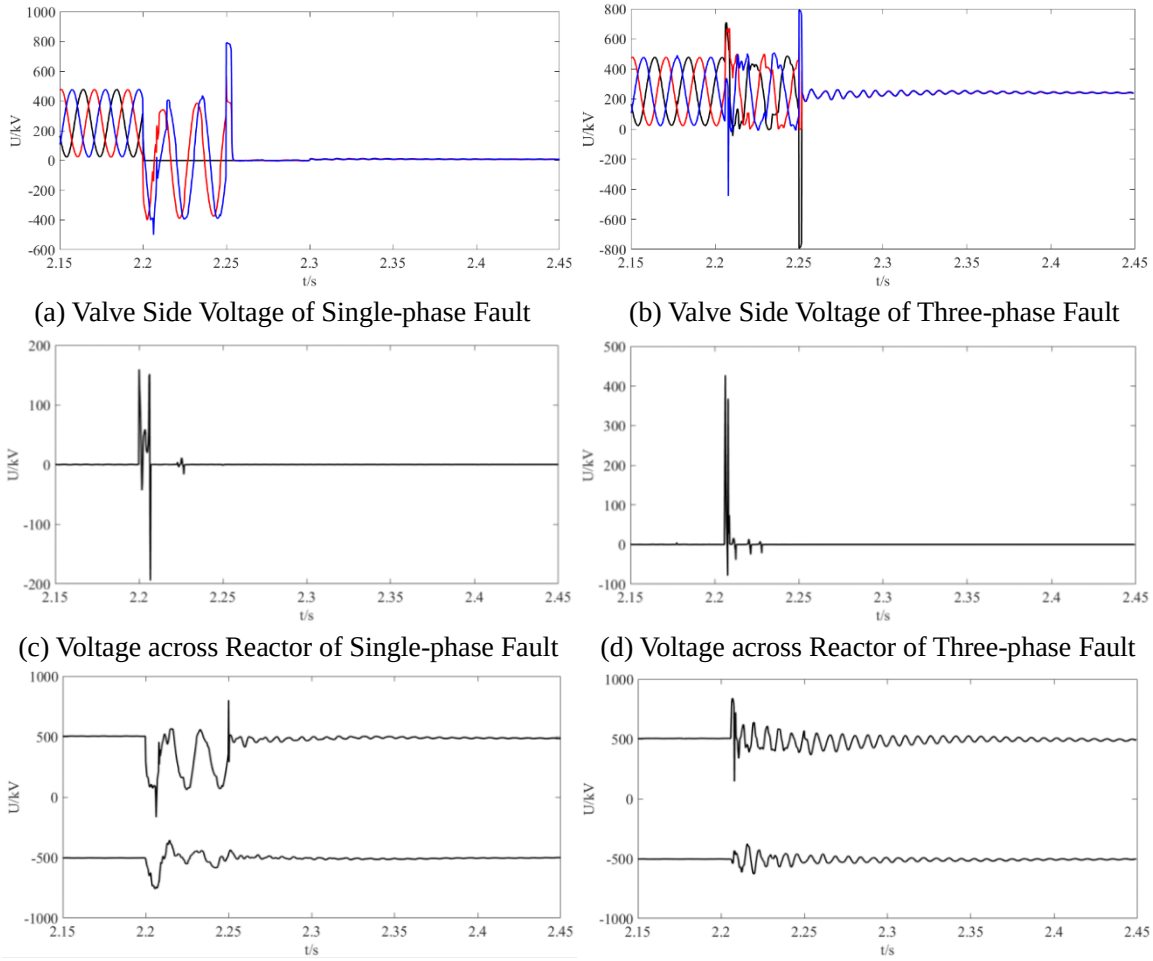

(a) Valve Side Voltage of Single-phase Fault (b) Valve Side Voltage of Three-phase Fault

(c) Voltage across Reactor of Single-phase Fault (d) Voltage across Reactor of Three-phase Fault

(e) DC Bus Voltage of Single-phase Fault (f) DC Bus Voltage of Three-phase Fault

Figure 3-8 System Switching Overvoltage after Converter Valve Side Failure

Four kinds of metallic ground faults are considered in the fault of the converter valve side. In order to prevent the fault current from being transmitted through the metal return line DC line to generate a large overvoltage affecting the unfaulty converter station, an action command should be issued to the DC breaker immediately. The faulty valve is locked and pole isolated, and the AC breaker on the grid side and the valve side is isolated to malfunction. Taking Kangbao Station as an example, figure 3-8 shows the overvoltage characteristics of key nodes in single-phase grounding and three-phase grounding faults.

Through the fault simulation calculations at the four converter stations, the critical nodes of the MMC-MTDC grid converter station and the switching overvoltage deterministic faults between the important equipment terminals are shown in table 3-3. The decisive faults in which the DC circuit breaker operates overvoltage include DC line bipolar short circuit fault, found fault between circuit breaker and smoothing reactor. The switching overvoltage levels at the DC bus, the point between circuit breaker and smoothing reactor, and DC line are 933kV, 940kV, and 860kV, respectively. The key nodes of different converter stations are

basically the same type of decisive faults. Therefore, the decisive fault can be scanned in a targeted manner when verifying the arrester parameters of each node.

Table 3-3 Decisive Failure of Key Nodes of MMC-MTDC Converter Station

Key Node	Beijing		Fengning		Kangbao		Zhangbei	
	U/kV	Decisive Fault	U/kV	Decisive Fault	U/kV	Decisive Fault	U/kV	Decisive Fault
A	668	B	621	B	307	B	351	B
AV	886	E	870	G	893	G	881	D
LV	1001	B	930	G	957	G	955	B
CBH	933	B	915	E	925	G	921	E
D	933	B	915	E	916	E	921	E
DB	940	G	924	G	916	E	921	E
DL	860	E	857	E	842	E	847	E
CBN	587	G	580	G	586	B	604	D
E	410	C	403	C	402	C	414	C
EM	324	E	328	E	324	E	324	E
AL	1008	B	906	B	908	B	1058	C
SR	658	E	720	G	738	G	706	E
V	1934	B	1494	B	1692	G	1717	G

In summary, the maximum DC switching overvoltage of the MMC-MTDC system with DC breakers appears in the DC breaker opening process. The decisive fault is the DC line bipolar short circuit fault, the overvoltage generated by the DC circuit breaker reclosing process is less than the tripping process, and the maximum DC switching overvoltage is 940kV.

3.1.3 Effect of Operation Mode on Switching Overvoltage

1）Influence of bipolar and unipolar operation mode on switching overvoltage

The normal operation of MMC-MTDC is bipolar operation mode, but due to the long construction period, the single pole metal return line operation mode can be adopted in the early stage of the project. In these two modes of operation, the overvoltage levels of the electrical nodes may be significantly different. In order to verify the impact of the operating mode on the switching overvoltage, the following is a simulation calculation using the Zhangbei converter station as an example. The fault point is set at the positive pole of the converter station, and each converter station is operated at rated power. The calculation results are shown in table 3-4.

Table 3-4 Beijing Station Overvoltage level under Bipolar and Unipolar operation mode (kV)

Operation Mode	Valve top grounding		Valve side of reactor grounding		Exit of DC line grounding	
	Bipolar	Unipolar	Bipolar	Unipolar	Bipolar	Unipolar

A	186.7	187.7	186.4	189.7	184.4	189.3
CBH	766.4	0.1	928.1	925.7	823.7	823.3
DL	771.4	465.1	848.2	842.2	793.8	793.9
LV	456.4	466.0	462.7	467.1	383.4	410.8
E	414.1	412.8	319.8	326.2	280.1	303.6
EM	315.9	326.1	319.7	326.1	280.0	303.6

The overvoltage levels of the bipolar and unipolar metal return modes are compared according to the three representative faults in the above table. In the bipolar operation mode, the switching overvoltage level of the DC busbar and other DC side positions is relatively high. In the case of the valve top grounding fault, the valve top voltage difference of the two modes reaches 1.53p.u, so the DC side overvoltage level check calculation is adopted in this way. . For the unipolar metal operation mode, the switching overvoltage level on the valve bottom and the metal return line is relatively high, and the maximum voltage difference is 0.06p.u. Therefore, the metal operation overvoltage level is calculated in this manner. In summary, the calibration of the switching voltage level of the converter station should take into account the operation mode of the bipolar and unipolar operation mode.

2）Influence of converter station control mode on switching overvoltage

In order to ensure the stable operation of the DC grid, the Zhangbei project uses a slope control with a voltage dead zone. As a balanced node, Fengning Station controls the four-terminal grid DC voltage according to a preset voltage reference value. When the DC side voltage of Fengning Station cannot be controlled within the steady-state operating voltage range after the fault, or the transmission power value of Fengning Station has exceeded the capacity of the converter station, Fengning Station will not be able to maintain the stability of the DC voltage of the system. As the system DC voltage changes beyond the voltage dead zone range, the other three converter stations change from the constant power control mode to the voltage slope control mode. The control principle is shown in figure 3-9. It can be seen that the droop control coefficient k is related to the power command value P_{dc} of the converter station.

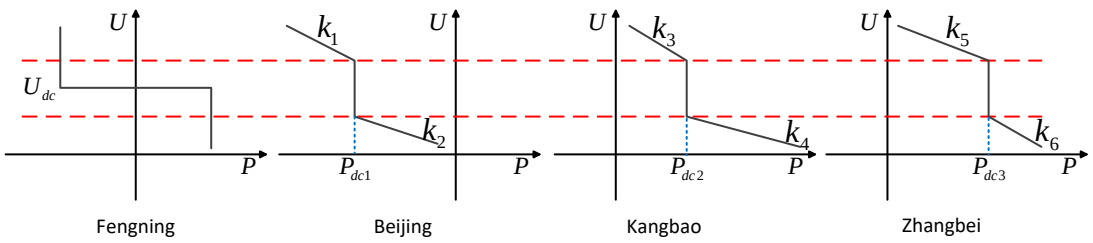

Figure 3-9 Slope Control of MMC-MTDC transmission system

Taking the DC bus grounding fault of Zhangbei Station as an example, the power converter values of the converter station are compared with different values. Exploring the influence of

the power command value on the switching overvoltage, the overvoltage level statistics of the key positions in the converter station are shown in table 3-5. Through a large number of calculations, it can be found that when the power command value of Zhangbei Station is gradually increased from 300MW to 3000MW, the overvoltage of the AC side, the valve top and the DC line is gradually increased, and the valve side and the bridge arm are gradually increased. The overvoltage level of the reactance valve side, the DC pole line, the valve bottom, and the metal return line gradually decreases. Among them, the maximum variation range of the AC side overvoltage amplitude is 0.05p.u, and the DC side operation overvoltage amplitude range is 0.08p.u. Since the overvoltage level of the electrical node is monotonous with the power command of the converter station, the two-state operation mode of the large mode and the small mode should be comprehensively considered to check the overvoltage. In the small mode, the power of each converter station is 10% of the rated value.

Table 3-5 DC Bus Grounding Switching Overvoltage under Different Power Command Value (kV)

Power Command Value	A	AV	CBH	DL	E	EM
300MW	427.28	448.13	741.82	884.01	430.52	178.93
1000MW	427.80	444.69	742.59	892.16	426.58	178.75
2000MW	428.47	437.78	743.93	908.53	422.11	178.65
3000MW	428.89	424.77	745.08	921.93	416.38	178.51

3）Influence of AC system coupling on switching overvoltage

In today's trend of large grid interconnection, the AC systems connected to different converter stations in multi-terminal systems are not necessarily independent of each other. Therefore, it is necessary to consider the coupling relationship between the AC systems of multiple converter stations in the networked operation mode to analyze the overvoltage level in the converter station. This section takes the Zhangbei project as an example to study the influence of the coupling relationship between the four AC systems on the overvoltage of the converter station. Considering the overvoltage comparison analysis of various typical faults of the converter station, figure 3-10 shows a representative comparison of the switching overvoltage levels of the converter station.

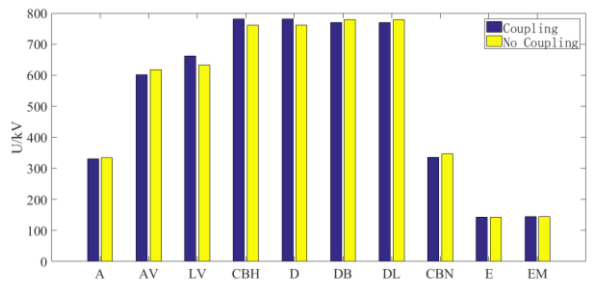

(a) AC Side Voltage of Three-phase Fault

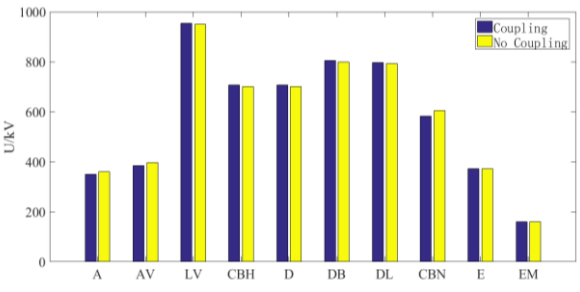

(b) Valve Side Voltage of Three-phase Fault

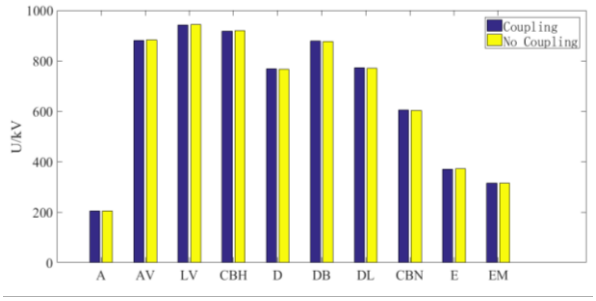

(c) DC Bus Grounding Fault

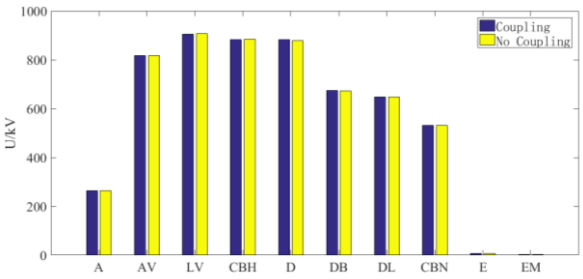

(d) Bipolar Short-circuit Fault

Figure 3-10 Switching Overvoltage Considering AC System Coupling Relationship

It is known from the fault at AC side and valve side of transformer that the coupling of the AC system will affect the switching overvoltage level of the key node of the converter station. In the three-phase ground fault of the AC side, the overvoltage levels on the side of the bridge arm reactance in the two cases are 30kV (0.05p.u.). The maximum difference of the overvoltage level of the electrical nodes on the DC side and the AC side under other AC side faults is less than 30 kV. From the typical DC side fault switching overvoltage comparison results, it can be seen that the overvoltage level of the electrical node in the AC system coupling and uncoupling is equivalent, and the maximum difference of overvoltage in both cases is less than 2kV (0.004p.u.).

The DC side overvoltage is very low under the condition that the AC system is coupled and uncoupled, and the influence is negligible. The coupling relationship of the AC system has a certain influence on the switching overvoltage level of the AC side fault, but its influence is small considering the insulation margin. Therefore, the coupling relationship between the AC systems can be neglected when calculating the switching overvoltage of the converter station of the MMC-MTDC system.

In summary, the power grid operation mode considers the three factors of bipolar and unipolar operation mode, converter station control mode and AC system coupling relationship. The unipolar operation mode has an overvoltage difference of 1.53p.u. at the top of the converter valve and a maximum switching overvoltage drop of 0.06p.u. on the metal return line. When the value of the converter station control command changes from small mode to large mode, the overvoltage in the station changes monotonously with the power command value, and the maximum differential overvoltage is 0.08p.u. In the case where the AC system is coupled and uncoupled, the overvoltage difference after the DC side fault is less than 0.004p.u., and the overvoltage difference after the AC side fault is less than 0.05p.u. In the case of the insulation margin, the coupling relationship of the AC system can neglect the influence of the switching overvoltage in the station. Therefore, the bipolar operation mode, the unipolar operation mode, the large mode, and the small mode should be considered to check the overvoltage of the converter station.

3.1.4 Effect of Control and Protection System on Switching Overvoltage

In the MMC-MTDC system, the failure in the converter station or the failure of the DC protection line after the failure of the DC protection line can ensure that the unfaulty pole or unfaulty converter station can continue to operate. The time that the protection system detects the fault and the time when the action command is issued will have an effect on the overvoltage of the converter station. Therefore, it is necessary to study the influence of the control protection system on the overvoltage in the station. Since the time of the lightning intruding wave is about microsecond and the control protection system is too late to operate, this section does not consider the influence of the control system on the lightning overvoltage.

1）Line protection action time is different

The DC circuit breaker will only operate after receiving the trip command of the control and protection system. According to the engineering parameters, the time when the system detects the line fault is 3ms. Considering the delay error and setting of the control and protection system in the actual project, the system fault detection time is set to change between 2ms and 5ms and the overvoltage level of the converter station is analyzed through simulation calculation. Taking the single-pole ground fault at the exit of the Beijing-Fengning line as an example, calculate the overvoltage level of the converter station under different protection action times. The simulation results are shown in figure 3-13.

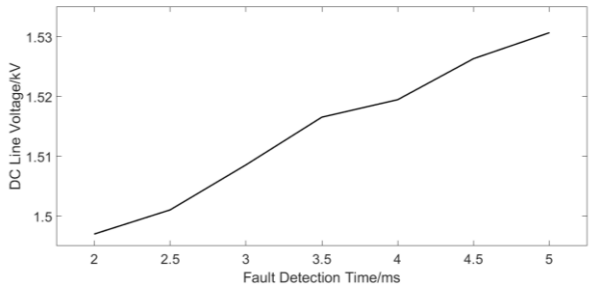

Figure 3-11 Relationship between the Line Overvoltage and the System Fault Detection Time

It can be seen from the above simulation results that the longer the line fault detection time, the higher the overvoltage level of the converter station. Considering that the fault detection time is between 2ms and 5ms, the overvoltage level of the converter station is increased from 801kV to 819kV, which is 0.03p.u. Therefore, the line fault detection time has little effect on the switching overvoltage in the converter station. The fault current rise rate of the MMC system is several tens kA/ms, and the fault current that rises sharply when the system fault detection time is too long may cause damage to the MMC system. Second, the system failure detection time is too short and may increase the probability of misjudgment. Therefore, it is more appropriate to consider the system line fault detection time as 3ms.

2）DC circuit breaker is not synchronized

When DC line has a ground fault, after the system detects the fault, the DC breaker at both ends of the fault line will act to cut off the line. Since the line connecting the four-terminal converter station is far away, the time for the control protection system to detect the fault and transmit it to the DC breaker at both ends of the fault line by the coordinated control system may vary. As a result, there are cases where the two circuit breakers cannot be opened simultaneously. Take the single-pole ground fault at the exit of Beijing-Fengning line as an example. Consider the operation time of the Fengning side DC circuit breaker is synchronized with the Beijing side circuit breaker, delay 1ms to 2ms and advance 1ms to 2ms. The overvoltage level of the converter station is shown in table 3-6.

Table 3-6 Switching Overvoltage When the DC Circuit Breaker is not Synchronized

Circuit breaker action	Single pole ground fault at Beijing				Single pole ground fault at Fengning			
	Beijing /kV	Beijing /p.u.	Fengni -ng/kV	Fengni -ng/p.u.	Beijing /kV	Beijing /p.u.	Fengni -ng/kV	Fengni -ng/p.u.
Advance 1ms	809	1.52	809	1.52	810	1.51	805	1.50
Advance 2ms	803	1.50	803	1.50	805	1.50	804	1.50
Synchronize	807	1.51	799	1.49	773	1.44	814	1.52
Delay 1ms	832	1.56	776	1.45	752	1.41	838	1.57
Delay 2ms	826	1.55	776	1.45	752	1.41	826	1.55

For the single-pole ground fault simulation on both ends of the same DC line, the following rules can be obtained. Since the long-distance traveling wave of the DC line has a delay effect on the opposite side of the line, the overvoltage of the converter station is not the most serious when the DC circuit breakers on both sides of the fault line operate synchronously. Switching overvoltage of the fault side line is slightly higher than the non-fault side (0.16p.u.). Switching overvoltage of the fault side line is slightly higher (0.07p.u.) when the fault side delay is opened, and the non-fault side overvoltage level is slightly lower (0.10p.u.) when the fault side delay is opened. Therefore, for a fault that needs to trip the DC circuit breaker at both ends of the line, if the fault side DC circuit breaker is delayed, the overvoltage level in the converter station will increase, which will increase the insulation level of the equipment and the line. Therefore, the control protection system should avoid the situation that the fault side DC circuit breaker is delayed.

3）Influence of failure of control system on switching overvoltage

In order to analyze the influence of the control system on the switching overvoltage, in the case of configuring the arrester, the overvoltage levels in the converter station are compared and analyzed considering the operation and failure of control and protection system. Calculate the switching overvoltage level generated by the operation and failure of the various control and protection systems in the converter station, and obtain the overvoltage of

each electrical node as shown in table 3-7.

Table 3-7 Switching Overvoltage during Operation and Failure of the Control System (kV)

C&P system	Beijing		Fengning		Kangbao		Zhangbei	
	No	Yes	No	Yes	No	Yes	No	Yes
AC side of transf.	726	668	651	621	569	445	584	438
Valve side of transf.	1099	886	1078	870	986	893	936	881
Valve side of bridge arm reactor	966	1001	963	930	952	957	965	955
Valve top	971	933	972	915	977	925	977	921
Valve side of smoothing reactor	971	940	972	924	977	916	977	921
DC line	984	860	980	857	982	842	983	847
Neutral bus outside the valve hall	618	587	603	580	606	586	635	604
Neutral bus	323	410	342	403	323	402	323	414
Metallic return	323	324	342	328	323	324	323	324

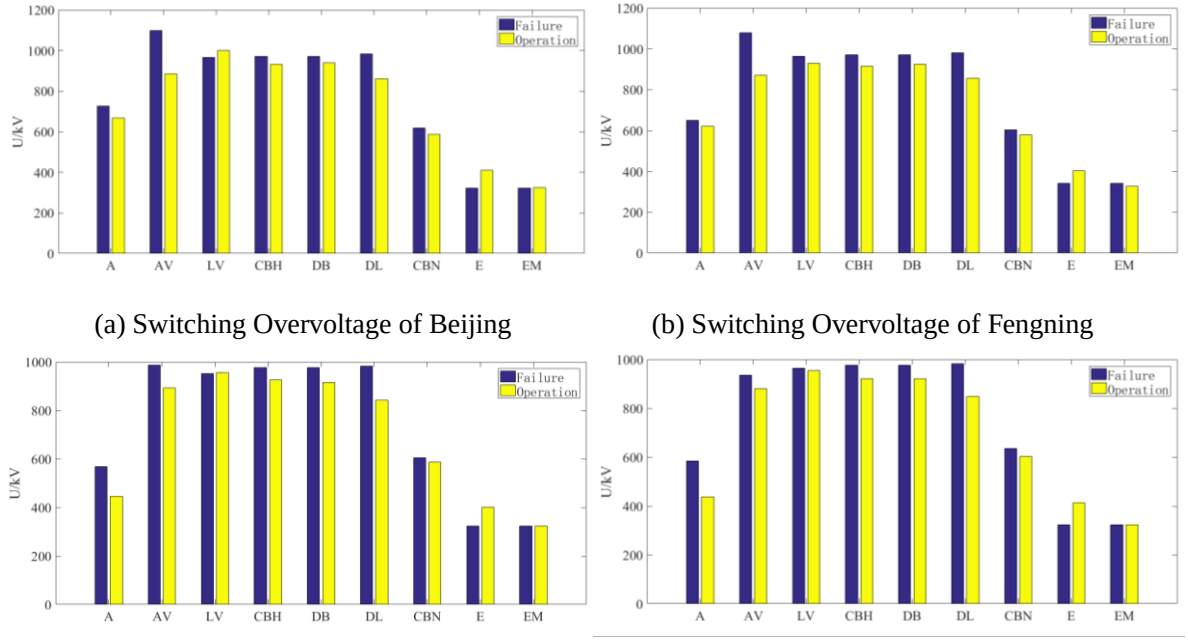

(a) Switching Overvoltage of Beijing

(b) Switching Overvoltage of Fengning

(c) Switching Overvoltage of Kangbao

(d) Switching Overvoltage of Zhangbei

Figure 3-12 Effect of the Control System on the Overvoltage in the Station

Figure 3-14 shows the impact of the control system on the four converter stations. It can be seen that the failure of the control system has a significant impact on the switching overvoltage level in the MMC-MTDC converter station. In addition to the neutral line and the metal return line, the node overvoltage in the case of failure of the control system is higher. The difference is obvious in the DC line, valve side of transformer and the neutral bus. The overvoltage level when the control fails is 1.17 times, 1.24 times and 0.78 times of the control action, respectively. Since the potential of the neutral line and the metal return line is close to zero under normal and stable operation, the operation of the control system after the fault will cause the overvoltage level to be high. In summary, the presence of the control and protection system can well limit the overvoltage level of the converter station.

4）Effect of valve blocking and circuit breaker action timing on switching overvoltage

This section focuses on the time and sequence of control and protection system actions after the grid fails. The effects of valve locking and circuit breaker action timing on overvoltage are studied in this thesis. Taking the three-phase ground fault and the valve ground fault on the valve side of transformer as an example, the fault transition resistance is 0.01 Ω, and the two DC breakers of the fault pole after the fault are activated, and the converter valve is blocked. In the following two cases, the different valve lockout time after the fault occurs, the DC breaker operation time is unchanged and the different DC breaker action time is unchanged in the valve lockout time, and the overvoltage of the key nodes in the converter station is obtained. The levels are shown in figure 3-15 and figure 3-16, respectively.

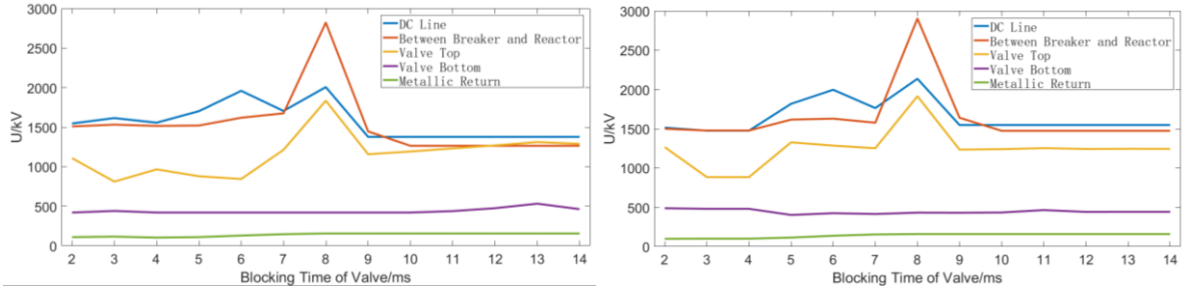

(a) Three-phase Ground Fault of Valve Side (b) Ground Fault of Valve Bottom

Figure 3-13 Effect of Valve Blocking Time on Switching Overvoltage

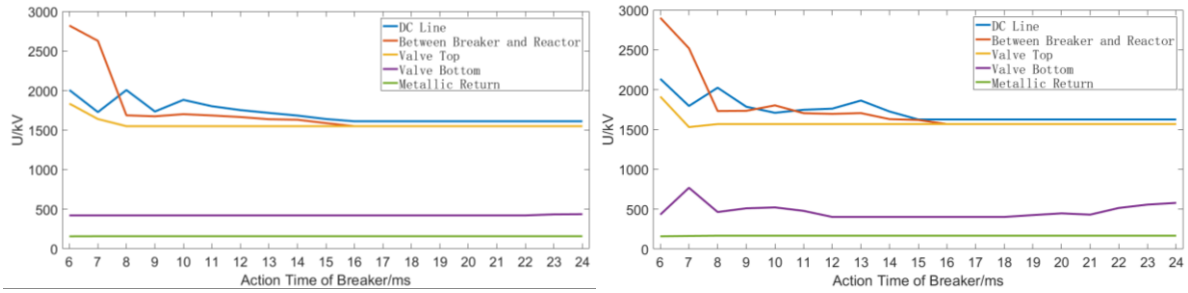

(a) Three-phase Ground Fault of Valve Side (b) Ground Fault of Valve Bottom

Figure 3-14 Effect of Breaker Operation Time on Switching Overvoltage

Under these two typical faults, the analysis of valve blocking and DC breaker action timing changes can be seen. After the fault occurs, the shorter the blocking time of the converter valve, the lower the overvoltage level of the electrical node in the converter station. When the blocking time gradually lags and is in the interval coincident with the circuit breaker operating time, the overvoltage level in the faulty converter station increases. After the valve blocking time t>10ms, the valve blocking time has no effect on limiting the overvoltage peak. When the valve blocking time is kept at 8ms, the DC breaker action time is changed from 6ms to 24ms. The DC side overvoltage level is higher when the DC breaker operates faster. In order to avoid a high overvoltage, the DC breaker action should not coincide with the valve blocking time. Comparing and analyzing figure 3-15 and figure 3-16, the DC breaker will be locked before the valve is locked in the event of a fault, and the overvoltage level in the converter station will be better limited when the two operating times do not coincide.

The control and protection system mainly consider the line fault detection time, the asynchronous operation of the DC breaker, the control protection timing, and the effect of the operation or failure of the protection system on the overvoltage in the station. When the line fault detection time changes from 2ms to 5ms, the overvoltage level of the converter station increases by 0.03p.u., and the fault current also rises sharply. However, considering that the system fault detection time is too short may increase the probability of misjudgment, it is more appropriate to consider the system line fault detection time as 3ms. When the fault-side DC breaker is delayed, the overvoltage in the station is slightly higher than the synchronous trip 0.07p.u. Therefore, the control protection system should avoid the delay-opening of the fault-side DC breaker. After the fault in the station, the DC circuit breaker is locked before the valve is locked, and the operation time of the two does not coincide, which will better limit the overvoltage level in the converter station. In the case of failure of the control system, the switching overvoltage on the DC side of the converter station is 1.24 times that of normal operation, so the presence of the control protection system can limit the overvoltage level of the converter station.

3.2 Lightning Overvoltage Analysis of Converter Station in MMC-MTDC

The lightning overvoltage of the converter station generally includes three aspects: the lightning intruding wave overvoltage from the AC side of the converter station, the lightning intruding wave overvoltage from the DC side of the converter station, and the direct lightning strike overvoltage of the converter station. Direct lightning strike overvoltage is not the main way to threaten the converter station equipment. The lightning protection line is generally used in conjunction with the lightning rod to protect the direct lightning strike, and the coverage is much greater than the lightning strike of the transmission line of the converter station [38,39]. Therefore, this section mainly considers the lightning overvoltage that invade the converter station along the AC side and along the DC side line, providing a theoretical basis for the insulation configuration scheme.

3.2.1 Model and Parameters of Lightning Invasion Wave

The lightning intruding wave simulation calculation needs to add the lightning current to the top of the tower or the DC line. The lightning current model adopts the double exponential wave equivalent model, and its expression is as shown in equation (3-1).

$$i(t) = I(e^{-\alpha t} - e^{-\beta t}) \qquad (2\text{-}1)$$

In the project, a typical lightning wave $2.6/50\mu s$ is used to verify the lightning intruding wave overvoltage, which is the wave front time $2.6\mu s$ and half wave time $50\mu s$. The lightning current waveform is generated by a controlled current source, and the lightning wave impedance is generally taken $Z_0 = \sqrt{L_0 / C_0} \approx 300\Omega$.

This paper will study the overvoltage generated by lightning intruding waves at the key

nodes of the converter station from the aspects of back flashover and shielding failure, and analyze its characteristics. Back flashover refers to the overvoltage generated by lightning strikes the tower or lightning conductor causing the insulator to flash. Shielding failure means that the lightning bypasses the protection range of the lightning protection line and directly hits the overvoltage generated by the wire. Because 75%~90% of the lightning current is negative, so in the engineering, the lightning current of the negative polarity is generally used for simulation calculation.

For the magnitude of back flashover lightning current, the probability distribution of the lightning current magnitude is calculated according to the power industry standard according to equation (3-2). Here, a lightning current with a magnitude of 216kA is selected for the calculation and analysis of the intruding wave overvoltage. Since the lightning protection measures of the incoming section of the converter station are relatively perfect, the lightning current with a probability of 0.35% will have a relatively high reliability.

$$\lg P = -I / 88 \qquad (2\text{-}2)$$

where, I is the lightning current amplitude, P is the probability of lightning current greater than I.

Shielding failure is related to the protection angle of the lightning protection line, the height of the tower and the inclination of the ground. At present, the method of electrical geometric model is generally used to calculate the maximum lightning current magnitude I_m [40], that is, the maximum lightning current that can directly strike the DC line on the protection line of the lightning protection line. In addition, it is also necessary to consider that a large shielding failure current may break through the insulator string, and part of the lightning current is amplified by the tower. Therefore, it is also necessary to consider the minimum shielding failure current I_o that causes the insulator string to flash. The maximum current around the lightning intruding wave should be a small value between I_m and I_o, and then the terrain factor and margin can be used to obtain the value of the surrounding current used in the simulation, as shown in table 3-8.

Table 3-8 Shielding Failure Current of Converter Station DC Line (kA)

Ground Inclination	Single Return Transmission Line		Double-circuit Transmission Line		
	500kV Line	Metallic Return	500kV Line (Upper）	500kV Line (Bottom）	Metallic Return
0°	9	4	8	13	11
5°	10.5	4.5	8	15	12
10°	12	5	8	17.5	14
Calculation Value	11	5	8	16	14

In the following, the shielding failure and back flashover simulations of the incoming tower

segments of the converter station are carried out to study the overvoltage and characteristics of the main equipment generated by the lightning intrusion converter station.

3.2.2 Influencing Factors of Lightning Overvoltage by Shielding Failure

The metal return line and the pole line of the ±500kV Zhangbei flexible DC power grid are erected on the same tower. Therefore, the tower height is higher than the conventional ±500kV DC tower, which is detrimental to the DC shielding failure performance. In this section, the influence of the intruding wave on the overvoltage of the converter station will be analyzed. After analyzing the influencing factors of the overvoltage, the parameters and arrangement of the tower will be improved.

The factors affecting the shielding failure voltage of the DC line are mainly the maximum current of the tower, the position of the strike point and the polarity of the line. The maximum shielding failure current of the tower is related to the tower type, tower height and ground inclination angle. Under the premise that the tower model has been determined, the maximum striking current of the tower is positively correlated with the ground inclination angle. According to experience, as the distance between the lightning strike point and the converter station increases, the level of the voltage across the station gradually decreases. The greater the magnitude or energy of the lightning current, the higher the overvoltage level in the converter station. The maximum lightning current of the tower of Fengning Station is 11kA, and the DC grid adopts bipolar operation mode and negative lightning current. The simulation calculation of the negative DC line of the six towers of Fengning-Kangbao line segment is carried out, and the simulation results are shown in figure 3-17.

It can be seen from the figure that when the polarity of the lightning current is constant, the lightning strikes the #1 to #6 towers respectively, and the level of the shielding failure overvoltage in the station gradually decreases. Due to the action of the smoothing reactor, the lightning strike wave has little threat to the converter valve. At this time, the overvoltage level generated at the DC line is the highest. When the lightning strike position changes six towers, the overvoltage is reduced by 0.12p.u. Therefore, in order to find the overvoltage extreme value in the station, the nearest tower of the converter station should be selected for the lightning calculation.

The lightning current amplitude increased from 16kA to 23kA, and the negative lightning was used to simulate the #1 tower. As the amplitude of the maximum shielding failure current of the tower increases, the overvoltage level in the station increases accordingly, and the overvoltage at the outlet of the DC line increases by 0.13p.u. Comparing figure 3-17(b) and figure 3-17(c), the overvoltage level of the intrusion wave is related to the polarity of the line voltage. When the lightning current and the voltage polarity are the same, the overvoltage level in the station is higher and the polarity is higher. On the contrary, the intruding wave overvoltage level is low, and the overvoltage difference in both cases is

0.35p.u. Therefore, on the basis of this, the most severe lightning strike situation can be used to obtain the lightning intruding wave overvoltage level of the converter station.

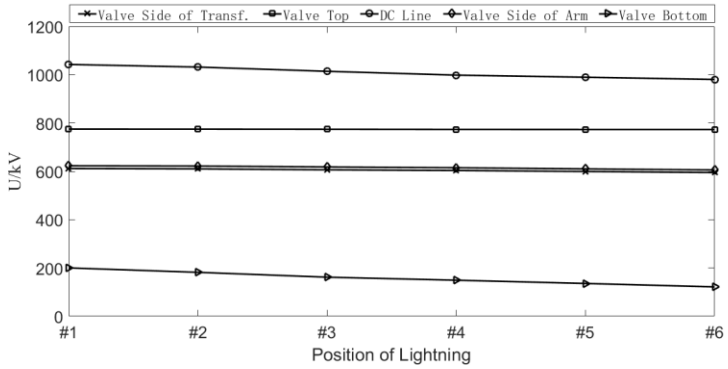

(a) Effect of Tower Position on Overvoltage

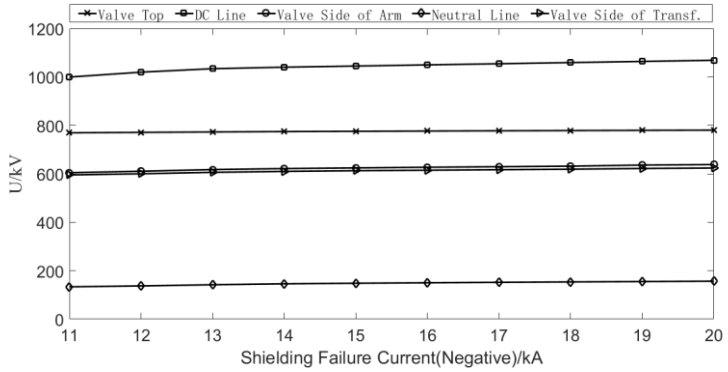

(b) Effect of Lightning Current Amplitude on Overvoltage

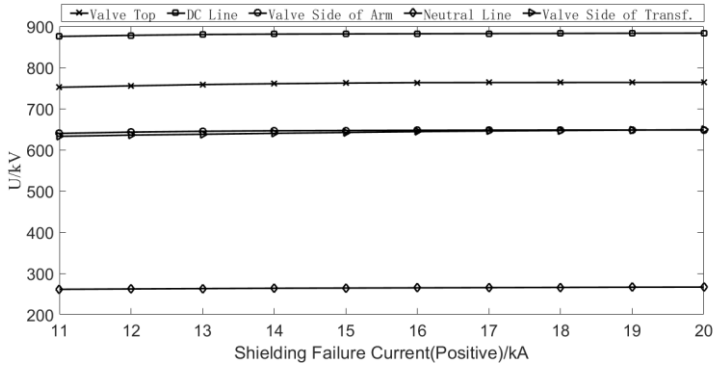

(c) Effect of Lightning Current Amplitude on Overvoltage

Figure 3-15 Influencing Factors of Shielding Failure

3.2.3 Influencing Factors of Lightning Overvoltage by Back Flashover

There are two cases of back flashover on transmission lines with lightning protection lines. One is to strike the top of the tower, and the other is to strike the lightning protection line between the two towers.

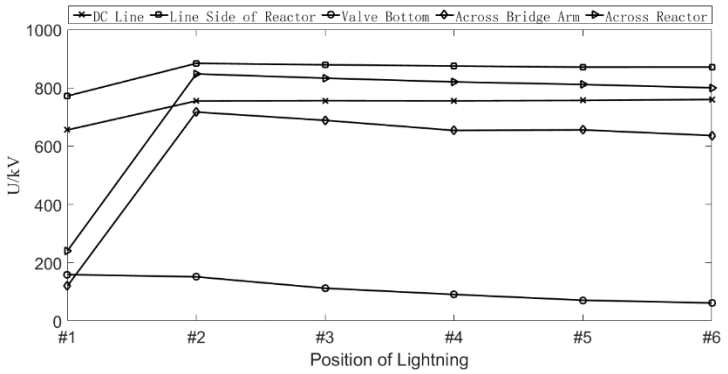

(a) Effect of Tower Position on Overvoltage

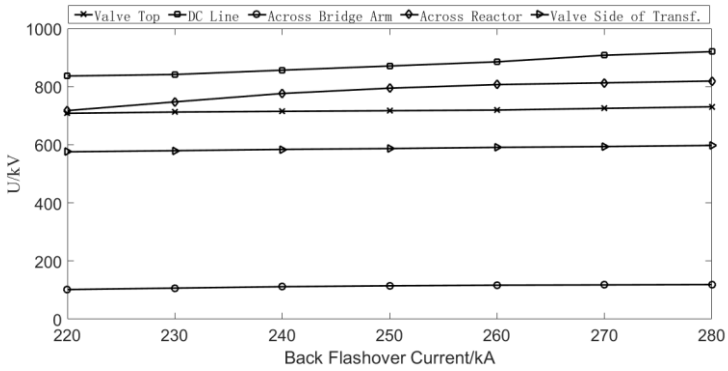

(b) Effect of Lightning Current Amplitude on Overvoltage

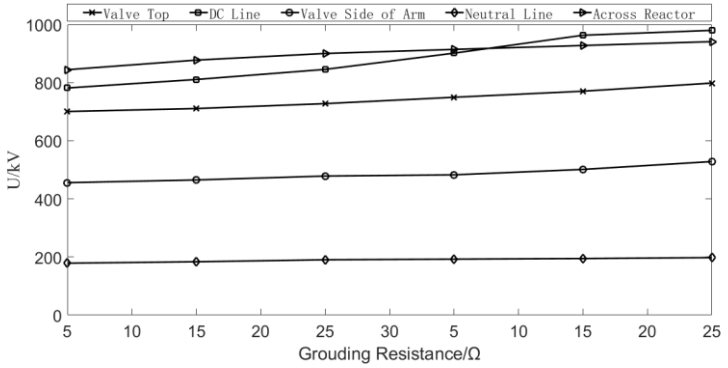

(c) Effect of Grounding Resistance on Overvoltage

Figure 3-16 Influencing Factors of Back Flashover

When the lightning strikes the top of the tower, the lightning current flows directly along the tower to the ground. When the lightning strikes the lightning protection line, the lightning current will have two components flowing along the lightning protection line to the adjacent two towers. This situation obviously has no great harm to the transmission line when the lightning strikes the top of the tower. When lightning strikes the top of the transmission line tower, lightning current will flow through the tower and flow into the earth to produce a high potential on the tower. When the voltage difference between the position of the insulator string and the transmission line is higher than the flashover voltage of the line insulator, the insulator will have a flashover phenomenon. This section first analyzes the impact of back flashover on the overvoltage of the converter station, and then focuses on the method of reducing the lightning overvoltage in the station.

The grounding resistance of the tower and the string length of the tower insulator string will cause the difference of the lightning overvoltage intruding wave overvoltage. The lightning current amplitude of 216kA with a probability of occurrence of 0.35% and the grounding resistance of the tower are taken as 10Ω, respectively, strike the tops of the six towers of the Fengning-Kangbao line segment. The simulation results are shown in figure 3-18.

It can be seen from the figure that in addition to the #1 tower, as the distance between the lightning strike point and the converter station increases, back flashover overvoltage level in the station gradually decreases. This is because the #1 tower is very close to the converter station, and the negative reflection wave is formed to reduce the overvoltage. Most of the lightning current is directly injected into the earth and the arrester in the station does not operate. The overvoltage generated by the lightning strike #2 tower is the highest, and the overvoltage level from #2 to #6 is gradually reduced, and the overvoltage drop on the reactance side of the bridge arm is most significant, 0.15p.u. Second, the greater the magnitude or energy of the lightning current, the higher the overvoltage level in the converter station. When the lightning current amplitude increases from 220kA to 280kA, the overvoltage in the station increases by 0.19p.u. It can be seen from figure 3-18(c) that as the resistance value of the grounding resistance of the tower increases, the component of the lightning current flowing into the ground through the grounding resistance decreases. The potential generated on the tower becomes high, and the lightning current component of the converter entering the converter station increases after the insulator flashes, so the overvoltage level in the station also increases. When the resistance of the grounding resistance of the incoming line tower changes from 5 Ω to 30 Ω, the DC line voltage rises by 0.37p.u. Therefore, in order to effectively suppress the intruding wave overvoltage level, it is necessary to reduce the resistance of the tower grounding resistance.

This section analyzes the influence of different factors on the lightning overvoltage, and can be used as the basis to obtain the most severe simulation conditions of lightning intruding wave overvoltage in the converter station.

(1) The intuitive factors that influence the shielding failure overvoltage are the maximum current of the tower, the position of lightning, and the polarity of the stricken line. When the lightning current increases from 16kA to 23kA, the overvoltage of the DC line outlet increases by 0.13p.u. When the stricken point changes from the near station to the far station, the voltage is reduced by 0.12p.u., and the lightning current is reduced. The overvoltage difference is the same as the voltage polarity and the difference between the two cases is 0.35p.u. Therefore, reducing the tower height, reducing the ground inclination angle and the lightning protection angle can improve the lightning strike performance of the pole line and reduce the voltage of the station.

(2) Intuitive factors affecting back flashover overvoltage include lightning current amplitude,

position of lightning and tower grounding resistance. When the current increases from 220kA to 280kA, the DC line overvoltage increases by 0.19p.u. When the stricken point changes from #2 tower to #6 tower, the overvoltage level decreases by 0.15p.u., and the tower grounding resistance increases by 25Ω to make the DC line. The lightning overvoltage rises by 0.37p.u. Therefore, the factors affecting the lightning strike performance of the pole line mainly consider the tower grounding resistance.

3.3 Intrinsic Overvoltage Characteristics in MMC-MTDC

In a multi-terminal MMC-HVDC system, the fault current after the failure of the converter station is transmitted along the direct current transmission line to the adjacent converter station, and an overvoltage is induced at the adjacent station. The relationship between the overvoltage level of adjacent converter stations and the overvoltage level of the faulty converter station is required to be studied in this section. Based on this, the overvoltage characteristics of multi-terminal MMC-HVDC system will be studied and analyzed.

3.3.1 Characteristics of Switching Overvoltage

A fault on the DC side of the converter station will cause the DC breaker on the opposite side of the line to trip. Figure 3-19 shows the overvoltage extreme value of adjacent converter stations after the DC side of the Beijing station fails.

For the failure of the DC breaker of the unfaulty converter station, the overvoltage level of the unfaulty converter station is higher than that of the unfaulty converter station that is not operating. However, the overvoltage level generated by the adjacent converter station will not be greater than the faulty converter station. Under the fault of the Beijing-Fengning line, the two stations with the highest overvoltage level were 1.74p.u. of Beijing Station and 1.48p.u. of Fengning Station. The overvoltage levels of the other two stations were 1.42p.u. Under the fault of the Beijing-Zhangbei line, the two stations with the highest overvoltage level are 1.74p.u. of Beijing Station and 1.51p.u. of Zhangbei Station. The overvoltage levels of the other two stations are 1.42p.u.

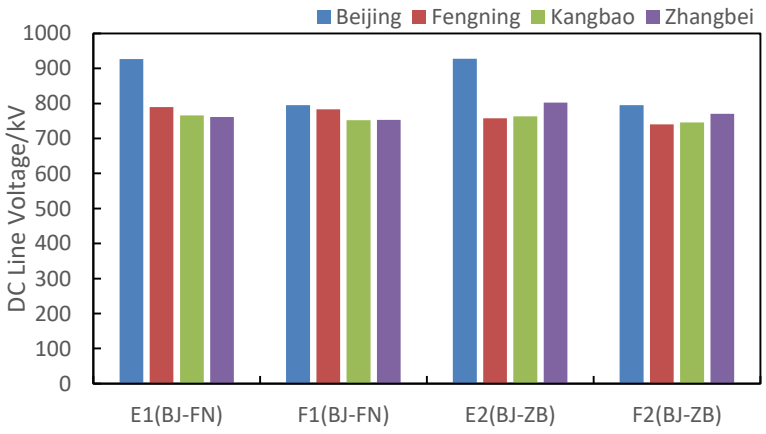

Figure 3-17 Overvoltage Level of Each Station when the DC side of Beijing Station Fails

In addition to the DC side fault of the converter station, the overvoltage distribution of multiple converter stations after the converter station area and the AC side fault occurs. The following is a simulation study on the faults of four converter stations in Zhangbei DC grid. The overvoltage generated by the key nodes of the converter station is shown in figure 3-20 and figure 3-21.

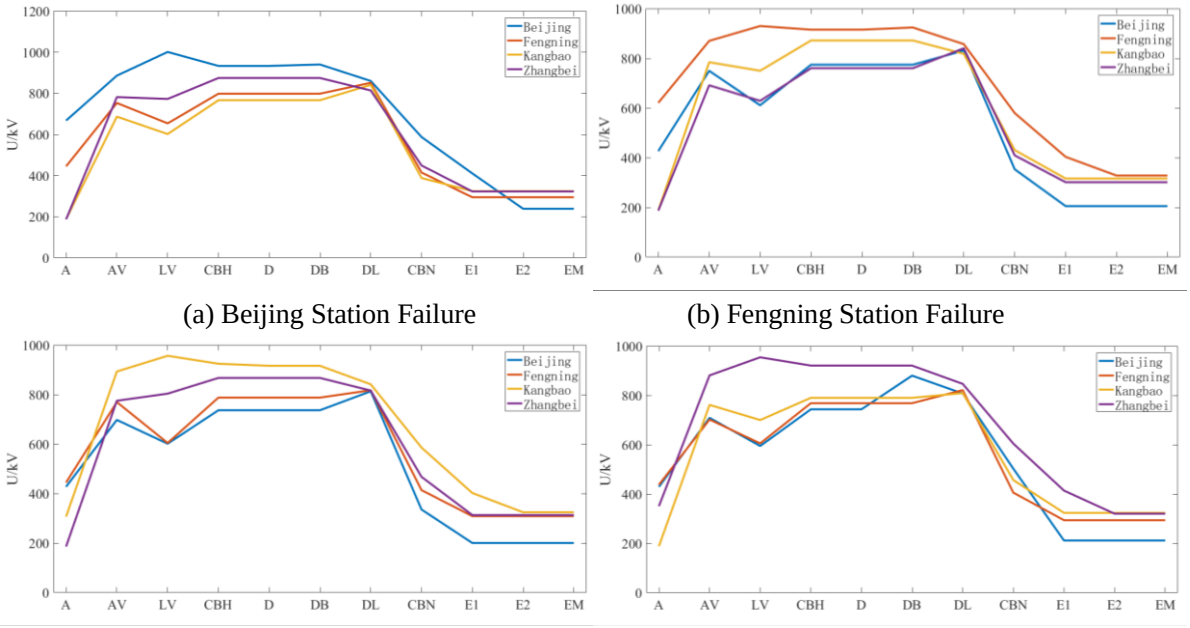

(a) Beijing Station Failure (b) Fengning Station Failure

(c) Kangbao Station Failure (d) Zhangbei Station Failure

Figure 3-18 Switching Overvoltage Level

Although for a certain fault, there is a possibility that the overvoltage level of the unfaulty converter station is higher than that of the faulty converter station. However, considering all typical faults of a single converter station of a multi-terminal system, it can be found that the switching overvoltage level of the faulty converter station is higher than that of the unfaulty converter station. It should be noted that because the fault current on the metal return line of the Beijing station can be directly discharged to the earth, its voltage will not rise significantly. Therefore, the metal return line overvoltage of the Beijing station as the grounding point of the entire DC grid is lower than the other three stations. In addition, the overvoltage level of the AC side of Kangbao Station and Zhangbei Station with rated voltage of 220kV is also lower than that of Beijing Station and Fengning Station with AC system voltage of 500kV.

Comparing the overvoltage of the key nodes of the four converter stations, it is found that the extreme values of overvoltage for each device are generated in the two high-power converter stations of Zhangbei Station and Beijing Station. Therefore, if you want to simplify the insulation coordination work of multiple converter stations, you can only study the switching overvoltage of the high-power station, and use this as a basis to determine the insulation level of each station equipment.

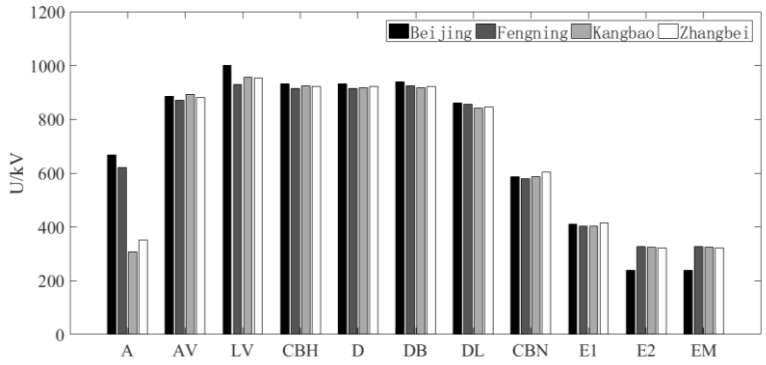

Figure 3-19 Comparison of Four Station Switching Overvoltage Level

3.3.2 Characteristics of Lightning Overvoltage

After the DC line of the converter station is subjected to lightning intruding waves, the DC circuit breaker of the station and the adjacent converter station will not operate. The consumption of the lightning wave energy is realized by the ground arrester at the DC line exit of the converter station, and the direction of the lightning wave transmission is bidirectional, and the high-frequency lightning current also induces the overvoltage at the opposite-side converter station.

Taking the lightning intruding wave on the DC side of Fengning Station as an example, figure 3-22 shows the DC side overvoltage level of each station. The overvoltage levels of the converter stations at both ends of the line subjected to lightning waves are 1.65p.u. and 1.06p.u., respectively, and the overvoltage levels of the other two stations are 0.97p.u. The overvoltage levels of the converter stations at both ends of the line subjected to lightning strikes are 1.75p.u. and 1.50p.u., respectively, and the overvoltage levels of the other two stations are 1.12p.u. Therefore, the lightning intruding wave generates an overvoltage of up to 1.50p.u. in the adjacent converter station, and the insulation level of the adjacent converter station equipment cannot be ignored when simulating the overvoltage calculation.

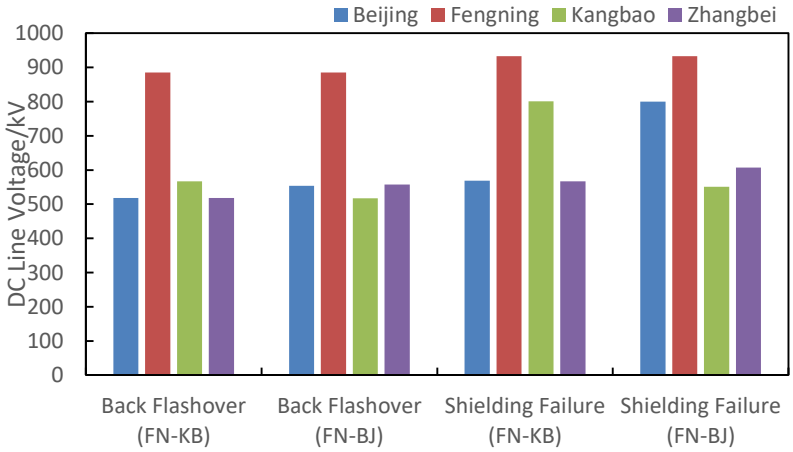

Figure 3-20 Fengning Station Suffered from Lightning Intruding Wave Station Overvoltage Level

Considering the overvoltage distribution of all converter stations after the lightning strike on

the AC side and DC side of the converter station, the overvoltage generated by the key nodes of the four converter stations in Zhangbei DC grid is shown in figure 3-23 and figure 3- 24 is shown. It can be found that the overvoltage distribution law of each converter station of the multi-terminal system after being subjected to lightning strikes is similar, that is, the overvoltage level of the converter station subjected to lightning strike is higher than other converter stations. Because the rated voltage of the AC network system of Kangbao Station and Zhangbei Station is 220kV, which is lower than the AC system voltage of 500kV between Beijing and Fengning Station, the AC side overvoltage of these two stations is lower.

The entrance section of Beijing Station is the double-circuit line of the same tower, and the other three stations is a single-circuit line. Therefore, the structure of the tower of the Beijing station is different from that of the other three stations. The value of the maximum shielding failure current and the tower of the incoming section are known from Section 3.2.1. The parameters and the terrain are determined, and the calculated maximum shielding failure current of the double-circuit tower of the same tower in Beijing station is larger than that of the single-circuit tower, so the overvoltage level on the DC side is the highest. Except for the overvoltage level of the DC side line of different converter stations except the Beijing station, the overvoltage level after the lightning strike is intrinsic. The overvoltage level of the AC line is related to the voltage level of the AC side after the lightning strike.

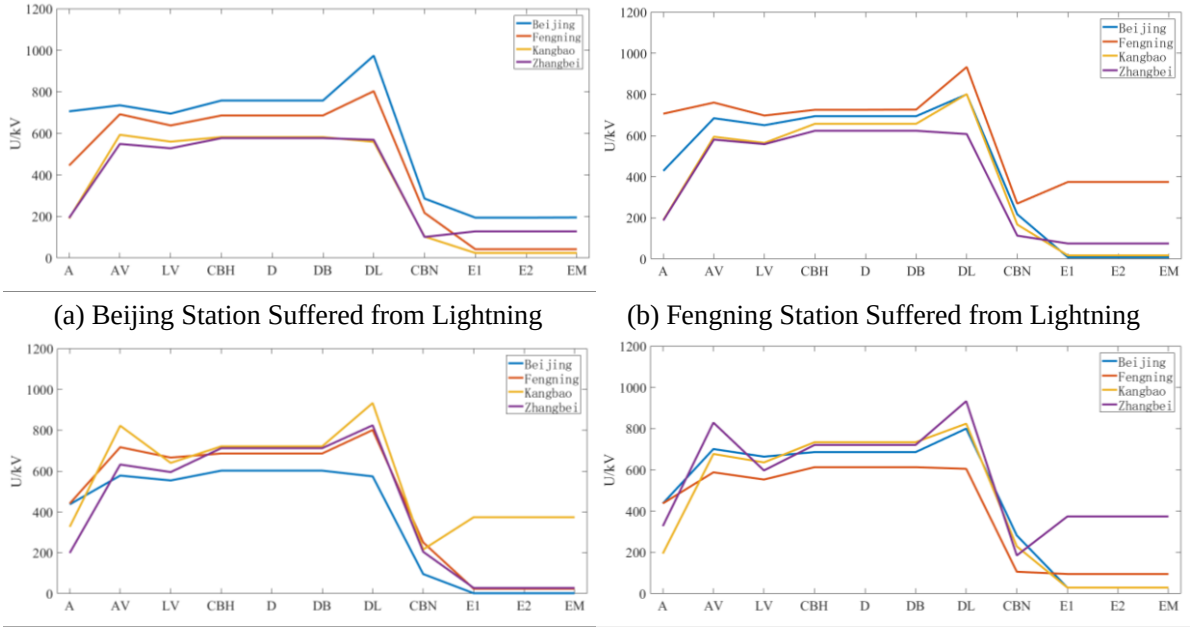

(a) Beijing Station Suffered from Lightning

(b) Fengning Station Suffered from Lightning

(c) Kangbao Station Suffered from Lightning

(d) Zhangbei Station Suffered from Lightning

Figure 3-21 Comparison of Lightning Overvoltage

In summary, the switching voltage level of key equipment nodes of high-power stations is relatively high. Therefore, multi-station configuration can be performed based on the overvoltage of the equipment of the high-power converter station, simplifying the insulation coordination work of the multi-terminal system. Secondly, the overvoltage of the lightning intruding wave of each converter station is related to the parameters of the tower of the

converter station and the topography. Therefore, the lightning overvoltage distribution law of each converter station is similar, and the lightning intruding wave will generate an overvoltage of up to 1.50p.u. in the adjacent converter station. The overvoltage level of adjacent converter stations on the line cannot be ignored in the simulation calculation.

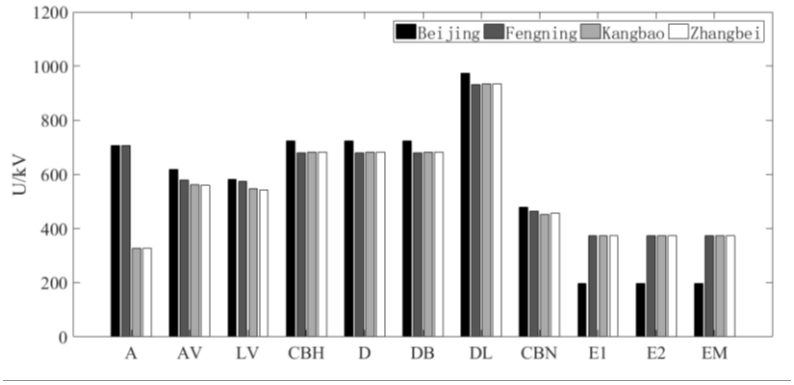

Figure 3-22 Comparison of Lightning Overvoltage of Four Stations

3.4 Brief Summary

In this chapter, the ±500kV four-terminal MMC-HVDC ring network is taken as an example. The PSCAD simulation software is used to simulate and analyze the typical faults and switching and lightning overvoltage of the flexible DC transmission system. The factors affecting the overvoltage and the intrinsic characteristics of the multi-terminal overvoltage are analyzed. The maximum switching overvoltage of the DC side of the converter station appears in the DC breaker opening process. When calculating the overvoltage of the converter station, the bipolar operation mode, the unipolar metal return line operation mode, the large mode and the small mode should be considered comprehensively. Factors affecting the switching overvoltage also include the grounding point of the DC grid and the fault detection of the control protection system and the time required for communication between stations. The factors affecting the back flashover and shielding failure intruding voltages mainly include the tower height, tower type, grounding resistance and the terrain of the incoming line tower. And the unfaulty station will generate a transmission overvoltage of up to 1.50p.u., and the overvoltage level of the adjacent converter station of the line cannot be ignored. Through the analysis results of the influencing factors of multi-terminal power grid overvoltage, the decisive faults of each node of the converter station and the most severe fault simulation conditions can be obtained, which can simplify the acquisition of representative overvoltage of the node. At the same time, in the multi-terminal flexible engineering design and operation stage, the overvoltage level of the converter station can be limited as much as possible according to the influencing factors.

4 Research on Insulation Coordination of Converter Station in MMC-MTDC System

The basic goal of insulation coordination is to determine the maximum steady state, transient overvoltage levels that different equipment in the converter station can withstand. Select the insulation strength and characteristics of the equipment, including the characteristics of the overvoltage protection device, to ensure that the equipment operates safely, economically and reliably at maximum overvoltage levels. The multi-terminal MMC-HVDC system with DC circuit breakers puts forward higher requirements for overvoltage protection. Therefore, it is very urgent and necessary to carry out research on overvoltage analysis and insulation coordination of the system [41-43].

The insulation coordination of MMC-HVDC converter station is generally divided into three steps. Arrange the arrester after determining the DC structure of the converter station. Calculate and analyze the overvoltage of each area of the converter station, determine the representative overvoltage of each node and the protection level of the arrester, and match the current and energy. The design of the insulation scheme is improved by repeatedly adjusting the insulation level of the equipment and the parameters of the arrester. This section studies the arrester configuration and equipment insulation level of MMC-HVDC transmission system converter station in the Zhangbei demonstration project.

4.1 Method and Influence of Arrester Configuration

4.1.1 Arrester Configuration Instructions

The configuration method of the arrester of the MMC-HVDC converter station has the same compatibility with the conventional HVDC converter station. The general principle of the conventional HVDC converter station configuration are as follows.

1）The overvoltage of the converter station shall be limited by the arrester in the respective area.

2）The key equipment of the converter station can be directly protected by an arrester connected across the two ends of the equipment.

3）Improve the ability of the arrester to absorb energy by paralleling the multi-column arrester.

According to the arrester configuration principle, on the basis of determining the overvoltage level of the key equipment and electrical nodes of the converter station, the electrical nodes with high overvoltage level and the key equipment are equipped with lightning arresters at

both ends of the ground or across the equipment. Then get a comprehensive protection of the arrester configuration.

At present, there is no perfect arrester configuration criterion for high-voltage large-capacity MMC converter stations. In general, the arrester configuration of the multi-terminal system can refer to a conventional HVDC transmission system and MMC transmission system. It is preliminarily determined that the HVDC converter station needs the electrical node and key equipment of the arrester. AC grid side, valve side of transformer, bridge arm reactive valve side, valve top, valve side of reactor, DC line, neutral bus, metal return line, bridge arm reactor, smoothing reactor, valve. Figure 4-1 shows the structure of a flexible DC converter station and the location of all possible arresters. Combined with the actual situation of the Zhangbei project and comprehensive analysis of economic and technical indicators, the initial configuration of the arrester can be increased or decreased as appropriate.

In figure 4-1, the AC bus arrester A of the converter station is mainly used to protect the AC bus equipment of the converter station. The overvoltage generated by the AC side of the converter station is limited, and the overvoltage generated by the AC transformer to the converter side and the DC side is limited. The valve side of transformer arrester AV is used to protect the converter valve side equipment. Directly protect the converter side and other related equipment, and indirectly protect the bridge arm reactor. In addition, the arrester can limit the overvoltage transmission on the AC side and the DC side to the opposite side.

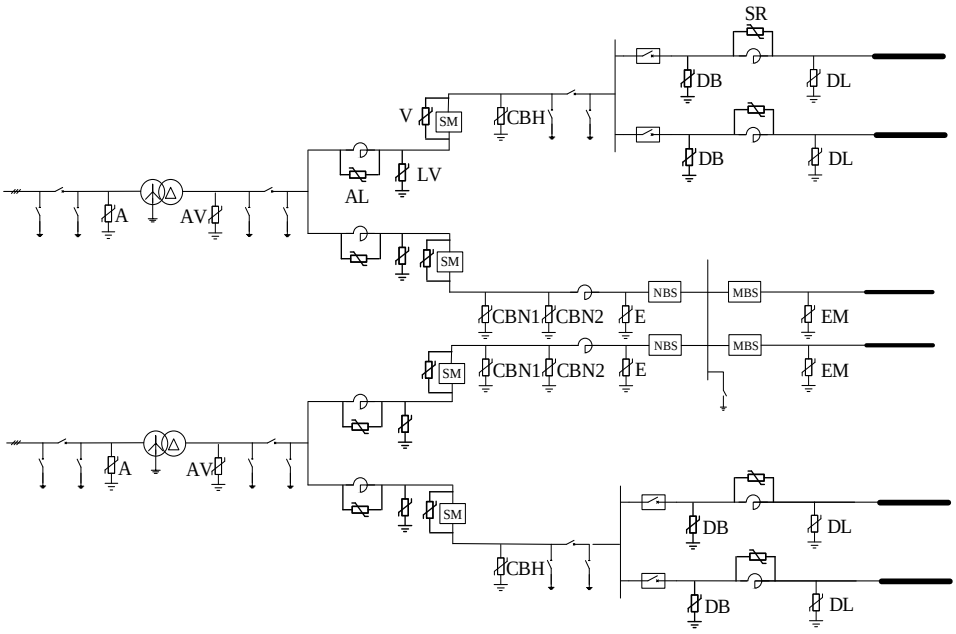

Figure 4-1 Arrester Configuration Diagram of Converter Station

The valve side arrester LV of bridge arm reactance is installed between the bridge arm reactance and the valve, and limits the bridge arm reactor overvoltage to indirectly protect the converter station sub-module cascade valve. The valve top arrester CBH is installed on the top of the converter valve. Since it is the high voltage end of the converter valve, the

rated operating voltage is very high. Therefore, arresters are needed to protect DC bus, wall bushings and other related equipment.

The valve side arrester DB of smoothing reactor is installed between the DC circuit breaker and the smoothing reactor to limit the switching overvoltage caused by the DC breaker action. In addition, the lightning intruding wave overvoltage will damage the DC circuit breaker after passing through the smoothing reactor, so the DC breaker is protected by installing the arrester DB. The DC pole lightning arrester DL is installed at the outlet of the DC pole line to protect the DC line of the converter station from lightning intruding waves and switching overvoltage. DL is used for lightning protection and is aimed at lightning intrusion wave overvoltage. Secondly, the operation of the circuit breaker is limited to the switching overvoltage of the smoothing reactor. The smoothing reactor is also protected with the valve side arrester DB of smoothing reactor to ensure that the voltage drop across the smoothing reactor does not damage the insulation.

The low voltage end of the converter valve CBN1 is installed in the neutral bus in the valve hall, and the CBN2 is installed in the neutral bus outside the valve hall. CBN2 is mostly a multi-column parallel arrester, which can withstand high energy. The neutral bus's reactor anti-absorption energy during neutral bus switch field operation is discharged through CBN2, which requires high requirements for CBN2. In addition, in order to prevent the CBN2 from jeopardizing the equipment in the valve hall, it is placed outside the valve hall. The reference voltage of the arrester CBN1 is higher than that of CBN2, mainly to limit the lightning intruding wave overvoltage generated by the metal return line.

The neutral bus lightning arrester E is installed on the neutral bus line. Its protection characteristics are higher than that of the metal return lightning arrester EM, and the DC bus and the neutral bus are protected together with the neutral bus arrester CBN2 outside the valve hall. Metal return lightning arrester EM is installed at the metal return line outlet. The EM is used to protect the metal return line of the converter station from lightning intruding waves and to limit the operating overvoltage. Usually multi-column arresters are connected in parallel. The parallel arrester AL directly protects its parallel bridge arm reactors, reducing the overvoltage at both ends of the equipment.

The valve arrester V is a typical arrester configuration for a conventional HVDC transmission project. In order to prevent the sub-module cascade valve from being overvoltage in MMC transmission converter station, the arrester can be connected in parallel at both ends of the converter valve. Although indirect protection can be achieved by the cooperation between the bottom arrester and the high voltage bus arrester of the inverter, this will increase the insulation level of the equipment and reduce the economy. In addition, the arrester V indirectly affects the overvoltage level of other key points through interaction with other arresters.

The smoothing reactor arrester SR is directly connected across the two sides of the smoothing reactor to suppress the reverse polarity transient overvoltage occurring at both ends of the smoothing reactor.

4.1.2 Calculation Principle of Arrester Parameters

After obtaining the preliminary configuration scheme of the arrester, it is necessary to select relevant parameters of each arrester.

The first parameter to determine is the rated voltage of the AC arrester U_f and the reference voltage of the DC arrester U_{ref}. They represent the maximum voltage at which the arrester does not absorb energy and the ability to withstand temporary overvoltage. The insulation level of the protected equipment is also closely related to this parameter. Secondly, the arrester parameter to be selected is the flow energy. After the arrester is operated, it is necessary to vent the fault energy, and the flow energy determines the energy consumption of the arrester.

The selection of these arrester parameters requires a combination of factors. The final selected parameters should be low on the premise of ensuring a small number of arresters and high economic efficiency. These factors mainly include the system's peak continuous operating voltage (PCOV), maximum continuous operating voltage (CCOV), and charge rate. Therefore, when determining the parameters of the arrester of MMC converter station, the optimization parameters of each type of arrester should be selected in combination with the overvoltage levels under various faults, operations, and lightning conditions. For the arrester configuration scheme proposed in this paper, the specific parameter selection will be described below.

1）AC side arrester

The selection of the lightning arrester parameters on the AC side of the converter station is the same as that of the AC system. The rated voltage of the AC arrester is the maximum allowable power frequency voltage applied between the terminals of the arrester. The operating characteristics of the system are characterized by the maximum continuous switching voltage of the system. Before determining the rated voltage of the AC arrester, the PCOV of the system should be determined.

For AC systems with a voltage level of 500kV, the highest extreme switching voltage is 550kV. The PCOV effective value of each of the three phases is calculated to be $\mathrm{MCOV} = 550/\sqrt{3} = 318\mathrm{kV}$, so the AC arrester must have a continuous operating voltage of not less than 318 kV. The power frequency overvoltage of the 500kV system generally does not exceed 1.3p.u., and the power frequency overvoltage duration does not exceed 1s. The power frequency overvoltage can be converted into an equivalent overvoltage U_{eq}, and the

duration of the equivalent overvoltage is set to 10s, and then the rated voltage of the selected arrester should be greater than the equivalent temporary overvoltage.

$$U_{eq} = 1.3 \times \frac{550}{\sqrt{3}} \times \left(\frac{1}{10} \right)^{0.02} = 394.2\text{kV} \qquad (4\text{-}1)$$

The AC bus arrester of 500kV voltage class can choose arrester with rated voltage of 396kV and above. Similarly, the 220kV voltage level AC bus arrester can choose arrester with rated voltage of 180kV and above. The 396kV and 180kV arresters have lower protection levels and can reduce the insulation level of the equipment. The protection level of the 420kV and 204kV arresters is higher, although the insulation level of the equipment will be increased, but the number of arresters and the absorbed energy will be reduced. Meet energy requirements and have a long service life and are lowest aging. It is recommended to select AC side of transformer arrester with rated voltages of 420kV and 204kV.

2）DC side arrester

In view of the current selection of MMC arrester parameters without reference, this topic directly calculates the relevant parameters of the arrester considering the influence of the chargeability.

（1）Chargeability

The chargeability of the DC arrester represents the ratio between the system's continuous operating voltage peak CCOV and the arrester reference voltage. The chargeability indicates the long-term charge on the zinc oxide valve. When the zinc oxide valve is in normal operation, it is uncharged, that is, it is not charged. Reducing the chargeability will make the arrester have less leakage current under long-term operating voltage and is not easy to age. At this time, the loss of the arrester is also reduced and the stability can be improved. When the chargeability is increased, the arrester reference voltage is lowered, which causes the voltage threshold of the arrester's bleeder energy to drop. The advantage is that the insulation level of the device is lowered and the economy is high. The disadvantage is that the aging speed of the arrester will be accelerated. Factors that need to be considered when selecting the chargeability of each arrester include system factors and environmental factors. The system factors mainly include the operating characteristics and voltage levels of the system. Environmental factors include temperature, installation area, and so on. According to the definition of the chargeability, the value is less than 1, and the DC arrester chargeability is generally greater than 0.8. The selection principle of the arrester chargeability of the converter station is as follows.

For the arrester AV and the arrester LV, they can cooperate to protect the converter valve and the converter transformer. Since only the bridge arm reactors are arranged between the two

arresters, the selection of the two parameters needs to be coordinated. Otherwise, there may be cases where one of the arresters does not operate and the other arrester has excessive aging energy, and their chargeability is generally selected as 0.82.

For the valve arrester V, considering that it is installed in the valve hall, it is basically not affected by external environmental factors (such as temperature, humidity, dust, etc.) during operation. The converter valve sub-module contains a capacitor-stabilized voltage, so the overvoltage level across the converter valve is limited. The valve arrester can have a higher chargeability, generally 0.9.

For the valve top arrester CBH, the valve side and line side of reactor arrester DB/DL, all three arresters are on the DC side of the converter station, so the voltage characteristics are similar to the DC line. The voltage at steady-state operation of the high-voltage terminal of the arrester is a DC voltage with little fluctuation, and the arrester has less loss, so the chargeability can be selected as 0.85.

The role of the bridge arm reactor is to suppress the circulation and to limit the sharp rise of the fault current. Therefore, the fault voltage at both ends of the bridge arm reactance is much larger than the voltage under normal operation mode, so the determination of the reference voltage of the bridge arm reactor arrester AL has nothing to do with the chargeability. For the reference voltage selection of AL, refer to the AC arrester. The rated voltage of the system can be taken as the rated voltage of the valve side of transformer, which is 290.88kV.

For the smoothing reactor arrester SR, the continuous operating voltage is very low, and the arrester reference voltage is generally determined by fault scanning. For the neutral bus arresters CBN1 and CBN2 in the valve hall and outside the valve hall, the CCOV of the arrester is very low, and the reference voltage of the arrester is not considered by the chargeability. For the neutral arrester E and the metal return arrester EM, when the fault current is transmitted to the neutral line and the metal return line, its overvoltage far exceeds its maximum continuous operating voltage. Therefore, the chargeability cannot be used to calculate the reference voltage of the arrester in this area.

（2）Reference voltage

After selecting the chargeability of the DC arrester and the maximum continuous operating voltage of each region, the minimum threshold of the reference voltage of the arrester can be calculated. The nominal voltage of Zhangbei project is ±500kV. Considering the measurement error and future DC grid expansion and various operating modes, the maximum voltage on the DC side is 535kV. Therefore, the maximum continuous operating voltage on the DC side is taken as 535 kV. For arresters at neutral line and across critical

equipment, the voltage in steady-state operation is close to zero. However, when the system is faulty or the DC line is subjected to lightning intruding waves, the energy of the arrester is very high. The reference voltage should be determined by considering the number and energy of the arrester. When the reference voltage of the selected neutral arrester is low, the energy discharged through the lightning arrester is large. The use of multi-column arresters in parallel to split the flow may cause uneven shunting. When the reference voltage of the selected neutral arrester is higher, the insulation level of the protected equipment is increased, and the improvement of the insulation requirement of the equipment causes economic decline. Therefore, we should consider these two factors to choose the reference voltage of the neutral line arrester.

（3）Number of parallel columns of arresters

Table 4-1 Arrester Selection Parameters

Converter station area	Arrester	*CCOV*/kV	U_{ref} /kV	Parallel Columns	Units
500kV AC bus	A（500kV）	318	420	6	2
220kV AV bus	A（220kV）	159	204	6	2
Valve side of transf.	AV	535	652	2	2
Valve side of bridge arm	LV	535	652	4	12
Valve top	CBH	535	629	4	2
Valve side of reactor	DB	535	629	6	4
DC line	DL	535	629	4	4
Across Valve	V	535	596	2	12
Across bridge arm reactor	AL	90	264	2	12
Across smoothing reactor	SR	90	629	1	4
Neutral line inside the valve hall	CBN1	90	428	6	2
Neutral line outside the valve hall	CBN2	90	396	8	2
Neutral line	E	80	296	3	2
Metallic return	EM	80	268	5	2

CCOV: Peak continuous operating voltage; **U_{ref}:** Arrester reference voltage.

In the HVDC transmission project that has been put into operation, many arresters are in the form of multi-column parallel. At this time, the current sharing problem of the multi-column arrester is something we need to consider. In the simulation calculation, if the energy of the arrester is too large, it is necessary to use a multi-column arrester and determine the number of parallel columns. Ideally, the arresters of each column are exactly the same, and the energy and current through the arresters of each column will be evenly divided after the action. If the performance of each column arrester is not completely consistent, the arrester

action will cause the energy of a column arrester to be released too much. In extreme cases, when a column with a weaker arrester bleeds more energy than the flow energy, it will endanger the directly protected equipment.

Therefore, the premise of selecting a multi-column arrester is that the insulation level of the arrester protection device needs to be reduced, and the matching current of each column arrester needs to be reduced. Different parameters of the converter station and the length of the overhead line between the stations in the multi-terminal system may result in different parameters of the arrester configured. When the arrester operation situation of each converter station is not much different, a uniform arrester configuration can be performed for all converter stations in consideration of the simplification of the design work.

Combined with the typical fault and lightning simulation calculation results, the parameters of the arrester in each area of the converter station and the installation quantity of various types of arresters are determined. The specific parameters are shown in table 4-1.

（4）Matching current and capacity

When the voltage across the arrester is exactly the protection level of the arrester, the current flowing through is the matching current of the arrester. Factors that should be considered in conjunction with the current include the surge energy of the arrester, the number of parallel columns of the arrester, and the peak discharge current of the single-column arrester. In the case where the flow energy of the whole arrester is constant, the matching current is small, the number of parallel columns of the arrester is large, and the peak value of the discharge current of the single-column arrester is small. On the contrary, with the large current, the number of parallel columns of the arrester is small, and the peak of the discharge current of the single-column arrester is large. When considering the capacity of the arrester, the continuous absorption and discharge current caused by the repeated action of the arrester should be considered, which requires higher capacity of the arrester. If the capacity of a single arrester cannot meet the requirements, a parallel multi-column arrester should be used. After research, it is necessary to repeatedly calculate and adjust under the representative overvoltage of the arrester node or equipment to find the optimal arrester matching current, flow energy and number of parallel columns.

4.1.3 Arrester Configuration Scheme

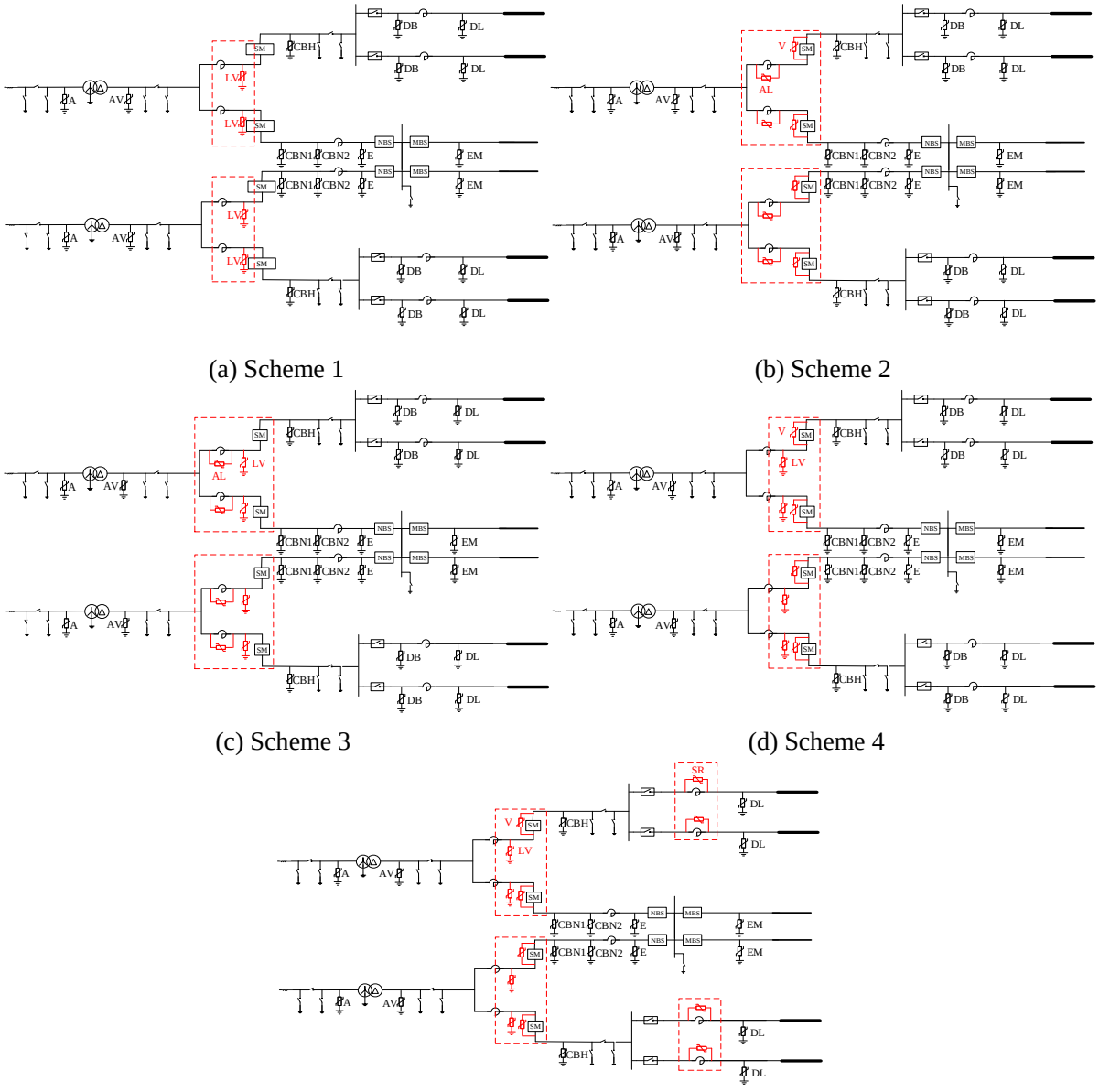

(a) Scheme 1

(b) Scheme 2

(c) Scheme 3

(d) Scheme 4

(e) Scheme 5

Figure 4-2 Five Kinds of Arrester Configuration Schemes for Converter Stations

From the perspective of insulation coordination, the reduction in the level of protection of the arrester means that the insulation level of the equipment in the station can be reduced accordingly. When the current of the arrester is constant, more arresters are needed to consume the overvoltage caused by the same fault. Although the insulation level can be reduced, the insulation cost of the equipment is reduced. However, the increase in the number of parallel columns makes the size of the arrester larger and takes up more valve room space, which causes heat dissipation problems and valve room equipment layout problems. Therefore, when selecting the specific configuration scheme of the arrester, the overvoltage level should be carefully checked. And repeatedly adjust the parameters through the action of the arrester to find the optimal balance between the insulation level of the

equipment and the parameters of the arrester.

In this section, considering the economic situation, the position of the arrester as shown in figure 4-1 is increased or decreased as appropriate, and five optimized arrester configuration schemes are finally determined. The main considerations are optimized converter valve protection and DC side equipment protection. Figure 4-2 shows the configuration of five arresters for MMC-HVDC converter station.

Table 4-2 Arrester Configuration of Scheme 1

Arrester	A	AV	CBH	DB	DL	CBN1	CBN2	E	EM	LV
U_{ref}/kV	420	652	629	629	629	428	396	296	268	652
Parallel Columns	6	2	4	6	4	6	8	3	5	4
Units	2	2	2	4	4	2	2	2	2	12

Table 4-3 Arrester Configuration of Scheme 2

Arrester	A	AV	CBH	DB	DL	CBN1	CBN2	E	EM	V	AL
U_{ref}/kV	420	652	629	629	629	428	396	296	268	596	264
Parallel Columns	6	2	4	6	4	6	8	3	5	2	2
Units	2	2	2	4	4	2	2	2	2	12	12

Table 4-4 Arrester Configuration of Scheme 3

Arrester	A	AV	CBH	DB	DL	CBN1	CBN2	E	EM	LV	AL
U_{ref}/kV	420	652	629	629	629	428	396	296	268	652	264
Parallel Columns	6	2	4	6	4	6	8	3	5	4	2
Units	2	2	2	4	4	2	2	2	2	12	12

Table 4-5 Arrester Configuration of Scheme 4

Arrester	A	AV	CBH	DB	DL	CBN1	CBN2	E	EM	LV	V
U_{ref}/kV	420	652	629	629	629	428	396	296	268	652	596
Parallel Columns	6	2	4	6	4	6	8	3	5	4	2
Units	2	2	2	4	4	2	2	2	2	12	12

Table 4-6 Arrester Configuration of Scheme 5

Arrester	A	AV	CBH	DL	CBN1	CBN2	E	EM	LV	V	SR
U_{ref}/kV	420	652	629	629	428	396	296	268	652	596	629
Parallel Columns	6	2	4	4	6	8	3	5	4	2	1
Units	2	2	2	4	2	2	2	2	12	12	4

The arrester configuration of the five arrester configurations is shown in table 4-2, table 4-3, table 4-4, table 4-5, and table 4-6. According to the proposed number of parallel columns of arresters and the number of units, calculate the engineering cost of the five configuration schemes, and find the weight relationship between the schemes.

The difference in the configuration of the five arresters at the converter station is mainly reflected in the converter valve and the smoothing reactor. Different protection measures for the converter valve are shown in scheme 1, 2, 3, and 4. The conventional DC transmission system converter consists of thyristor and is directly protected by arrester that is connected across the converter valve. The MMC transmission system is more complicated, and the inverter has a bridge arm reactor in addition to the converter valve, and the two devices need to be protected. The converter valve is made up of a series of submodules of IGBT shunt capacitors. In order to protect MMC converter, there are three types of optional arresters. Bridge arm reactor ground-side arrester, converter valve and bridge arm reactor parallel arrester, combined into four different arrester configuration options.

The different protection measures for the smoothing reactor are shown in scheme 4 and 5. The voltage across the smoothing reactance of the conventional DC converter station is relatively high, so a parallel arrester is configured. The voltage at the two ends of MMC converter station is lower than that of the conventional DC converter station, and the grounding arrester placed on both sides of the smoothing reactor can effectively protect the reactor. Secondly, if a parallel arrester is used, when the arrester operates, the fault current will flow to the converter valve, and the overvoltage level of the converter valve device rises. The weaker ability of the converter valve to withstand the inrush current can cause the IGBT to burn out.

4.2 Determination of Insulation Level of Converter Station

4.2.1 Process of Insulation Coordination

The steps to determine the insulation level of the equipment are mainly divided into three steps. First, a representative overvoltage of each device is obtained according to the simulation calculation. Secondly, the protection level of the arrester is obtained after determining the arrester configuration. Finally, comprehensively consider the safety margin, technical and economic factors to determine the insulation level recommended value. Therefore, the ultimate goal of insulation coordination is to properly determine the insulation withstand voltage of electrical equipment.

Insulation coordination methods include deterministic methods, statistical methods, and simplified statistical methods. This section uses the deterministic method, which is to determine a suitable coefficient between the expected overvoltage level of the critical equipment and the withstand voltage of the equipment, which is selected based on the operating experience of other projects and equipment manufacturing parameters. The representative overvoltage U_{rp} of each electrical node is the maximum overvoltage obtained after various simulations of various faults, operations, lightning strikes, etc. of the converter station and the line. According to the representative overvoltage level of the

equipment we can obtain, considering the aging of the insulation material after long-term operation and the factors such as rain and fog weather and environmental pollution, the insulation capacity of the equipment can be reduced, and a reasonable margin can be obtained according to experience to obtain the required withstand voltage of the equipment U_{rw}.

$$U_{rw} = U_{rp} \times K \tag{4-2}$$

where, K is insulation margin factor. This factor takes into account the insulation factor, withstand voltage, altitude correction factor and safety factor.

Switching, lightning specified withstand voltage U_w equal to or higher than the corresponding operation, lightning requirements withstand voltage U_{rw}. The rated withstand voltage of U_w shall be the next standard value equal to or higher than the calculated value from the series of standard rated withstand voltages given by GB 311.1-2012 [11,12].

4.2.2 Insulation Margin Selection of Equipment

The converter station of MMC-MTDC grid has an important function of mutual conversion between AC and DC. The cost of the converter station will affect the cost of the entire project, and the cost of the converter station is mainly composed of equipment cost and operation and maintenance cost. The decisive factor is the insulation level of the equipment. Considering that different equipment at the converter station have different insulation margin requirements, it is very important to properly select the insulation margin factor. The safety and stability of the system under the small insulation margin coefficient is difficult to guarantee, but the excessive insulation margin coefficient will make the engineering cost increase economically low. Refer to the ratio of the impact withstand voltage and the impact protection level in the national standard, and combine the characteristics of the Zhangbei four-terminal flexible DC transmission project to determine the insulation margin coefficient applicable to the multi-terminal high-voltage flexible DC engineering converter station equipment. The equipment insulation margin coefficient proposed for the Zhangbei project converter station is shown in table 4-7.

Table 4-7 Insulation Margin Coefficient of Zhangbei Project

Device Type	Switching Impulse	lightning Impulse
AC field equipment	1.20	1.25
AC side of transformer	1.20	1.25
Valve side of transformer	1.20	1.25
Valve	1.15	1.20
Equipment in DC valve hall	1.15	1.20
Smoothing reactor	1.20	1.25
DC field equipment	1.20	1.25

Table 4-8 Insulation Level and Insulation Margin of Each Electrical Node under Five Arrester Configurations

Nodes	Scheme 1				Scheme 2				Scheme 3				Scheme 4				Scheme 5			
	SIW *V*/kV	Marg in/%	*LIW* *V*/kV	Marg in/%	*SIW* *V*/kV	Marg in/%	*LIW* *V*/kV	Marg in/%	*SIW* *V*/kV	Marg in/%	*LIW* *V*/kV	Marg in/%	*SIW* *V*/kV	Marg in/%	*LIW* *V*/kV	Marg in/%	*SIW* *V*/kV	Marg in/%	*LIW* *V*/kV	Marg in/%
AC bus	804	20	1157	25	852	27	885	25	852	27	885	25	852	27	885	25	852	27	885	25
Valve side of transformer	1073	15	1068	20	987	15	791	25	965	15	808	25	965	15	808	25	965	15	759	25
Valve side of arm reactor	1073	15	1068	20	1415	15	805	25	1080	23	763	25	1080	24	763	25	1080	22	729	25
Valve top	1054	20	1173	25	1136	20	948	30	1080	20	948	30	1080	20	948	30	1109	20	943	30
Valve side of reactor	1054	20	1173	25	1136	20	948	30	1328	20	948	30	1128	20	948	30	1510	20	943	30
DC line	1034	20	1218	25	1030	20	1218	25	1025	20	1218	25	1025	20	1218	25	1060	20	1218	25
Neutral line out the valve hall	477	15	568	20	639	15	576	20	675	15	576	20	628	15	576	20	628	15	573	20
Neutral line	472	15	565	20	472	15	449	20	472	15	449	20	472	15	449	20	472	15	449	20
Metallic return line	378	15	500	20	374	15	449	20	374	15	449	20	374	15	449	20	374	16	449	20
Across bridge arm reactor	1160	15	840	20	485	20	204	25	510	20	196	25	1023	20	196	25	1023	20	203	25
Across smoothing reactor	790	20	1458	25	809	20	1069	25	1104	20	1069	25	893	20	1069	25	964	20	1045	25
Across valve	2225	15	612	20	1046	20	612	23	1975	15	624	20	1108	20	624	23	1108	20	612	23

SIWV：Switching impulse withstand voltage; **LIWV**：Lightning impulse withstand voltage.

4.2.3 Insulation Level of Equipment in Converter Station

After determining the parameters of the arrester, the overvoltage calculation of the arrester is performed one by one to obtain the lightning impulse and the switching impulse protection level of each arrester. Refer to the design experience of ±500kV conventional DC engineering, and according to the protection level of the arrester, lightning overvoltage level and switching overvoltage level, insulation margin. The switching impulse withstand voltage SIWV, the lightning impulse withstand voltage LIWV, and the recommended insulation level of the equipment for the key equipment nodes of the converter station in the five arrester configurations can be obtained separately, as shown in table 4-7. Considering the safety of the equipment and the switching voltage level, the insulation level should be appropriately increased according to the application environment.

4.3 Optimization of Arrester Configuration Scheme

In the insulation configuration plan planning, each configuration scheme has different advantages and disadvantages, and it is difficult to directly determine the optimal solution through a large amount of data. Therefore, the main factors influencing the decision-making can be selected when the optimal scheme is selected, and the trade-off comparison is made on all the schemes. In order to comprehensively consider the influence of both technical and economic aspects, this paper uses the Analytic Hierarchy Process (AHP) to give an effective comprehensive decision-making method. Finally, the technically optimal arrester configuration scheme can be given from several alternatives.

4.3.1 Evaluation Model of Arrester Configuration Scheme

AHP is a new type of decision-making method that combines quantitative and qualitative methods proposed by American operations researcher Professor Thomas L. Saaty in the 1970s. It is necessary to classify a variety of complex factors, group them in a logical order and form an ordered hierarchical structure. According to the relative importance degree of each layer, the judgment matrix is obtained, and the corresponding weight vector can be obtained by calculating the eigenvector of the matrix [44-46].

According to the basic idea of AHP, the complex decision problems are hierarchical into four categories. For the optimal selection of the arrester scheme for MMC-HVDC converter station, the goal is to select the optimal technical and economic insulation coordination scheme. The criteria layer mainly contains relevant criteria to be considered in order to achieve the objectives, including insulation level, insulation margin, installation difficulty, maintenance difficulty and engineering cost. Among them, the insulation level, engineering cost, installation difficulty and maintenance difficulty are all reverse indicators, that is, the smaller the better, the insulation margin is the positive indicator, the bigger the better. The third layer of the indicator layer considers the electrical node of the converter station that can

be configured with the arrester, which is the specific assessment content of each factor of the criterion layer. The solution layer consists of five arrester configurations that consider optimized converter valve protection and DC side equipment protection. According to the theory of analytic hierarchy process, the technical and economic evaluation model of the insulation coordination scheme of MMC converter station is established, and the hierarchical structure of the technical economy is shown in figure 4-3.

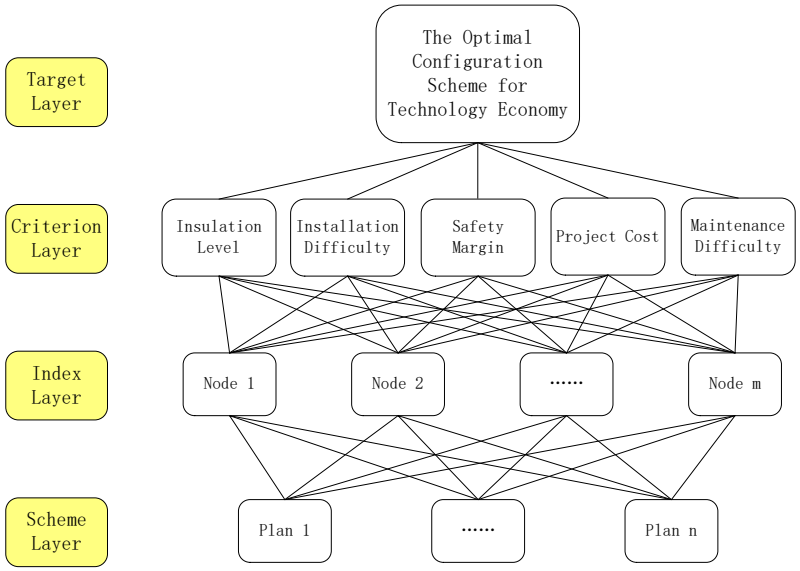

Figure 4-3 Hierarchical Structure Diagram of Insulation Coordination Scheme

4.3.2 Application of Improved AHP in Arrester Configuration Scheme

1）Determination of weights at each level

After determining the level assessment indicator system, it is necessary to determine the weight of each level factor.

（1）Criterion layer weights

For the criterion layer indicators, due to the different extension and connotation of the indicators, they are qualitative indicators. You can consider the expert opinion and calculate the weight by comparing the judgment matrix by two. We use a scale of 1 to 9 and its reciprocal as the ratio of the importance of the two factors. The larger the value, the stronger the importance, and the resulting judgment matrix must satisfy the consistency test. By comparing the two factors of the criterion layer, the following judgment matrix $\boldsymbol{G}$ can be obtained.

$$G = \begin{bmatrix} G_{11} & G_{12} & G_{13} & G_{14} & G_{15} \\ G_{21} & G_{22} & G_{23} & G_{24} & G_{25} \\ G_{31} & G_{32} & G_{33} & G_{34} & G_{35} \\ G_{41} & G_{42} & G_{43} & G_{44} & G_{45} \\ G_{51} & G_{52} & G_{53} & G_{54} & G_{55} \end{bmatrix} \quad (4\text{-}3)$$

According to the above judgment matrix ***G***, use $Gw_1 = \lambda_{\max} w_1$ to calculate the largest eigenvalue $\lambda_{\max}$ of the matrix ***G***, and the normalized eigenvector w_1. The components of the vector w_1 are the weights of the five criterion layer factors, which is $w_{1,i},(i=1,2,\ldots,5)$.

The method of calculating the weight has three steps: First, the column vectors of the judgment matrix ***G*** are separately normalized to obtain a column vector and a 5×5 matrix which are both 1. Second, sum the row elements of the matrix obtained in the previous step to obtain a 1 × 5 row vector. Finally, the eigenvector of the judgment matrix can be obtained by normalizing the row vector $w_1 = \left[w_{1,1} \quad w_{1,1} \quad \cdots \quad w_{1,i} \right]$. According to the calculated feature vector, the maximum eigenvalue of the matrix can be calculated according to the following formula.

$$\lambda_{\max} = \frac{1}{n} \sum_{i=1}^{n} \frac{G w_{1,i}}{w_{1,i}} \tag{4-4}$$

After that, it is necessary to perform consistency check on the feature vector to ensure whether the established pairwise comparison judgment matrix is in reality, and the consistency value can prove that the weight value obtained by the matrix is logical. CR in equation (4-5) is a random consistency ratio, and CI in equation (4-6) is a consistency index, and their calculation formula is as follows.

$$CR = \frac{CI}{RI} \tag{4-5}$$

$$CI = \frac{\lambda_{\max} - n}{n-1} \tag{4-6}$$

where, n is the number of criterion layer elements, RI represents average random consistency indicator. When the number of criteria layer elements is less than 9, the value RI can be selected from table 4-9.

Table 4-9 Average Random Consistency Indicator RI

n	1	2	3	4	5	6	7	8	9
RI	0.00	0.00	0.58	0.90	1.12	1.24	1.32	1.41	1.45

Finally, CR is calculated. When $CR \le 0.10$, the supervisory weight of the criterion layer can be considered to pass the consistency test. If it does not pass, it is necessary to adjust the pairwise comparison values of the judgment matrix ***G*** and repeat the above steps.

（2）Index layer

The factor of the index layer is the *m* important electrical nodes of the model to be evaluated. Because there are many factors in the index layer, if the judgment matrix obtained by the

9-scale method is still very complicated, the matrix may not pass the consistency test. Therefore, an improved analytic hierarchy process can be used to establish an accurate comparison matrix of the relative importance of electrical nodes, and finally a reasonable weight value between the 12 factors of the indicator layer is calculated. This method can eliminate the step of consistency check and does not require multiple adjustments of the decision matrix. Taking the insulation margin as an example, the specific method is as follows.

Using the 3-scale judgment method to establish the pairwise comparison matrix between the index factors, according to the degree that the m electrical nodes are vulnerable to overvoltage threats and considering the overvoltage level value when the arrester is not configured, the comparison matrix is.

$$F = \begin{bmatrix} F_{11} & F_{12} & \cdots & F_{1m} \\ F_{21} & F_{22} & \cdots & F_{2m} \\ \vdots & \vdots & \ddots & \vdots \\ F_{m1} & F_{m2} & \cdots & F_{mm} \end{bmatrix} \tag{4-7}$$

where, F_{ij} is the importance of the i^{th} electrical node relative to the j^{th} electrical node. When *I* is larger than *j*, it is 2. When *I* is equal to *j*, it is 1. When *I* is smaller than *j*, it is 0.

It can be known that if ***B*** is an antisymmetric matrix, the optimal transfer matrix ***C*** of ***B*** satisfies $c_{ij} = \frac{1}{m}\sum_{k=1}^{m}(b_{ik} - b_{jk})$. If A is reciprocal matrix, then the matrix ***B***=lg***A*** is an antisymmetric matrix. When ***C*** is the optimal transfer matrix for ***B***, then $\boldsymbol{A}^{*}=10^{\boldsymbol{C}}$ is the quasi-optimal consistent matrix. The quasi-optimal consistency matrix does not need to pass the consistency test [47].

Therefore, a reciprocal matrix ***A*** should be constructed from the comparison matrix ***F*** first. Find the importance index of each electrical node of the comparison matrix ***F***, that is, obtain the row sum $f_i = \sum_{j=1}^{m} f_{ij}$. The judgment matrix ***A*** is constructed according to the importance degree index a_i, and the elements of the matrix can be calculated by the formula (4-8).

$$a_{ij} = \begin{cases} f_i - f_j + 1, f_i \geq f_j \\ (f_j - f_i + 1)^{-1}, f_i < f_j \end{cases} \tag{4-8}$$

The judgment matrix ***A*** is the reciprocal matrix, and then the quasi-optimal consistent matrix $\boldsymbol{A}^{*}$, whose element is

$$a_{ij}^{*}=10^{\frac{1}{m}\sum_{k=1}^{m}(b_{ik}-b_{jk})} \tag{4-9}$$

where $b_{ij}=\lg a_{ij}$.

In the weight calculation part of the index layer, the square root method can be obtained

$$w_{2,i}^{*}=\sqrt[m]{\prod_{j=1}^{m}a_{ij}^{*}},(i=1,...,m) \tag{4-10}$$

Finally, normalization can directly determine the weight coefficient of each node to a certain technical index in the criterion layer $w_2^{(1)}=\begin{bmatrix} w_{2,1} & w_{2,2} & \cdots & w_{2,m} \end{bmatrix}$. By repeating the above steps, the weight coefficient of the index layer relative to other factors of the criterion layer can be obtained $w_2=\begin{bmatrix} w_2^{(1)} & w_2^{(2)} & \cdots & w_2^{(5)} \end{bmatrix}^T$.

2）Judgment of quantitative indicators

After determining the weight of each level of factors, it is necessary to judge the quantitative indicators. For a certain factor of the criterion layer, the evaluation index is the corresponding data at *m* key device nodes. The number of configuration schemes that need to be determined is *n*, and a quantitative indicator decision matrix can be constructed by *m* evaluation indicators of the *n* schemes, which is $X=(x_{ij})_{n\times m}$. The evaluation indicators under different criteria are not the same, and their units and dimensions are also different. Therefore, it is necessary to standardize this quantitative indicator decision matrix so that the evaluation indicators under various factors can be compared intuitively. The standardization process is to perform dimensionless processing on the magnitude and then perform standardization operations to obtain weights.

（1）Dimensionless processing

For positive indicators,

$$y_{ij}=\frac{x_{ij}}{\sum x_{ij}} \tag{4-11}$$

For negative indicators,

$$y_{ij}=\frac{\sum x_{ij}-x_{ij}}{\sum x_{ij}} \tag{4-12}$$

（2）Standardization

$$d_{ij} = \frac{y_{ij}}{\sum_{i=1}^{n} y_{ij}} \tag{4-13}$$

Get weight $D = (d_{ij})_{n\times m}$.

3）Computational ordering at each level

After the quantitative indicators are judged, the insulation configuration scheme can be comprehensively evaluated. Taking the insulation margin as an example, consider the weight of the quantitative indicators under the criterion for the five insulation configuration schemes.

$$D_1 = \begin{bmatrix} d_{11}^{(1)} & d_{12}^{(1)} & \cdots & d_{1m}^{(1)} \\ d_{11}^{(2)} & d_{12}^{(2)} & \cdots & d_{1m}^{(2)} \\ \vdots & \vdots & \ddots & \vdots \\ d_{11}^{(n)} & d_{12}^{(n)} & \cdots & d_{1m}^{(n)} \end{bmatrix}_{n\times m} \tag{4-14}$$

where, $d_{ij}^{(k)}, (k = 1, ..., n)$ is the judgment value of the j^{th} node under the i factor for the k^{th} scheme.

Similarly, quantitative indicator weights can be obtained under the other four criteria D_2, D_3, D_4, D_5.

Then the technical and economic comprehensive evaluation of the k-th scheme is

$$Y^{(k)} = w_{1,1}\sum_{j=1}^{m} w_{2,j}\cdot d_{1j}^{(k)} + w_{1,2}\sum_{j=1}^{m} w_{2,j}\cdot d_{2j}^{(k)} + \cdots + w_{1,5}\sum_{j=1}^{m} w_{2,j}\cdot d_{5j}^{(k)} \tag{4-15}$$

Finally, according to the size of each insulation configuration $Y^{(k)}$, the technical economy of each insulation configuration can be obtained to obtain the optimal solution.

$$Y_{\max}^{(k)} = \max\left\{ Y_i^{(k)} \middle| i = 1, 2, \cdots, n \right\} \tag{4-16}$$

4.3.3 Results and Analysis of Evaluation

Five kinds of arrester configuration schemes for Zhangbei MMC-MTDC transmission system were selected as the research objects for analysis and calculation. The first thing that needs to be determined is the weighting factor of the criteria layer. Among them, the insulation level and insulation margin data of key nodes can be obtained from the results of 4.2 insulation cooperation research.

The main difficulty in installation is the installation of the arrester at each location. The

decisive factors related to it are the installation method of the arrester and the installation location. Parallel arresters are more difficult to install. The parallel arrester for the converter valve also needs to consider the heat dissipation problem of the converter valve. Parallel arresters for smoothing reactor need to consider the connection problems caused by separate arrangement of smoothing reactor. The value of maintenance difficulty is affected by the number of arresters and the installation location.

The main consideration of the project cost is the purchase cost of each equipment of the converter station, the installation cost in the previous period and the maintenance cost in the later period. For the optimization choice of the arrester configuration scheme, the main consideration is the cost of the purchase, installation and maintenance of the arrester. The arrester of the HVDC converter station generally adopts a gap-free zinc oxide arrester. The cost of the arrester with different reference voltages is given by formula (4-17).

$$P = \sum \frac{V_{refi}}{V_i} \cdot a_i \cdot b_i \cdot P_i \tag{4-17}$$

where, V_{refi} is reference voltage for the i^{th} arrester, V_i is valve plate rated voltage, a_i is Number of parallel columns for arrester, b_i is number of arresters, P_i is single valve price.

According to the analytic hierarchy process and the characteristics of Zhangbei project, the index decision matrix of insulation level, installation difficulty, insulation margin, engineering cost and maintenance difficulty can be obtained. The weight coefficients of the criterion layer are shown in table 4-10.

Table 4-10 The Weight Coefficients of the Criterion Layer

Criterion layer	Insulation level	Installation difficulty	Insulation margin	Engineering cost	Maintenance difficulty	Weight coefficients
Insulation level	1	2	3	1/2	3	0.2625
Installation difficulty	1/2	1	2	1/2	2	0.1681
Insulation margin	1/3	1/2	1	1/4	2	0.1037
Engineering cost	2	2	4	1	4	0.3876
Maintenance difficulty	1/3	1/2	1/2	1/4	1	0.0782

The weighting coefficients of the five indicators of the obtained criterion layer are,

$$w_1 = \begin{bmatrix} w_{1,1} & w_{1,1} & \cdots & w_{1,5} \end{bmatrix} = \begin{bmatrix} 0.2625 & 0.1681 & 0.1037 & 0.3876 & 0.0782 \end{bmatrix}$$

Second, the weighting factor of the indicator layer should be determined. For the several scenarios to be evaluated, consider the important nodes. It is necessary to determine the weighting coefficients of each node of the indicator layer with respect to each factor in the criterion layer. Except for the economic indicator of project cost, it is not necessary to consider the relative importance between nodes. The other four technical indicators can calculate the weight coefficients of m nodes by using the 3-scale method. Finally, the weight coefficients of the 12 observation nodes for each indicator in the criterion layer are determined as shown in table 4-11.

After determining the weight coefficients of the criterion layer and the index layer, it is necessary to determine the weights of the quantitative indicators of the five insulation configuration schemes under each criterion. Among them, the two technical indicators of insulation level and insulation margin are related to the operating overvoltage and lightning overvoltage of each node. The weighting factors of the switching overvoltage and the lightning overvoltage can be directly taken as $w_s = 0.6$ and $w_l = 0.4$.

Table 4-11 The Weight Coefficients of the Index Layer

w_2	1	2	3	4	5	6	7	8	9	10	11	12
Insulation level	0.0047	0.1092	0.0218	0.1092	0.1092	0.1092	0.0098	0.0098	0.0098	0.1689	0.1689	0.1689
Installation difficulty	0.0188	0.0554	0.1041	0.0554	0.0188	0.0188	0.0081	0.0046	0.0046	0.1558	0.2292	0.3259
Insulation margin	0.0047	0.1092	0.0218	0.1092	0.1092	0.1092	0.0098	0.0098	0.0098	0.1689	0.1689	0.1689
Engineering cost	0.0833	0.0833	0.0833	0.0833	0.0833	0.0833	0.0833	0.0833	0.0833	0.0833	0.0833	0.0833
Maintenance difficulty	0.2791	0.0687	0.0687	0.0101	0.1585	0.2791	0.0056	0.0039	0.0101	0.0234	0.0234	0.0687

Quantitative indicator weights under five criteria can be calculated from Section 4.2 data D_1, D_2, D_3, D_4, D_5.

Finally, the final weighted result can be calculated by equation (4-15). The result is shown in figure 4-4. The comprehensive evaluation coefficients obtained by the final weighting of the five configuration schemes are $Y = \begin{bmatrix} 0.2041 & 0.2021 & 0.2035 & 0.1988 & 0.1917 \end{bmatrix}^T$.

The size of the pair can be obtained $Y^{(1)} > Y^{(3)} > Y^{(2)} > Y^{(4)} > Y^{(5)}$. The weight coefficient of the scheme 1 is the largest, so the scheme 1 is the optimal scheme among the five arrester configuration schemes. By comparing the arrester configuration schemes of five high-voltage flexible DC converter stations, the following conclusions can be obtained.

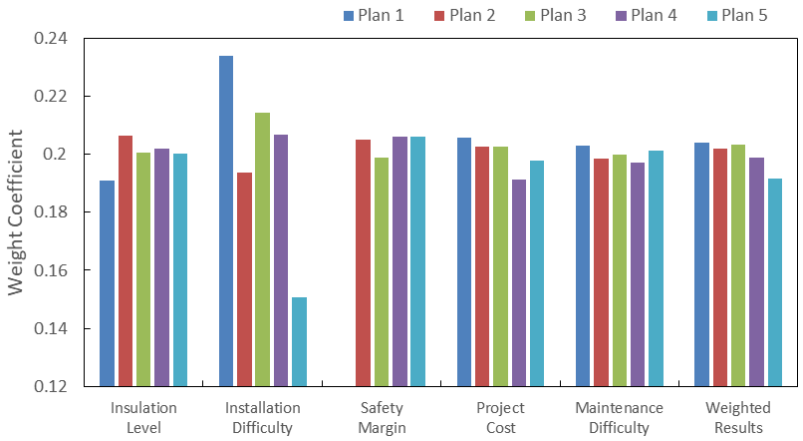

Figure 4-4 Comprehensive Evaluation Results of Five Configuration Options

(1) Scheme 1

The arrester configuration scheme 1 is an optimal configuration scheme obtained through comprehensive evaluation and analysis. The scheme takes into account the difficulty in designing and installing the parallel arrester at both ends of the converter valve and the heat and heat dissipation problems after the system is running, and the parallel arresters at both ends of the converter valve and the reactance of the bridge arm are subtracted. For the protection of the converter valve, the ground arrester LV disposed on the side of the bridge arm reactance valve is selected. Under this scheme, the overvoltage levels at both ends of the bridge arm and at both ends of the valve reach 1058kV and 1934kV, which requires high insulation level for the converter valve equipment. Although the requirements for the insulation level of the valve hall equipment have been improved, the number of arresters has been reduced and the economy has been improved while ensuring the full operation of the system.

(2) Scheme 2

Arrestor configuration scheme 2 parallel protection arrester V and AL direct protection valve block and bridge arm reactor at both ends of MMC converter valve and bridge arm reactance, to prevent excessive overvoltage of converter valve and bridge arm reactance. Under this configuration scheme, the fault current can form a loop through V and AL, the charging current of the converter valve arm sub-module is reduced, and the tendency of the sub-module voltage to rise is relatively reduced. Therefore, the overvoltage levels at both ends of the converter valve and the bridge arm reactor are reduced to 872kV and 404kV, respectively, thereby reducing the insulation level of the converter valve device. However, since there is no arrester on the valve side of the bridge arm reactor, the overvoltage level of the node rises to 1230kV, which still poses a threat to the converter valve. Compared with Option 1, this scheme adds 12 arresters and is economically low.

(3) Scheme 3

The arrester configuration scheme 3 adds a bridge arm reactor arrester AL to the

configuration scheme 1. In the MMC transmission system, the existence of the smoothing reactor limits the lightning intruding wave overvoltage on the DC side to the converter valve. The existence of the converter transformer and the bridge arm reactor limits the lightning intruding wave overvoltage transmission on the AC side. Therefore, when considering the arrester arrangement of the converter valve, the influence of the lightning intruding wave overvoltage can be ignored. Only the switching overvoltage level is considered. The voltage from the side of the bridge arm reactance valve to the ground drops to 880kV, and the voltage at the end of the bridge arm reactor drops to 425kV, but the voltage across the converter valve is still high, 1717kV. At this time, the energy of the arrester AL is small, and it is considered that the bridge arm reactor has a certain ability to withstand overvoltage. Therefore, the AL configuration of this scheme is less economical in the case of ensuring safe and stable operation of the system, and 12 arresters are added in comparison with scheme 1 in scheme 3.

(4) Scheme 4

On the basis of the scheme 1, the configuration scheme 4 adds a V arrester connected in parallel to both ends of the bridge arm module. The overvoltage levels of the bridge arm reactance valve side, both ends and the bridge arm module are respectively 872kV, 853kV and 923kV. Therefore, the insulation level of important equipment and electrical nodes of the converter valve is low, and the manufacturing difficulty of the equipment is reduced. The reference voltages for the LV and V arresters for the converter valve protection configuration are 652kV and 596kV, respectively, and the engineering cost of this configuration is the highest of the five configurations. Schemes 2, 3, and 4 all increase the number of arresters. In order to improve economy, the number of parallel columns of various arresters can be appropriately reduced while ensuring that the arrester energy and current are both satisfied.

(5) Scheme 5

In the configuration scheme 5, the DB arrester is removed on the basis of the scheme 4, and the SR arrester connected in parallel at both ends of the smoothing reactor is added. In the lightning overvoltage of the converter station equipment, the overvoltage level at both ends of the smoothing reactor is reduced to 836 kV. The DC line intruding wave overvoltage is limited by the DL arrester, and the overvoltage level of the DC side line does not change much. In terms of the operating overvoltage of the converter station equipment, the overvoltage level at both ends of the smoothing reactor is reduced to 803 kV, and the reduction is not large. The overvoltage level on the flat valve side rises to 1259kV, threatening the hybrid DC circuit breaker on the DC side of the converter station. At the same time, the energy of the lightning arrester on the line side is increased, and the number of parallel columns of the DL arrester increases, so the economy is low.

From the previous engineering experience and the implementation of DC engineering, with the increase of voltage level, the volume and weight of the equipment are further increased,

and the manufacturing process and difficulty of the equipment are further increased. For ±500kV HVDC systems, the primary consideration should be to reduce the cost of the arrester equipment and the valve hall space, and then consider reducing the insulation level of the equipment. From the above analysis, the protection level and safety margin of the scheme 1 meet the requirements, and have lower engineering cost, and the system's long-term safe and stable operation capability is considered, which is the best choice among the five schemes. Table 4-12 shows the final arrester parameters and protection levels in the converter station. Table 4-13 shows the recommended insulation levels for the converter station equipment under the optimal arrester configuration.

Table 4-12 Converter Station Arrester Parameters and Protection Level

Arrester	U_{ref} /kV	*SIPL* (kV/kA)	*LIPL* (kV/kA)	Energy/MJ	Number of columns
A(500kV)	420	670/10	925/20	-	6
A(220kV)	304	448/10	458/10	-	6
AV	652	894/2	890/2	8	2
LV	652	930/4	890/2	10	4
CBH	629	878/4	938/10	10	4
DB	629	878/6	938/10	20	4
DL	629	861/4	974/10	10	4
CBN1	428	-	473/2	10	4
CBN2	396	414/6	426/2	10	6
E	296	-	375/5	5	3
EM	268	328/6	375/10	10	4

SIPL: Switching Impulse Overvoltage Level; **LIPL:** Lightning Impulse Overvoltage Level

Table 4-13 Equipment Specified Withstand Voltage and Insulation Level Recommended Value

Position	Arrester	SO/kV	*SIWV* /kV	*SSIWV* /kV	LO/kV	*LIWV* /kV	*SLIWV* /kV
500kV AC Bus	A1	670	804	850	925	1157	1300
220kV AC Bus	A2	448	538	550	458	573	650
Valve side of transformer	AV	894	1073	1175	890	1068	1175
Valve side of bridge arm	LV	930	1073	1175	890	1068	1175
Valve top	CBH	878	1054	1175	938	1173	1300
Valve side of reactor	DB	878	1054	1175	938	1173	1300
Line side of reactor	DL	861	1034	1175	974	1218	1300
Neutral line-valve side	CBN	414	477	550	473	568	650
Neutral line-line side	E	328	378	450	416	500	550

SSIWV: Specified switching impulse withstand voltage; **SLIWV:** Specified lightning impulse withstand voltage.

4.4 Brief Summary

In this chapter, the principle of arrester configuration of MMC converter station is given with reference to the principle of insulation configuration of conventional DC transmission converter station. The influence law of different arrester configuration schemes on system overvoltage is analyzed. The influence of the parameters, capacity, installation quantity and installation position of the arrester on the insulation coordination is analyzed, and five arrester configuration schemes for the demonstration project are proposed. At the same time, the principle and method of insulation coordination for the converter station of MMC transmission system are given. Combined with the protection level of the arrester, the lightning overvoltage level, the switching overvoltage level and the insulation margin, the insulation level of the key equipment of the converter station under different arrester configuration schemes can be obtained.

According to the optimization choice of the arrester configuration scheme, this paper uses the idea of analytic hierarchy process to analyze the five technical and economic indicators of insulation level, insulation margin, installation difficulty, maintenance difficulty and engineering cost. According to the characteristics of the criterion layer and the index layer factor, the nine-scale method and the three-scale method are used to solve the weight coefficient respectively, and the configuration scheme of the lightning arrester with the best technical economy is determined as the scheme 1. That is, the scheme of retaining the ground arrester of the key equipment node of the converter station and removing the parallel arrester of the converter station equipment. Finally, with reference to the design experience of ±500kV conventional DC engineering, the recommended values of insulation level for key equipment of ±500kV demonstration project converter station are given.

5 Conclusions

This thesis is based on ±500kV Zhangbei MMC-MTDC transmission system to carry out system modeling and simulation, multi-terminal converter station overvoltage characteristics analysis and insulation coordination research. The modeling of the four-terminal MMC grid is realized in the PSCAD electromagnetic transient simulation software. Based on the simulation model, the typical overvoltage of the converter station of the MMC-MTDC transmission system and the switching overvoltage characteristics generated after operation and the lightning overvoltage characteristics caused by the lightning intruding wave at the converter station are studied. The influencing factors and intrinsic characteristics of overvoltage of multi-terminal systems are analyzed. Based on the overvoltage analysis, the insulation coordination method of the converter station of MMC-MTDC transmission system is deeply studied. The configuration scheme of the arrester suitable for the MMCC converter station is proposed and the insulation level of the converter station equipment is determined.

The main findings of the thesis are as follows：

1）Taking the typical fault of the MMC converter station as an example, the effects of DC breaker action, grid operation mode, AC side fault and control protection system on the switching overvoltage in the multi-terminal converter station are analyzed. The overvoltage generated by the DC circuit breaker reclosing process is less than the opening process, and the DC side switching overvoltage extreme value of the MMC-MTDC system appears in the DC breaker opening process. Whether the converter station is grounded will affect the switching overvoltage distribution and the decisive faults of each node. The overvoltage of the station operation varies monotonously with the power command value, and the maximum switching overvoltage difference of the single-pole operation mode at the top of the converter valve reaches 1.53p.u. The operation mode of the converter station should be checked by considering different operation modes. In the case of failure of the control system, the DC side overvoltage of the converter station is 1.24 times that of the control operation, and the overvoltage of the fault side DC breaker is more than 0.07p.u. In the case of a correct judgment by the control system, the system line fault detection time should be shortened and the delay action of the fault side DC circuit breaker should be avoided.

2）The influencing factors of DC line shielding failure and back flashover intruding wave overvoltage are studied. Based on this, the most severe simulation conditions of lightning intruding wave overvoltage in converter station are obtained. The lightning protection performance of the pole wire is mainly affected by the tower parameters and the ground inclination angle. The tower height is lowered, and the ground inclination angle and the lightning protection angle are improved to improve the lightning strike performance of the

transmission line. The overvoltage difference between the lightning current and the voltage polarity is the same and different, and the difference of the overvoltage reaches 0.35p.u. The factors affecting the lightning strike performance of the line mainly consider the tower grounding resistance. The increase of the grounding resistance by 25Ω will cause the DC line overvoltage to rise by 0.37pu. Therefore, the lightning overvoltage level can be obtained by using the most severe lightning strike conditions according to the influencing factors.

3）In a MMC-MTDC transmission system, the fault current after a converter station fails will be transmitted to the adjacent converter station along with the DC transmission line, and a maximum switching overvoltage of 1.51p.u. and a maximum lightning overvoltage of 1.50p.u. will be generated at the adjacent converter station. Thus, the overvoltage level of the adjacent converter station of the line cannot be ignored in the simulation calculation. The lightning overvoltage level of each converter station in the MMC-MTDC transmission system is related to the parameters and terrain of the incoming line tower. The switching voltage level of the key equipment nodes of the high-power converter station is relatively high. If you want to simplify the insulation of multiple converter stations. The multi-station configuration can be carried out based on the overvoltage of the equipment of the high-power converter station.

4）The complete insulation coordination method of the MMC-MTDC converter station is introduced in detail, that is, the arrangement of the arrester of the converter station and the determination of the insulation level of the converter station equipment. The arrester configuration schemes of five flexible DC converter stations are proposed for different protection modes of converter valve, bridge arm reactor and smoothing reactor. Then, an improved analytic hierarchy process is used to determine the technically optimal arrester configuration. That is to say, the ground arrester for the key electrical nodes of the converter station of the MMC-MTDC transmission system is reserved, and the parallel arrester of each device is omitted under the premise of ensuring safe operation.

Reference

[1] Zhong JF, Chen LP, Yuan KL, etc. Current status and application prospects of multi-terminal flexible DC transmission technology [J]. Southern Energy Construction, 2015, (02): 38-45.
[2] Wang J. Thoughts on the impact of new energy power access on power grid planning [J/OL]. Science and Technology Innovation Guide, 2018, 36:1-2 [2019-04-11]. Http:// /doi.org/10.16660/j.cnki.1674-098X.2018.36.220.
[3] Zhangbei renewable energy flexible DC power grid demonstration project design start [J]. Rural Electrification, 2017, (02): 62.
[4] Xu Z. Flexible DC transmission system [M]. Mechanical Industry Press, 2016.
[5] Zhao YJ. HVDC transmission engineering technology [M]. Beijing: China Electric Power Press, 2004.
[6] Marquardt R. Modular multilevel converter: an universal concept for HVDC-networks and extended DC-bus applications[C]//2011 International Power Electronics Conference (IPEC). Sapporo, Japan: 2010: 502-507.
[7] Marquardt R. Modular multilevel converter topologies with dc-short circuit current limitation [C]// 2011 IEEE 8th International Conference on Power Electronics and ECCE Asia (ICPE & ECCE). Jeju, Korea: 2011: 1425-1431.
[8] Luo YJ, Li YH, Li ZX, etc. Full-bridge MMC-HVDC DC short-circuit fault ride-through control protection strategy [J]. Chinese Journal of Electrical Engineering, 2016, 36(7): 1933-1943.
[9] Mitra B, Chowdhury B, Manjrekar M. HVDC transmission for access to off-shore renewable energy: a review of technology and fault detection techniques [J]. IET Renewable Power Generation, 2018, 12(13): 1563-1571.
[10] Song Q, Zeng R, Yu ZQ, et al. A modular multilevel converter integrated with DC circuit breaker [J]. IEEE Transaction on Power Delivery, 2018, 33(5): 2502-2512.
[11] GB/T 311.3-2017, Insulation coordination Part 3: Insulation coordination process of HVDC converter station [S]. Beijing: China Standard Press, 2017.
[12] GB/T 311.3-2012, Insulation coordination Part 1: Definitions, principles and rules [S]. Beijing: China Standard Press, 2012.
[13] Zhao CY. Flexible DC transmission modeling and simulation technology [M]. Beijing: China Electric Power Press, 2014.
[14] Tang GF, He ZY, Pang Hui. Research, application and development of flexible DC transmission engineering technology [J]. Automation of Electric Power Systems, 2013, (15): 3-14.
[15] Wu SX, Li L, Zhang X, etc. Analysis of AC and DC interaction of multi-terminal flexible DC transmission project in South Australia [J]. Guangdong Electric Power, 2013, 37 (4): 26-30.
[16] Li J, Fan CY, Zhang J, etc. Research on insulation coordination of converter station of

±500kV DC transmission project [J]. Electrical Engineering, 2016, (02): 47-49.
[17] Wu B, Li HM, Be R, etc. Development status and research prospects of multi-terminal flexible direct current transmission [J]. Modern Electric Power, 2015, 32(2): 9-15.
[18] Guo XH, Zhao W, Fu Y, etc. Changji-Guquan ±1100kV UHV DC Engineering Insulation Coordination Scheme [J]. High voltage technology, 2018, 44 (4): 1343-1350.
[19] Zhou H, Wang DJ. Overvoltage protection and insulation coordination of ±1100kV UHV DC converter station [J]. Power Grid Technology, 2012, 36(9): 1-8.
[20] Ma WM, Jiang WY, Li YN. System design of Dalian flexible DC transmission project [J]. Power Construction, 2013, 34 (5): 1-5.
[21] Chen D, Le B, Mei N, etc. Design of ±320kV Xiamen Bipolar Flexible DC Transmission Engineering System [J]. Automation of Power Systems, 2018, 42(14): 180-185.
[22] Zhang ZR, Xu Z, Xue YL, etc. Research on overvoltage protection and insulation coordination of MMC-HVDC system [J]. Power System Protection and Control, 2013, 41(21): 58-64.
[23] Liu DP, Cheng XT, Qi RF, etc. Asynchronous networking engineering flexible DC converter station overvoltage and insulation coordination [J]. High-voltage electrical appliances, 2015, 51 (4): 104-108.
[24] Li TW, Liu DP, Lei YY, etc. Three-terminal flexible DC transmission system lightning intrusion wave overvoltage [J]. Power Construction, 2014, 35(3): 13-17.
[25] Yu SF, Ma WM, Nie D, etc. Over-voltage and insulation coordination of Zhoushan multi-terminal flexible DC project [J]. Power Construction, 2014, 35(3): 7-12.
[26] Zhou Hao, Shen Yang, Li Min, etc. Insulation coordination of Zhoushan multi-terminal flexible DC transmission project converter station [J]. Power Grid Technology, 2015, 28(4): 879-890.
[27] Li G, Liang J, Ma F, et al. Analysis of single-phase-to-ground faults at the valve-side of HB-MMCs in HVDC systems [J]. IEEE Transactions on Industrial Electronics, 2019, 66 (3): 2444-2453.
[28] Cui SH, Lee HJ, Jung JJ, et al. A comprehensive AC-side single-line-to-ground fault ride through strategy of an MMC-based HVDC system [J]. IEEE Journal of Emerging and Selected Topics in Power Electronics, 2018, 6 (3): 1021-1031.
[29] Freytes J, Akkari S, Rault P, et al. Dynamic analysis of MMC-based MTDC grids: Use of MMC energy to improve voltage behavior[J]. IEEE Transactions on Power Delivery,2019,34(1):137 -148.
[30] Xu JZ, Li CY, Xiong Y, etc. A review of the research on efficient modeling methods for modular multilevel converters [J]. Chinese Journal of Electrical Engineering, 2015, 35(13): 3381-3392.
[31] Zou YZ, Zhang HT, Liu CY, etc. New virtual synchronous generator control method and its transient process adaptive control strategy [J]. Grid Technology, 2018, 42 (3): 933-943.
[32] Xu JZ, Zhao CY, Aniruddha MG, etc. Multi-level converter Thevenin equivalent overall modeling method [J]. Chinese Journal of Electrical Engineering, 2015, 35 (08): 1919-1929.

[33] Zhao YC, Xu YL, Zhao CY, etc. Single port submodule MMC electromagnetic transient universal equivalent modeling method [J]. Journal of China Electrical Engineering, 2018, 38(16): 4658-4667+4971.
[34] Lan YN, Zheng CD. Research on broadband frequency converter module of flexible DC converter valve [J]. Electrical Engineering, 2017, (05): 31-35.
[35] Sun HF, Zheng CD, Wu XM, etc. Flexible DC converter station broadband model and lightning overvoltage calculation [J]. Power Grid Technology, 2015, 39 (01): 103-109.
[36] Tang Y. UHV DC converter valve integrated broadband equivalent circuit model and its application research [D]. Beijing: North China Electric Power University, 2017.
[37] Huang WW, Xiao MJ, Yang X, etc. Research on tower model in lightning strike analysis of transmission lines [J]. High-voltage electrical appliances, 2015, 51 (6): 166-172.
[38] He JL, Tu YP, Zeng R, et al. Numeral analysis model for shielding failure of transmission line under lightning stroke [J]. IEEE Transactions on Power Delivery, 2005, 20(20): 815-822.
[39] Asif M, Lee HY, Khan UA, et al. Analysis of transient behavior of mixed high voltage DC transmission line under lightning strikes [J]. IEEE Access, 7, 2018, 2169-3536.
[40] Ma H, Guo J, Ma W, etc. The influence of topography and geomorphology on the maximum bypass current of 330kV double-circuit transmission line on the same tower [J]. Electric porcelain arrester, 2014, 261 (5): 71-75.
[41] Zhang CX, Zhang LC. Insulation coordination optimization study for ±800kV UHVDC project with increased transmission capacity [J]. IEEE Power and Energy Society General Meeting, 2013, 1932-5517.
[42] Asha S, Vittal KP. Insulation coordination studies and selection of lightning arrester for 765kV switchyard[C]// 2017 International Conference on Intelligent Computing, Instrumentation and Control Technologies (ICICICT). Kannur, India: 2017: 1421-1425.
[43] Huang YR, Li FF, He QL, etc. Research on insulation coordination of converter station of ±800kV UHV DC transmission system [J]. High-voltage electrical appliances, 2015, 51 (7): 81-86.
[44] Duan RC, Wang FH, Gu CY, etc. Comprehensive evaluation of the effect of lightning protection on 500kV transmission lines by improved analytic hierarchy process [J]. High Voltage Technology, 2014, 40(1): 131-137.
[45] Wang D, Chen DZ. The application of solar power system on closed landfill based on the analytic hierarchy process method [C]// 2013 International Conference on Materials for Renewable Energy and Environment. Chengdu, China: 2014: 1008-1011.
[46] Li ZX, Rong XY. Accounting information system risk assessment algorithm based on analytic hierarchy process [C]// 2015 Seventh International Conference on Measuring Technology and Mechatronics Automation. Nanchang, China: 2015: 72-75.
[47] Wang MJ, Qi HS, Sun JS, etc. Comprehensive evaluation of quality and safety of Ganoderma lucidum based on improved analytic hierarchy process [J]. Journal of Agricultural Engineering, 2017, 33(4): 302-308.